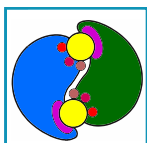


STRUCTURE, GATING, AND REGULATION OF THE CFTR ANION CHANNEL

László Csanády,  Paola Vergani, and David C. Gadsby

Department of Medical Biochemistry, Semmelweis University, Budapest, Hungary; MTA-SE Ion Channel Research Group, Budapest, Hungary; Department of Neuroscience, Physiology and Pharmacology, University College London, London, United Kingdom; and Laboratory of Cardiac/Membrane Physiology, The Rockefeller University, New York, New York



Csanády L, Vergani P, Gadsby DC. Structure, Gating, and Regulation of the CFTR Anion Channel. *Physiol Rev* 99: 707–738, 2019. Published December 5, 2018; doi:10.1152/physrev.00007.2018.—The cystic fibrosis transmembrane conductance regulator (CFTR) belongs to the ATP binding cassette (ABC) transporter superfamily but functions as an anion channel crucial for salt and water transport across epithelial cells. CFTR dysfunction, because of mutations, causes cystic fibrosis (CF). The anion-selective pore of the CFTR protein is formed by its two transmembrane domains (TMDs) and regulated by its cytosolic domains: two nucleotide binding domains (NBDs) and a regulatory (R) domain. Channel activation requires phosphorylation of the R domain by cAMP-dependent protein kinase (PKA), and pore opening and closing (gating) of phosphorylated channels is driven by ATP binding and hydrolysis at the NBDs. This review summarizes available information on structure and mechanism of the CFTR protein, with a particular focus on atomic-level insight gained from recent cryo-electron microscopic structures and on the molecular mechanisms of channel gating and its regulation. The pharmacological mechanisms of small molecules targeting CFTR's ion channel function, aimed at treating patients suffering from CF and other diseases, are briefly discussed.

I.	INTRODUCTION	707
II.	CFTR DOMAIN TOPOLOGY AND...	709
III.	THE CFTR ANION PERMEATION...	711
IV.	REGULATION OF CFTR GATING...	715
V.	REGULATION OF CFTR GATING...	725
VI.	TARGETING CFTR FUNCTION TO...	728
VII.	CONCLUDING REMARKS	730

The primary defect in CF patients is a reduction in chloride (190, 259) and bicarbonate (208) transport capacity across the apical membrane of epithelial cells. In 1989, the gene mutated in CF patients was identified on chromosome 7 by positional cloning (201), and the protein product was named the cystic fibrosis transmembrane conductance regulator (CFTR) to reflect its presumed involvement in the regulation of other anion transport proteins. Purification of the CFTR protein and its functional reconstitution in lipid bilayers soon provided proof that CFTR is, itself, the anion channel responsible for cAMP-dependent anion transport across epithelial surfaces (16).

I. INTRODUCTION

A. CFTR and Cystic Fibrosis

Cystic fibrosis (CF) is the most common life-threatening, inherited monogenic disorder among Caucasian populations; it affects 1 in ~2500 newborns in Europe and 1 in ~3500 newborns in the United States. CF is a multiorgan disorder, with symptoms including airway blockage by thickened mucus, leading to chronic lung infections, inflammation and bronchiectasis, blockage of pancreatic ducts and consequent pancreatic insufficiency, bowel obstruction in newborns, male infertility because of obstruction of the vas deferens, and a characteristic high-salt sweat diagnostic of the disease. Although at present efficient causative treatment is still restricted to a small subset of CF patients, in the past decades, improvements in patient care and symptomatic treatment have greatly prolonged the life expectancy of people born with CF, from ~1 yr in 1950 to ~40 yr at present (171).

B. The ABC Protein Superfamily

CFTR is a member of the large superfamily of tens of thousands of ATP binding cassette (ABC) proteins that are found in all kingdoms of life (147) and that serve to transport a large variety of substrates into and out of cells at the expense of ATP hydrolysis. ABC proteins share a conserved general architecture based on the modular assembly of four canonical domains: two transmembrane domains (TMDs) and two cytosolic nucleotide binding domains (NBDs). The number of polypeptide chains that this “core” functional unit comprises is variable. In prokaryotes, the four domains are often expressed as four individual polypeptides or as two TMD/NBD “half transporters” that coassemble post-translationally. The human genome encodes 48 ABC pro-

teins, which have been grouped into seven subfamilies (ABCA–G) (69). Except for the E and F subfamilies, which contain no TMDs, the human ABC proteins consist either of half transporters that homo- or heterodimerize or of full transporters in which the four canonical domains are linked in a single polypeptide chain. The ABCC subfamily, to which CFTR (ABCC7) belongs, falls into the latter class. In CFTR, each TMD contains six transmembrane (TM) helices, and the two homologous TMD-NBD halves (TMD1-NBD1 and TMD2-NBD2) are linked by a contiguous, unique, cytosolic regulatory (R) domain (201) (FIGURE 1A). At the sequence level, CFTR's two homologous halves display a marked asymmetry, a general feature of ABCC subfamily proteins (187). Within the entire ABC superfamily, CFTR is the only protein shown to form a transmembrane ion channel pore, in contrast to the vast majority of its homologs that serve as active transporters. The only other exceptions among human ABC proteins are the soluble E and F subfamily members, that are not involved in transmembrane transport, and CFTR's close relatives SUR1 (ABCC8) and SUR2 (ABCC9) that serve as regulatory subunits of ATP-sensitive potassium (K_{ATP}) channels (69).

C. Basic Functional Properties of the CFTR Anion Channel

Opening and closing (gating) of the CFTR anion pore is largely regulated by two processes. First, for a CFTR channel to become activated, its cytosolic R domain must be phosphorylated by cAMP-dependent protein kinase (PKA) (20, 48, 183, 225). Second, gating of a phosphorylated CFTR channel is driven by binding of ATP to its cytosolic NBDs (9). In single-channel recordings, CFTR channel activity displays typical bursting behavior, with brief (intra-burst) closures interrupting longer periods of channel opening, yielding open bursts that are separated by long (interburst) closures (32, 95, 261). Gating kinetics are relatively slow; the duration of a burst and interburst cycle is on a second timescale (0.1–2 s, depending on species, phosphorylation level, and temperature) rather than the millisecond timescale of voltage-gated channels. Moreover, except for the kinetics of intra-burst closures, which little affect channel open probability (30), CFTR gating is largely voltage independent (20). Anion permeation through the open pore follows simple ohmic behavior: in symmetrical 140 mM of chloride, the unitary current/voltage relationship is relatively linear (20, cf. Ref. 30) with a slope conductance of ~10 pS at 35–37°C (20) or ~7–8 pS at 20–25°C (227). These basic biophysical properties serve as a fingerprint that allows reliable identification of CFTR currents both in native tissues and in heterologous expression systems.

D. Root Cause of CF Disease Symptoms

To date, more than 2,000 CFTR mutations have been identified in CF patients (<http://www.genet.sickkids.on.ca>), a

remarkable number for a 1480-residue protein, although a subset of these variations is likely to have no functional consequence. The roughly 200 mutations that are known to cause CF are traditionally classified (68, 282) based on how they affect the encoded protein, that is, whether they abolish or reduce the production of the full-length CFTR polypeptide (truncation mutations, Class I; alternative splicing, Class V), impair protein trafficking/maturation (Class II), impair regulation of channel gating (Class III) or anion permeation through the open channel pore (Class IV), or affect the lifetime of the channel protein in the apical membrane (Class VI). Despite the large number of identified CFTR mutations, a single mutation, deletion of phenylalanine 508, is responsible for the majority of CF cases worldwide. The $\Delta F508$ allele represents ~70% of all CF-associated alleles; thus, given the recessive inheritance of the disease, >90% of CF patients carry at least one $\Delta F508$ allele. The $\Delta F508$ mutation belongs to several classes. Because of a severe folding defect resulting in degradation of most of the protein translated at the endoplasmic reticulum (Class II) (42, 148) coupled with thermal instability and an increased rate of degradation once at the plasma membrane (Class VI) (173, 251), the amount of mature, fully glycosylated $\Delta F508$ CFTR protein in the plasma membrane is estimated to be only ~2% of that of wild type (WT) (239). In addition, the small amount of $\Delta F508$ CFTR present in the plasma membrane is phosphorylated by PKA at a diminished rate (246), and even fully phosphorylated $\Delta F508$ channels display a severe gating defect (Class III) characterized by a >40-fold reduction in channel open probability because of a lower rate of pore opening (66, 125, 161).

A reduction of CFTR anion permeability is undoubtedly one of the root causes of abnormal lung secretions that lead to the ultimately lethal CF lung symptoms. However, CF airway epithelia also show enhanced amiloride-sensitive transepithelial potentials and short-circuit currents (28, 121, 122). Loss of an inhibitory effect of WT CFTR on the amiloride-sensitive epithelial Na^+ channel (ENaC), and consequent ENaC overactivation, was thought to underlie this observation, and increased Na^+ absorption together with the loss of Cl^- secretion was suggested to cause dehydration of the airway surface liquid, impairing mucociliary clearance and increasing susceptibility to infection (27). Although initial electrophysiological studies of coexpressed CFTR and ENaC in *Xenopus* oocytes did not detect any inhibitory effect of CFTR on ENaC (165), studies in more native systems do support this hypothesis. In primary nasal epithelia, a Na^+ -permeant channel had a higher open probability in cells obtained from CF patients than in those from normal individuals (44). Biochemical studies demonstrated that WT CFTR could protect ENaC from protease-dependent activation in airway epithelial cells, but $\Delta F508$ CFTR failed to do so (89, 128). This consistent picture was questioned, however, when CF pigs (both $-/-$ and homozygous $\Delta F508$) were developed by the Welsh laboratory. These,

like humans, developed lung disease and showed increased susceptibility to bacterial infection when newborn. A reduced pH of the airway surface liquid was found to be crucial in developing the disease (181) (see Section III C), but increased Na^+ absorption was not detected (39, 110), suggesting that amiloride-sensitive changes in epithelial properties might be secondary to reduced apical Cl^- permeability. However, using a biophysical model of transepithelial ion fluxes, alterations in bioelectric properties of CF epithelia were found to be too large to be accounted for by electrical coupling alone (170). Thus, a more complex interpretation of CF pathogenesis might be required before decades of controversy can be finally laid to rest.

II. CFTR DOMAIN TOPOLOGY AND STRUCTURE

A. Domain Boundaries

Cloning of the CFTR sequence revealed its domain organization (FIGURE 1A) and allowed a rough prediction of transmembrane topology and domain boundaries (201). The suggested topology has stood the test of time, except for some small adjustments of helical boundaries [e.g., (86, 255)]. However, the originally predicted NH_2 - and COOH -termini of NBD1 and 2 turned out to be quite inaccurate. Exploiting ABC transporter modular architecture, coexpression of complementary CFTR segments was used to provide a functional definition of NBD1 boundaries (33): this approach extended the NBD1 COOH -terminus from amino acid position (a.a.) 586 to 633, but left its NH_2 -terminus uncorrected. The crystal structure of mouse CFTR NBD1 (130) finally assigned correct NBD1 NH_2 - and COOH -terminal boundaries to ~a.a. 390 and ~670, respectively, although residues distal from ~a.a. 645 form a helix that is not conserved among ABC proteins and contains two consensus serines (S660 and S670) phosphorylated by PKA, suggesting that it might be considered part of the R domain. For NBD2, the crystal structure of a fusion protein of human CFTR NBD2 with the regulatory domain of *Escherichia coli* MalK (PDBID: 3GD7) allowed adjustment of NBD2 NH_2 - and COOH -terminal boundaries to a.a. 1208 and ~1427, respectively, largely confirmed (1207–1436) by the first atomic structure of full-length human CFTR (145). Given that much of the R domain of CFTR is unstructured (145, 177), its exact NH_2 - and COOH -terminal boundaries are still uncertain and might be assigned to ~a.a. 645 (670) and ~845, respectively, largely based on the boundaries of its bracketing domains (NBD1 and TMD2; see FIGURE 1A) as well as on the locations of consensus sites for PKA phosphorylation.

B. The ATP Binding Cassettes

NBD1 and NBD2 are also known as CFTR's ATP binding cassettes, the highly conserved (both at a sequence and

three-dimensional structure level) ATPase subunits characteristic of all ABC proteins (FIGURE 1B). ABC NBD structures consist of two subdomains. The nucleotide binding core subdomain (the "head") comprises an F1-like parallel β -sheet (FIGURE 1B, *light green*), which is stabilized by α -helices (FIGURE 1B, *dark green*) and contains the conserved Walker A (consensus GXXXXGKS/T; FIGURE 1B, *red*) and B (consensus $\Phi\Phi\Phi\Phi\text{DE}$, Φ hydrophobic; FIGURE 1B, *marine*) motifs important for Mg-ATP binding (245) and is completed by an ABC-specific, three-stranded antiparallel β -sheet (FIGURE 1B, *cyan*). The two β -sheets surround a central α -helix preceded by the P-loop, which is formed by residues of the Walker A motif (FIGURE 1B, *dark green helix and red loop*). The NBD α -helical subdomain (the "tail"; FIGURE 1B, *orange*) contains the highly conserved, ABC-specific "signature sequence" (consensus LSGGQ; FIGURE 1B, *magenta*). In nucleotide-bound, high-resolution NBD structures, the P-loop is seen to coordinate the phosphate chain, with the conserved Walker A lysine (K464 and K1250 in CFTR; FIGURE 1B, *red sticks*) playing a dominant role by coordinating all three phosphates of ATP. The antiparallel β -sheet provides a conserved aromatic residue that stacks against the adenine base of the bound nucleotide (W401 and Y1219 in CFTR; FIGURE 1B, *blue sticks*). The Walker B motif ends in a conserved aspartate (D572 and D1370 in CFTR; FIGURE 1B, *marine sticks*) important for Mg^{2+} coordination and is followed by a conserved glutamate (E1371 in NBD2 of CFTR; FIGURE 1B, *salmon sticks*), which acts as the general base that polarizes the attacking water molecule during the ATP hydrolysis reaction (162, 174, 175). A conserved glutamine (Q493 and Q1291 in CFTR; FIGURE 1B, *orange sticks*) in the loop that links the head and tail subdomains (the "Q-loop") acts as the γ -phosphate sensor and plays a key role in an induced fit conformational change elicited by ATP binding; an ~15° rotation of the tail subdomain toward the core subdomain in ATP compared with ADP-bound, or apo, structures (115, 268). These key catalytic residues are held together by the conserved "switch histidine" (H1402 in NBD2 of CFTR; FIGURE 1B, *light magenta sticks*), also called the "linchpin" (174, 269). In CFTR, there is substantial asymmetry between NBD1 and NBD2 regarding the key consensus motifs. In NBD1, the post-Walker B glutamate and the switch histidine are replaced by serines (S573 and S605, respectively), whereas in NBD2, the signature sequence is atypical (LSHGH). In addition, CFTR's NBD1 contains two unique sequence segments (130): an ~30-residue unstructured segment (a.a. 406–436) inserted into the antiparallel β -sheet [regulatory insertion (RI)], and an ~30-residue helical extension [a.a. 641–670; regulatory extension (RE)]. Both segments contain consensus serines phosphorylated by PKA (S422 and S660 and S670, respectively), and both are unstructured in full-length CFTR (FIGURE 1B; *light magenta dotted lines*).

In the presence of ATP, but under conditions that preclude ATP hydrolysis, isolated ABC NBDs form head-to-tail dimers that occlude two molecules of ATP at the dimer

interfaces. Such NBD dimerization can be observed both for isolated soluble NBD domains [e.g., (38, 215, 269)] or in the context of full-length ABC proteins [e.g., (46, 67, 256)], including CFTR [(99, 159, 207, 274); **FIGURE 1C**]. In both composite nucleotide binding sites, an ATP is sandwiched between the Walker motifs of one NBD (**FIGURE 1C**, Walker A, *red*) and the signature sequence of the other NBD (**FIGURE 1C**, *magenta*). This arrangement explains the crucial role the signature sequence plays in catalysis despite its distance from the bound nucleotide within an NBD monomer (**FIGURE 1B**). Furthermore, in CFTR, the head-to-tail arrangement of the NBD dimer collects all noncanonical substitutions into a single-composite binding site formed by the head of NBD1 and the tail of NBD2 (site 1; **FIGURE 1D**, *upper site*); in this degenerate site, the catalytic glutamate and the switch histidine are ablated by mutation, and the signature sequence is aberrant. In contrast, in the composite binding site formed by the head of NBD2 and the tail of NBD1 (site 2; **FIGURE 1D**, *lower site*), all key residues are canonical. A similar asymmetrical distribution of consensus versus atypical residues is found throughout the entire ABCC subfamily as well as in many other prokaryotic and eukaryotic heterodimeric ABC proteins (101, 187).

C. Structural Organization of Full-Length CFTR

The overall three-dimensional arrangement of full-length CFTR was resolved in a series of recent atomic resolution structures obtained by cryo-electron microscopy (cryo-EM), two from zebrafish CFTR (273, 274) and one from the human protein (145). Although at present no functional information is available on zebrafish CFTR, which is only ~55% identical in sequence to the human protein, the structures of the two orthologs in their dephosphorylated apo-states are virtually identical (root mean square deviation ~1.9Å across the entire protein), suggesting that structural information obtained from the zebrafish ortholog is largely relevant to the human protein.

The global arrangement of the CFTR protein (**FIGURE 1E-F**) resembles that of other ABC exporters (46, 67, 212, 256), as had been predicted by extensive cross-linking studies (99, 159, 207). The membrane-spanning components are formed by the twelve transmembrane helices, six from TMD1 (**FIGURE 1E-F**, *light gray*) and six from TMD2 (**FIGURE 1E-F**, *dark gray*), which also extend deep into the cytosol. TMD/NBD interactions occur via four short coupling helices (CH1–4; **FIGURE 1E-F**, *magenta*) formed by intracellular loops 1 (CH1; aa. 168–174) and 2 (CH2; aa. 269–275) of TMD1 and the analogous intracellular loops 3 (CH3; aa. 961–966) and 4 (CH4; aa. 1062–1068) of TMD2. As for other ABC exporters, TMD1 and TMD2 do not form distinct, separate bundles of transmembrane helices but are closely intertwined with each other as well as with the NBDs. In particular, a unit formed by TM4/CH2/

TM5 reaches out from TMD1 and contacts NBD2 and in a similar fashion, TM10/CH4/TM11 extends from TMD2 toward NBD1 [domain swap (67)]. Thus, the full-length CFTR molecule can be seen to be formed by two structural halves [TM helices 1, 2, 3, 6 plus 10, and 11 with NBD1 and TM helices 7, 8, 9, 12 plus 4, and 5 with NBD2 (274), **FIGURE 1E**]. The coupling helices run roughly parallel with the plane of the membrane and fit into corresponding clefts on the NBD surfaces, forming ball-and-socket-like joints that are the transmission interfaces for communications between the NBDs and the TMDs. Because of deletion of a short helix from NBD1, the “socket” on the NBD1 surface that accepts CH4 is shallower than the NBD2 socket that accepts CH2 (compare sockets in **FIGURE 1B**), rendering the NBD1/CH4 interface more sensitive to deleterious effects of mutations. This explains the severe structural destabilization caused by deletion (or mutations) of phenylalanine 508 (**FIGURE 1B**, NBD1, *purple sticks*), which contributes a hydrophobic side chain to formation of the shallow NBD1 socket (273).

Experimentally observed conformations of ABC proteins fall into two major classes. First, in most structures solved in the absence of nucleotide (apo-structures), the TMDs adopt an inward-facing conformation in which the extracellular ends of the TM helices are tightly bundled, whereas their cytosolic extensions, including the coupling helices, are spread apart, and the NBDs are separated (8, 101, 212, 256). Among the many solved inward-facing structures of ABC proteins, the observed degree of separation between NBD interfaces is highly variable. In the structure of dephosphorylated apo-CFTR [both zebrafish (273) and human (145)], the NBD interface separation is relatively large (>17Å; **FIGURE 1E**). Second, in nucleotide-bound ABC-exporter structures solved under conditions that preclude ATP hydrolysis, the TMDs typically adopt an outward-facing orientation in which the cytosolic ends of the TM helices are tightly bundled, the coupling helices approach each other, and the NBDs are tightly dimerized. In such structures, a variable degree of separation is observed between the extracellular ends of the TM helices, ranging from widely splayed extracellular loops (67, 256) to more compact bundling (46). The structure of phosphorylated, ATP-bound zebrafish CFTR is in an outward-facing conformation (274) resembling the latter, tighter extracellular bundling arrangement, with the TM helices largely parallel to each other [**FIGURE 1F**; see also (52)].

In addition to these mostly expected general ABC protein characteristics, the recent CFTR structures revealed several unpredicted features. The NH₂-terminal ~60 residues, conserved throughout the ABCC subfamily and unique to it, form a “lasso motif” (**FIGURE 1E-F**, *red*). The lasso contains two α -helices, the first of which is partly inserted in the membrane, packed against TMD2. The second, amphi-

pathic helix, which runs parallel to the membrane and exposes a highly charged surface to the aqueous environment, has been implicated in both channel trafficking and gating regulation (166, 167). Further unique features of CFTR's TMDs are likely essential for its ion channel function. The pseudosymmetry of the TM helices is disrupted by a discontinuity of TM helix 8 [TM8 (51)], which makes two sharp breaks within the membrane (FIGURE 1F, right; TM8 external segment and helical breaks are highlighted in cyan), thereby displacing TM7 from its ABC-typical location (FIGURE 1F, right, pale green). As a consequence, the central ion pore is mostly lined by TM1 and 6 of TMD1, and by TM8 and 12 of TMD2, consistent with earlier accessibility studies (12, 85, 88, 188, 254, 255, 271). In ABC transporters, access to the substrate translocation pathway is gated at both ends: the external gate is open in the outward-facing TMD conformation, whereas the internal gate opens in the inward-facing state. In contrast, in the CFTR channel, the open pore provides a continuous aqueous transmembrane pathway permeable to anions. Given that the open CFTR pore corresponds to an outward-facing TMD conformation, an aqueous pathway must exist that bypasses the closed internal ABC transporter gate. Consistent with results of functional (76, 77) and modeling (52, 163) studies, in the corresponding CFTR structure (274), that pathway is formed by a lateral opening (FIGURE 1F, red arrow) between TM4 (FIGURE 1F, yellow) and 6 (FIGURE 1F, orange) that connects the cytosolic environment with the internal vestibule of the pore.

D. Structural Information on the R Domain

The entirely unique amino acid sequence of the R domain is a consequence of its evolutionary origin from an intronic DNA sequence (205). Although early circular dichroism (CD) spectra of an R domain peptide, based on the originally suggested domain boundaries (a.a. 595–831), reported some α -helical content to a degree influenced by phosphorylation and identified an NH₂-terminal subdomain with high sequence conservation among CFTR orthologs (residues 587–672) (72), the latter segment, in fact, largely belongs to NBD1. In contrast, CD spectra of an R domain peptide encompassing a.a. 708–831 predicted this domain to be largely unstructured (177), consistent with its origin from noncoding sequence. Nevertheless, biochemical pull-down assays and NMR studies with isolated peptides suggested that the R domain interacts with other parts of the channel in a phosphorylation-dependent manner (29, 36, 249). In the dephosphorylated closed apo-structures of both zebrafish (273) and human (145) CFTR, a large amorphous density corresponding to the R domain is seen wedged between the two CFTR halves, interacting with NBD1 and the cytosolic ends of the TM helices; in the dephosphorylated human structure, a part of the density that interacts with the TM helices can be modeled as an α -helix (FIGURE 1E, yellow surface plot) and likely corre-

sponds to the COOH-terminal end of the R domain (a.a. 825–843). Such an intercalated arrangement of the dephosphorylated R domain is sterically incompatible with NBD dimerization or with an outward-facing conformation of the TMDs. Indeed, in the phosphorylated, ATP-bound, outward-facing zebrafish CFTR structure (274) (FIGURE 1F), no density corresponding to the R domain is observed, indicating that this region does not adopt a common conformation in most of the analyzed particles but, instead, becomes disordered.

III. THE CFTR ANION PERMEATION PATHWAY

A. Structural Segments Lining the Pore

Long before the availability of high-resolution structural information, several of CFTR's helices had been probed for their contributions to the ion permeation pathway by use of the substituted cysteine accessibility method. Such studies identified TM helices 1 (85, 88, 254), 5 (271), 6 (11, 75, 88), 11 (78, 255), and 12 (17, 78, 188) as pore lining. The accessibility patterns were generally consistent with helical structures, with each third-to-fourth-substituted residue being accessible from the ion permeation pathway, and the patterns even predicted some symmetry break by suggesting that TM7 does not participate in forming the pore (255, 271). A lateral portal serving as the cytosolic entrance of the pore vestibule between the cytosolic extensions of TM4 and 6 was hypothesized (52, 163) and later experimentally confirmed. It is lined by a number of positively charged amino acid side chains that play a role in attracting cytoplasmic chloride ions to the inner mouth of the pore [(76, 77); some of the corresponding residues in zebrafish CFTR are highlighted as blue spheres in FIGURE 1F, right]. Except for the unanticipated helical break observed in TM8 (FIGURE 1F, right, cyan), the recent cryo-EM structures largely confirmed the predictions of these functional studies and revealed that the entire inner surface of the pore is lined by positively charged residues, as expected for an anion channel (273).

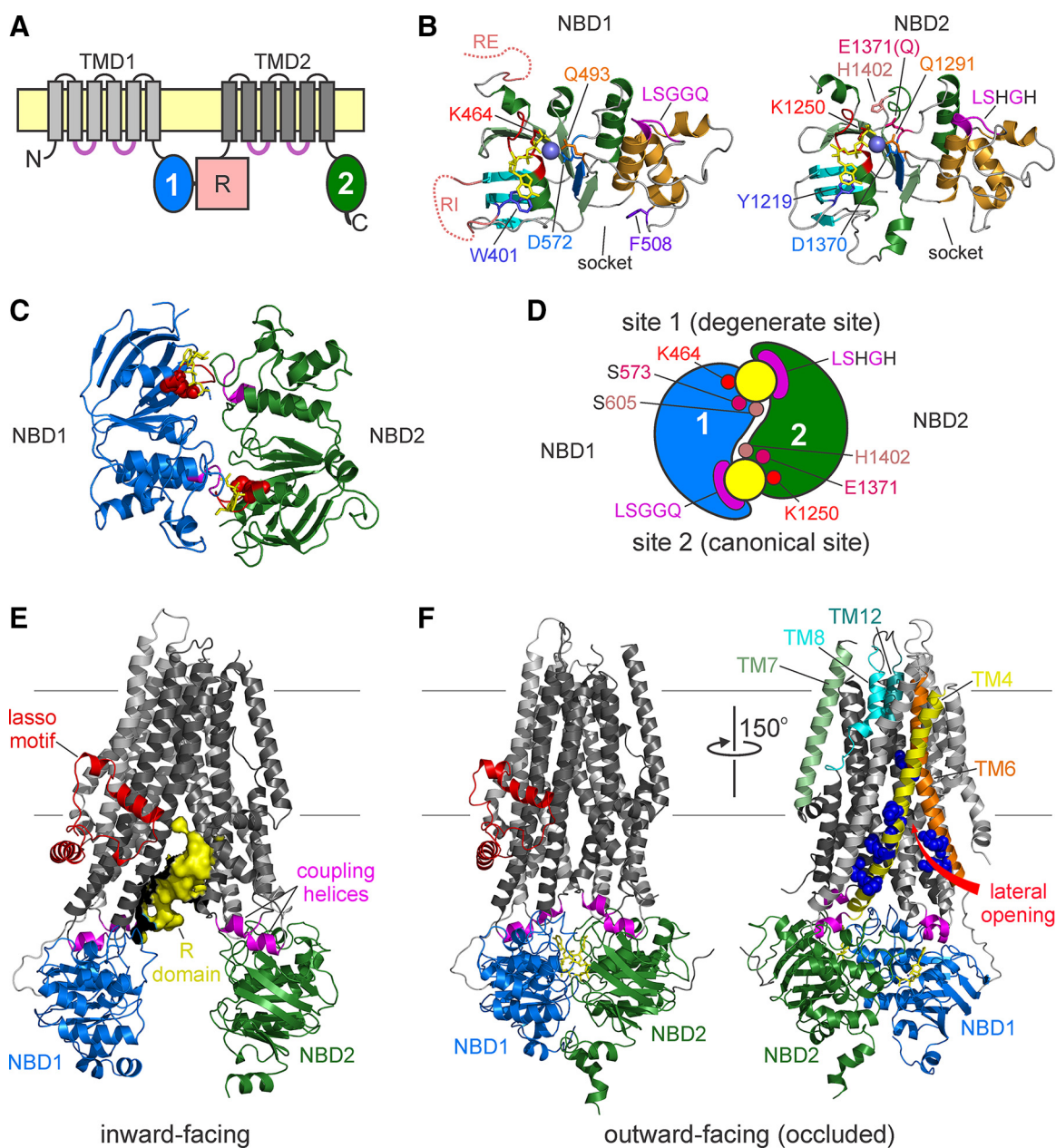
B. Location of the Channel Gate

A deep and wide intracellular (12, 141, 211, 221, 279), and a shallower extracellular (169, 218), vestibule predicted from the voltage dependence of pore block by various large organic anions suggested an asymmetric hourglass shape for the CFTR pore. This shape positioned the gate, corresponding to a narrow constriction in the permeation pathway [with a functional diameter of ~ 5.3 Å (106, 144) in the open conformation], close to the extracellular membrane surface, at the level of TM6 residues 338–341 (63, 75, 87). Consistent with a gate located at the extracellular end of the pore, binding of large organic anion pore blockers (59) or

ATP (219) in the intracellular vestibule does not prevent gate closure. In the inward-facing structures of zebrafish (273) and human [(145); **FIGURE 1E**], CFTR, the funnel-shaped intracellular vestibule, indeed tapers down to a narrow tunnel at the predicted location of the gate, consistent with those structures representing closed CFTR channels. Interestingly, however, in the outward-facing structure of phosphorylated ATP-bound zebrafish CFTR (274), although this gate constriction between TM6, TM1, and TM11 widens as expected, access to the pore from the extracellular space is nevertheless prevented by the extracellular segments of TM helices 8 and 12 (**FIGURE 1F, right, cyan and dark cyan**); this results from a local reorientation of these two secondary structure elements with respect to the rest of the half molecule. A structure of the CFTR pore in its fully conductive conformation remains to be captured.

C. Mechanism of Anion Selectivity

The CFTR pore shows high anion versus cation selectivity [the relative permeability of Na^+ compared with Cl^- ($p_{\text{Na}^+}/p_{\text{Cl}^-}$) is ~ 0.03 (226)] but poorly selects among anions. Experimentally obtained anion permeability sequences (which report relative ease of ion entry into the pore) are consistent with a lyotropic selection mechanism; relative permeability of a given anion is inversely proportional to its energy of dehydration (140, 157, 216). For instance, compared with chloride, large anions like SCN^- and nitrate, which more easily shed their hydration shell, display higher permeability through CFTR [e.g., $p_{\text{SCN}^-}/p_{\text{Cl}^-} > 2.4$ (140, 157)]. On the other hand, these high-permeability, large anions also typically bind very tightly within the pore, resulting in a low throughput rate operationally defined by measuring relative



conductance [e.g., the relative conductance for SCN^- compared with Cl^- ($g_{\text{SCN}}/g_{\text{Cl}}$) is <0.2 (135, 157)]. Thus, evolution seems to have optimized the CFTR pore to provide maximal conductance for the physiologically most relevant anion, chloride (135). Besides chloride, the other physiologically relevant ion that permeates through CFTR is bicarbonate. CFTR's relative permeability ($p_{\text{HCO}_3}/p_{\text{Cl}}$) and relative conductance ($g_{\text{HCO}_3}/g_{\text{Cl}}$) for bicarbonate are both ~ 0.25 (144, 184). Low permeability ratios were initially also found in isolated pancreatic ducts (91), and CFTR's role in bicarbonate secretion was thought to be indirect, mediated by regulation of $\text{Cl}^-/\text{HCO}_3^-$ exchangers of the SLC26A family [reviewed in (129)]. However, several studies have raised the possibility that direct HCO_3^- permeation through CFTR might become important, especially in some physiological conditions (108), and that CFTR anion permeability might be dynamically regulated (178, 198). Regardless of the exact mechanism, CFTR-dependent bicarbonate secretion clearly plays an important physiological role in controlling the pH of the fluid layers that line various epithelial surfaces (189, 202), including the lung (181, 210), as demonstrated by the correlations seen between levels of CFTR, bicarbonate fluxes, and strength of lung host defense defects (208).

The region responsible for CFTR's lyotropic selectivity (i.e., the region that provides sites of interaction for permeating anions) corresponds to the narrow region of the pore, as evidenced by changes in anion selectivity sequences upon mutation of residues F337, T338, S341, S1118, or T1134 (90, 135, 140, 157, 158, 275). In addition, the large number of positively charged residues that line the entire internal surface of the pore [in particular, residue K95 in the internal vestibule (137, 139)] or flank the cytoplasmic lateral opening [(76, 77); cf., **FIGURE 1F**, right, blue spheres] contribute to enhancing chloride conductance by attracting chloride ions to the pore (139). Thus, it has been suggested that the anion selectivity characteristics of CFTR might result from at least two distinct selectivity filters operating in series, interactions between permeant anions and the pore con-

striction around F337 being largely responsible for determining the selectivity of permeability, whereas anion/pore interactions in the inner vestibule and around the entrance of the lateral portal determine anion over cation selectivity and boost anion conductance (139). Some evidence suggests that overall high conductance and tight pore binding of CFTR might result from simultaneous, multiple interactions of permeating anions along the permeation pathway (138). Channel pores with multiple ion binding sites often show a nonlinear dependence of unitary conductance on the mole fractions of two types of permeant ion that are simultaneously present. In the case of CFTR, such anomalous mole fraction behavior has been reported for the anion pairs Cl^-/SCN^- (136, 139) and $\text{Cl}^-/\text{SO}_4^{2-}$ (60).

By stabilizing the open-pore structure, anion/pore interactions contribute to the energetic stability, and therefore the life time, of the open-channel state. Thus, anion replacement affects not only permeation properties, but also the kinetics of gating transitions: nitrate and bromide, which bind more tightly than chloride delay, whereas formate, which binds less tightly than chloride, accelerates pore closure (219, 266). These effects of tight-binding permeating ions to retard the closing of the CFTR gate might be analogous to the influence exerted by a substrate bound to an outward-facing exporter; extracellular release of the substrate favors closing of the extracellular gate, and thus restoration of the inward-facing conformation [see Section IVG; see also (266)].

D. Pore Blockers

Many large organic anions block the CFTR pore when applied from the intracellular side. The resulting brief closed events (flickery block) reflect the brief residence time of the blocker at its binding site in the pore. Pore block is more pronounced at hyperpolarized (more negative) membrane potentials that drive the negatively charged blocker into the

FIGURE 1. CFTR domain topology and structure. *A:* CFTR domain topology. TMD1 (light gray), TMD2 (dark gray), intracellular loops (light purple), NBD1 (blue), NBD2 (green), regulatory (R) domain (rose), and membrane (yellow). *B:* Ribbon representation of NBD1 (left) and NBD2 (right) from the cryo-electron microscopy (cryo-EM) structure of the phosphorylated, ATP-bound form of zebrafish CFTR (PDBID: 5W81). F1-like parallel β -sheet plus α -helices (green), ABC-specific antiparallel β -sheet (cyan), α -helical subdomain (orange), Walker A motif (red), Walker B motif (marine), signature motif (magenta), ATP (yellow sticks), and Mg^{2+} ion (slate sphere). The numbering of the conserved residues shown in stick representation is based on the human CFTR sequence. An E-Q mutation of the catalytic glutamate in NBD2 was used to trap the protein in an ATP-bound form. In NBD1, light magenta dotted lines mark the locations in the primary sequence of the unresolved regulatory insertion (RI) and regulatory extension (RE). *C:* Organization of the ATP-bound, head-to-tail NBD1/NBD2 heterodimer (from PDBID: 5W81). NBD1 (blue), NBD2 (green), ATP molecules (yellow sticks), Walker A motifs (red), and signature sequences (magenta). The conserved Walker A lysines are shown as red spheres. *D:* Cartoon representation of residue asymmetry in the CFTR NBD dimer; color coding of conserved residues as in *B*. The upper site (site 1, degenerate site) harbours all noncanonical substitutions, whereas in the lower site (site 2, canonical site), all catalytically important side chains are intact. *E:* Ribbon representation of the dephosphorylated human CFTR apo-structure (PDBID: 5UAK); domain color coding as in *A*. Lasso motif (red), R domain helix modeled into observed density (yellow surface), coupling helices (magenta), ATP (yellow sticks), and membrane (horizontal gray lines). *F:* Ribbon representations of the structure of phosphorylated, ATP-bound CFTR (PDBID: 5W81) viewed from two different orientations; left view and domain color coding as in *E*. The view to the right shows the cytoplasmic opening of the ion permeation pathway (red arrow, lateral opening) flanked by transmembrane (TM) helices 4 (yellow) and 6 (orange); positively charged residues lining the opening are shown as blue spheres. Outer segments of TM8 and TM12 are colored (cyan and deep cyan); TM7 is pale green; the lasso motif has been removed for clarity.

intracellular pore vestibule but is alleviated at depolarized (more positive) membrane potentials. The steepness of this voltage dependence allows estimation of how deep the blocker binding site is [i.e., what fraction of the membrane electrical field the blocker traverses before reaching its binding site (θ)]. Similar voltage dependences suggest a common binding site for a structurally diverse group of blockers including diphenylamine-2-carboxylate, flufenamic acid [$\theta = \sim 0.41$ for both (156)], glibenclamide [$\theta = \sim 0.45\text{--}0.48$ (211, 279)], 5-nitro-2-(3-phenylpropylamino)benzoate (NPPB) [$\theta = \sim 0.5$ (59)], 3-(*N*-morpholino)propanesulfonic acid (MOPS) [$\theta = \sim 0.5$ (59, 109)], and anthracene-9-carboxylic acid [$\theta = \sim 0.5$ (1)]. In line with the notion of a common binding site, glibenclamide and isethionate (279), or NPPB and MOPS (60), were shown to compete for pore block. Mutagenesis studies highlighted how the positively charged side chain of the pore-lining residue K95 plays an important role in interacting not only with permeant anions, but also with blockers (137). In the atomic structure of human CFTR, K95 is located at a position where the intracellular vestibule tapers down to the narrow tunnel believed to comprise the gate (145). Of note, an intrahelical salt bridge between the side chains of K95 and E92 was recently noted in the cryo-EM structure of human CFTR and proposed to play a role in anion/pore and blocker/pore interactions (104). Consistent with the binding site for diverse blockers being located intracellular to the channel gate, the presence of NPPB or MOPS in the pore does not delay gate closure (59). More modest voltage dependences reported for block by the disulfonic stilbenes 4,4'-diisothiocyanostilbene-2,2'-disulfonic acid and 4,4'-dinitrostilbene-2,2'-disulfonic acid [$\theta = \sim 0.16$ and $\theta = \sim 0.34$, respectively (141)] suggest that a more superficial blocker binding site might also exist.

Whereas the above compounds block from the cytosolic side and show low affinity for the CFTR pore (K_d in the hundreds of micromolar to millimolar range at 0 mV membrane potential), high-throughput screening has led to the discovery of a higher-affinity pore blocker that acts from the extracellular side; *N*-(2-naphthalenyl)-[(3,5-dibromo-2,4-dihydroxyphenyl)methylene]glycine hydrazide (GlyH-101) blocks CFTR currents with a K_d of $\sim 4 \mu\text{M}$ at 0 mV membrane potential and shows the inverse voltage dependence expected for an anionic blocker that binds in the extracellular vestibule (164). The electrical distance of the GlyH-101 binding site ($\theta = 0.35$) and strong reductions in apparent affinity by mutation R334C (62) or upon covalent modification of a cysteine engineered into position 338 (169) suggest that GlyH-101 binds at the bottom of the shallow extracellular vestibule, just above the constriction that forms the channel gate (169).

E. Intraburst (Flickery) Closures

Under all experimental conditions, gating of single CFTR channels shows clear bursting behavior; groups of open

events interrupted by brief ($\sim 1\text{--}3$ ms at 37°C and ~ 10 ms at 25°C) flickery closed events form bursts that are separated from each other by long ($\sim 0.1\text{--}0.2$ s at 37°C and $\sim 0.4\text{--}2$ s at 25°C) interburst closed events. Some of the brief intraburst closures represent block by large cytosolic anions (278) or by anionic buffer molecules present in the recording solution that bathes the cytosolic membrane surface (109); indeed, even cytosolic ATP causes low-affinity pore block (219). But not all intraburst closures may be accounted for by such a mechanism, because flickery closures can be observed for locked/open channels long after ATP has been washed away, even in a cytosolic solution buffered with a cationic buffer (279), and also when channel currents are studied at positive voltages (243), which deter cytosolic anion entry. Thus, at least a fraction of the observed flickery closures must represent a gating mechanism intrinsic to the channel protein.

Several studies have addressed the dependence of intraburst gating kinetics on a variety of factors, including voltage, pH, or the concentration of ATP used for channel activation. Both the frequency and the duration of flickery closures increases at positive membrane potentials, reporting a weak voltage dependence of intraburst gating (30). Acidification of the bath solution to pH = 6.3 prolongs the average duration of flickers by approximately twofold (40). In contrast, neither the frequency nor the duration of intraburst closures is sensitive to the concentration of applied ATP (243, 261). Finally, mean flickery closed time is prolonged by catalytic site mutations that disrupt ATP hydrolysis (243) because of the appearance of a second population of intraburst closed events with an average life time of $\sim 50\text{--}100$ ms (25, 61). As a result, intraburst closures lasting up to several hundred milliseconds may be observed during long locked/open bursts and have been dubbed “gating” in some reports (172). Although temperature dependence of intraburst kinetics has not yet been addressed systematically, comparison of studies conducted at room temperature ($20\text{--}25^\circ\text{C}$) and those obtained at 37°C suggests approximately three- to fivefold briefer flickers at the higher temperature [e.g., (243) versus (30)].

Two alternative kinetic mechanisms, $C_{\text{slow}} \leftrightarrow C_{\text{fast}} \leftrightarrow O$ and $C_{\text{slow}} \leftrightarrow O \leftrightarrow C_{\text{fast}}$, with C_{slow} and C_{fast} denoting the interburst and intraburst closed states, respectively, have been used to model CFTR bursting behavior. Because these two schemes cannot be distinguished by steady-state recordings, all data available to date may be explained equally well by either scheme. In such situations, it is customary to prefer the scheme which requires adjustment of the smaller number of parameters to describe two data sets obtained under two different experimental conditions. However, even that “parsimony argument” has been of no help so far as for either model, only one rate was found to be sensitive to ATP

concentration (243, 261), but several to both voltage (30) and intracellular pH (40).

The physical mechanism underlying flickery closures is still elusive. The slow and fast gates that cause inter- and intraburst closures, respectively, may or may not be formed by two physically distinct protein regions. But slow and fast gating certainly reflect two distinct types of TMD conformational change; slow gating (i.e., entering and exiting a burst) likely represents flipping between TMD conformations that are analogous to inward- and outward-facing conformations of ABC exporters, respectively (146, 242), whereas fast gating (i.e., intraburst flickering) is likely caused by a smaller-scale, more localized conformational change. One possibility is that the outward-facing occluded structure seen for phosphorylated zebrafish CFTR (274), in which the pathway is blocked by a local distortion of the outer segments of TM helices 8 and 12, represents the flickery closed state. As described above, in that conformation, the gate constriction is widened, but the external extremity of the ion conduction pathway is blocked by a localized conformational change of the outer-leaflet segments of TM helices 8 and 12 (FIGURE 1F, right, cyan and dark cyan). However, given that the (human) CFTR channel dwells in the flickery closed state only for a small fraction of the total duration of a burst, capturing this conformation in a cryo-EM structure is unlikely, unless it is stabilized by some factor specific to the cryo-EM conditions (e.g., species difference or low temperature). Thus, an alternative interpretation of the outward-facing occluded zebrafish CFTR structure is that it represents an intraburst closed state with a high occupancy probability but a lifetime too short ($\sim 1 \mu\text{s}$) to be resolved in limited-bandwidth electrophysiological recordings; in that case, the experimentally measured unitary conductance of 7–10 pS would reflect the full conductance multiplied by the fraction of time the pore is truly open within a burst (274). Molecular dynamics simulations, encompassing 1.5 μs , highlight the relative stability of the outward-occluded conformation seen in the ATP-bound zebrafish structure (51), disfavoring the latter scenario. Thus it remains possible that for both interburst and conventional flickery closures, the ion conduction pathway is interrupted by a similar conformation of the narrow constriction between TM helices 1, 6, 8, and 12 observed at the height of TM6 residues 338–341 [the gate (273)].

IV. REGULATION OF CFTR GATING THROUGH NUCLEOTIDE INTERACTIONS AT THE NBDs

Because phosphorylation and ATP regulate slow gating, in the following sections, channel “opening” and “closing” will be used synonymously with entering and exiting a burst.

A. ATP Hydrolysis at One of Two Nonequivalent Composite ATP Binding Sites

The catalytic turnover rate of CFTR ATPase activity ($0.5\text{--}1 \text{ s}^{-1}$), estimated for phosphorylated human CFTR protein purified to homogeneity (131, 145), falls into the range of channel gating (bursting) rates. An early hint that ATPase activity might be coupled to pore gating was provided by the observation that lowering free Mg^{2+} to 4 nM, or adding Na-azide, inhibited both processes (131). The catalytic activity of the CFTR protein must originate from composite site 2 of the NBDs, because mutation of the Walker A lysine in site 2, but not that in site 1, abolishes ATPase activity (192). Indeed, photocrosslinking experiments revealed that site 1 retains ATP bound and unhydrolyzed for up to tens of minutes (7, 14). The presence of canonical consensus motifs in site 2, but noncanonical residues in site 1 (FIGURE 1D), readily explains such functional asymmetry between CFTR’s two composite ATP binding sites and is likely a shared feature of asymmetric ABC proteins (102, 186, 235) [including the entire human ABCC subfamily as well as many heterodimeric prokaryotic homologs (187)].

B. Coupling of Pore Opening/Closure to Formation/Disruption of a Head-to-Tail NBD Heterodimer

Decades of experimental work gathering information on both CFTR and related ABC proteins have clarified the basic mechanism by which ATP binding and hydrolysis at the NBDs drives pore gating in CFTR. Early studies demonstrated that preventing (or attenuating) ATP hydrolysis in site 2 by mutations of the Walker A lysine (K1250A/G/M/T) or the catalytic glutamate (E1371Q/S) in NBD2 (FIGURE 1B, right; FIGURE 1D) locks channels in the open bursting state (32, 96, 242, 243) for time intervals at least two orders of magnitude longer than the mean burst duration of WT CFTR. These results clearly demonstrated that site 2 ATP hydrolysis is required for normal (fast) termination of a burst. Mixtures of ATP either with nonhydrolyzable ATP analogs, such as 5'-adenylyl-imidodiphosphate (AMPPNP) or adenosine 5'-(gamma-thiotriphosphate) (ATP γ S), or with pyrophosphate (PP_i) also lock channels open (95, 103), suggesting that these analogs prevent closure by binding at site 2. A similar lock-open effect of mixtures of ATP with the inorganic phosphate (P_i) analog orthovanadate (V_i) is believed to reflect formation of a stable $\text{ADP}\cdot\text{V}_i$ complex that resembles the pentacovalent transition state of the ATP hydrolysis reaction in site 2 (15, 95). Formation of such complexes by the hydrolysis product ADP and a P_i analog that binds tightly in place of the released P_i has been observed in atomic structures of ABC proteins (174).

Contrary to early conclusions obtained mostly on single CFTR channels (9, 103, 203), nonhydrolyzable ATP ana-

logs, such as AMPPNP, ATP γ S, β,γ -methyleneadenosine 5'-triphosphate (AMPPCP) (4, 243), or PP_i (234), alone are capable of opening CFTR channels, although the nucleotide analogs are poor substitutes for ATP, supporting a maximal opening rate only ~5% of that observed in saturating ATP (243). Although the hydrolysis-abolishing K1250A mutation was found to reduce not only closing, but also channel opening rate (32, 192), the latter effect was later shown to be largely due to a reduced ATP binding affinity in site 2 (243). Indeed, another site 2 mutation expected to disrupt hydrolysis, E1371S, does not impair channel opening (243). Thus, pore opening requires nucleotide binding, but, in contrast to channel closure, not hydrolysis.

By what mechanism is ATP binding at the NBDs translated into pore opening? The hyperbolic dependence of channel opening rate (i.e., the rate of entering a burst) on ATP concentration [$K_{1/2} = \sim 50 \mu\text{M}$ (55, 241, 243, 270)] indicates a rate-limiting step for pore opening other than ATP binding. That step is Mg²⁺ dependent (71, 131) and must follow ATP binding because its rate is sensitive to nucleotide structure; maximal opening rates supported by 8-azido-ATP (14) or AMPPNP (243) are much lower than that observed in ATP. Furthermore, ATP binding must have happened at least at the NBD2 head before the pore opens, because mutations of the Walker A lysine (K1250A, *red*), the Walker B aspartate (D1370N, *marine*), or the stacking aromatic residue (Y1219G, *blue*) in NBD2 (**FIGURE 1B, right**), all of which destabilize ATP binding there, dramatically reduce the apparent affinity for ATP to open the pore (243, 281). In contrast, prior ATP binding to the NBD1 head (**FIGURE 1B, left**) seems less essential for channel opening as the apparent potency of ATP in opening the pore is decreased by some mutations that impair ATP binding [K464A, removal of the Walker A lysine side chain, *red* (243)], but not by others [W401G, removal of the stacking aromatic side chain (281)]. The observation of tight NBD dimers in ABC proteins in the presence of ATP and the suggestion that NBD dimer formation/dissociation might underlie the coupling of ATPase cycles to vectorial transport of substrates by ABC transporters (162) prompted the proposal that CFTR and transporters might share a common mechanism. Thus, in CFTR, the rate-limiting step for pore opening (to a burst) would reflect formation of a tight head-to-tail NBD1/NBD2 heterodimer, whereas closure (from a burst) would occur upon disruption of that heterodimer [**FIGURE 2E** (243)].

A first formal proof of that hypothesis was provided by the demonstration that two residues on opposing surfaces of composite site 2 (arginine 555 just downstream of the NBD1 signature sequence and threonine 1246 in the NBD2 Walker A motif) become energetically coupled upon channel opening, but not upon binding of ATP (which occurs on closed channels, see above) (242). For steric reasons, a hydrogen bond observed between the side chains of the cor-

responding residues in dimeric ABC NBD structures (38, 215) is expected to form either between an arginine/threonine (R/T) pair, as found in the sequence of CFTR and a subset of ABC proteins, or between a lysine/asparagine (K/N) pair, as present in a smaller subset of the ABC superfamily (**FIGURE 2A**), but not between R/N or K/T pairs (which are poorly represented in naturally occurring ABC sequences). A large reduction in channel opening rate (i.e., an increase in interburst duration, τ_{ib}) observed when introducing the R555K or T1246N mutations in the WT CFTR background (**FIGURE 2C, blue and red bars versus black bar**) was not seen when introducing the same mutations into a background already mutated at the other position (**FIGURE 2C, purple bar versus blue or red bar**). This suggests that formation of the R555/T1246 hydrogen bond in WT CFTR facilitates channel opening and that the hydrogen bond is disrupted in each single mutant but restored in the double mutant. These mutation-induced changes in opening rate report mutational effects on the stability of the transition state for opening (T^\ddagger) relative to the closed state ($\Delta\Delta G_{T-C}^\ddagger$; numbers next to arrows in **FIGURE 2D**). The R555K mutation destabilizes the transition state when a threonine is present at position 1246 (**FIGURE 2D, left vertical arrow**) but stabilizes it when the residue at position 1246 is an asparagine (**FIGURE 2D, right vertical arrow**). The difference between $\Delta\Delta G_{T-C}^\ddagger$ values along two parallel sides of the mutant cycle quantifies the change in interaction energy between the native side chains upon entering the transition state from the closed state [$\Delta\Delta G_{\text{int}(\text{opening})}$], and is of a magnitude and sign consistent with formation of a hydrogen bond. A similar mutant cycle built on the closed/open equilibrium constant of a hydrolysis deficient mutant, in which gating is reduced to reversible $C_1 \leftrightarrow O_1$ transitions, confirmed the presence of the R555/T1246 hydrogen bond also in the open ground state (242). Chemical cross-linking experiments (159) later confirmed the canonical head-to-tail NBD dimer arrangement seen in all dimeric ABC NBD structures (**FIGURE 1C-D**) to be present in full-length, gating CFTR channels in their native environment.

Thus, the rate-limiting step for channel opening (**FIGURE 2E, step $C_1 \rightarrow O_1$**) consists of tight dimerization of ATP-bound NBDs coupled to TMD rearrangements that open up a transmembrane pathway for anions. Demonstration of salt bridge formation between cytosolic TMD loops in the open state (252), but between extracellular TMD loops in the closed state (64, 107), as well as a proposed narrowing of the intracellular vestibule in open channels (12) all suggested that upon pore opening, CFTR's TMDs undergo a conformational change similar to the flipping of ABC transporter TMDs from an inward- to an outward-facing conformation. All these predictions, based on functional studies, were largely confirmed by the recent cryo-EM structures of dephosphorylated apo- and phosphorylated ATP-bound CFTR [**FIGURE 1E-F** (145, 273, 274)].

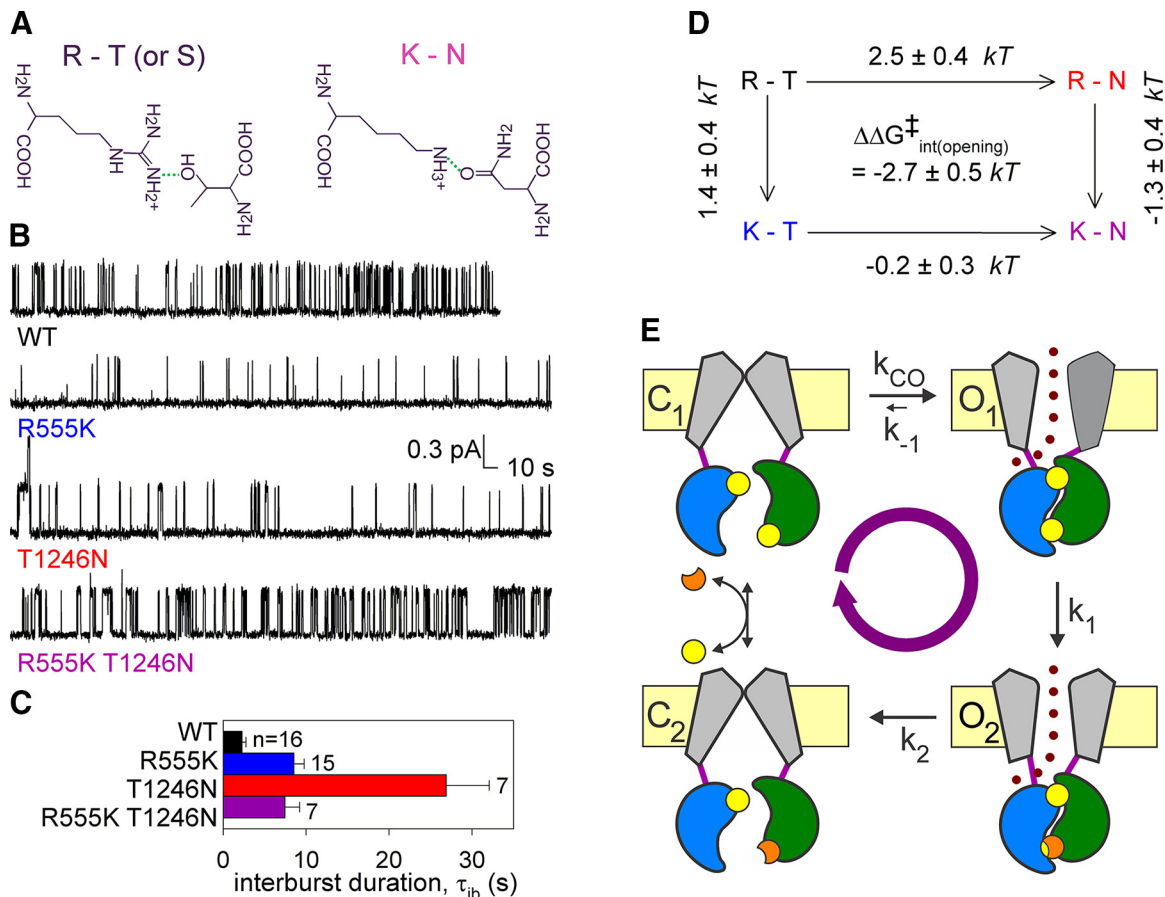


FIGURE 2. Coupling of CFTR pore opening to NBD dimerization. *A*: An arginine/threonine (serine) or a lysine/asparagine side chain pair is optimally positioned to form a salt bridge between CFTR positions 555 and 1246. *B* and *C*: Single-channel outward current traces (*B*: $V_m = +40 \text{ mV}$) and mean closed (interburst) durations (*C*) of prephosphorylated WT, R555K, T1246N, and R555K/T1246N CFTR channels gating in 5 mM Mg-ATP. *D*: Thermodynamic mutant cycle illustrating mutation-induced changes in $\Delta G_{\text{T-C}}^{\ddagger}$ (numbers next to arrows); $\Delta\Delta G_{\text{int(opening)}}^{\ddagger}$ is the difference between $\Delta\Delta G_{\text{T-C}}^{\ddagger}$ values along two parallel sides of the cycle. The four corners of the cycle are represented by the pairs of residues present at positions 555 and 1246, respectively. *E*: Cartoon gating cycle of phosphorylated CFTR. Color coding as in **FIGURE 1A**; the R domain is not depicted. Site 1 (degenerate site), *upper site*; site 2 (canonical site), *lower site*; ATP, yellow circles; ADP, orange crescent; chloride ions, dark red dots. [*A–D* adapted with permission from Vergani et al. [242]].

C. Thermodynamics and Timing of the Pore-Opening Transition

Among the steps that a phosphorylated WT CFTR channel follows around its gating cycle (**FIGURE 2E**), the pore-opening transition (**FIGURE 2E**, step $C_1 \rightarrow O_1$) is the slowest ($\sim 0.5\text{--}2 \text{ s}^{-1}$ at 25°C and $\sim 5\text{--}8 \text{ s}^{-1}$ at 37°C), reflecting a high energetic barrier characterized by an unstable, high-free-energy transition state. The most common CF mutation, deletion of phenylalanine 508, further slows this step by >40 -fold (125, 161). What is the nature of this transition state, and what causes its high free energy? The steep temperature dependence of WT CFTR opening rate signifies a large activation enthalpy [$\Delta H_{\text{T-C}}^{\ddagger} = \sim 100\text{--}150 \text{ kJ/mol}$ (6, 57, 155)], suggesting molecular strain. On the other hand, the discrepancy between $\Delta G_{\text{T-C}}^{\ddagger}$ and $\Delta H_{\text{T-C}}^{\ddagger}$ signals a large entropy increase in the transition state [$T\Delta S_{\text{T-C}}^{\ddagger} \geq 40 \text{ kJ/mol}$ (57)]. Given that the NBD interface is already tightened

around ATP site 2 in the transition state [**FIGURE 2A–D** (242)], the large activation entropy has been interpreted to reflect the dispersal of the layers of ordered water molecules that cover the interfacial NBD surfaces when the NBDs are separated and the interface is open and accessible to solvent (57).

The relative timing of motions in different regions of a channel protein during the submicrosecond process of pore opening (transition from state C to O) can be determined by studying the kinetic consequences of structural perturbations, typically point mutations, introduced into various protein regions. If the perturbation-induced change in the transition-state free energy linearly interpolates the difference, $\Delta\Delta G^{\ddagger}$, between the free energy changes of the C and O ground states ($\Delta\Delta G^{\ddagger} = \Delta G_{\text{O}}^{\ddagger} - \Delta G_{\text{C}}^{\ddagger}$) (94, 153), then the free energy of the transition state for opening, T^{\ddagger} , will change by $\Phi\Delta\Delta G^{\ddagger}$ ($0 \leq \Phi \leq 1$). A larger Φ value indicates

earlier, and a smaller Φ value later, movement of the target position during pore opening. In particular, $\Phi = \sim 1$ indicates that, in the transition state, the target position is already near its open-state conformation, whereas $\Phi = \sim 0$ suggests it has not yet moved much from its closed conformation (10, 277). Because the perturbation will change the logarithm of the opening rate constant (k_{CO}) by $-\Phi\Delta\Delta G^\circ$ (RT), but the logarithm of the equilibrium constant (K_{eq}) by $-\Delta\Delta G^\circ$ (RT), Φ can be estimated from the slope of a rate-equilibrium free energy relationship (REFER) plot of $\log k_{CO}$ versus $\log K_{eq}$ for a series of mutations at the target position. Importantly, because the REFER approach assumes equilibrium gating, with opening and closure reflecting reversible transitions along a single kinetic pathway (53), this approach cannot be applied to address the dynamics of the ATP-dependent slow-gating process of WT CFTR channels (5, 204), which obey a nonequilibrium cyclic gating mechanism (FIGURE 2E). However, the technique may be adapted to studying the pore-opening step (FIGURE 2E, step $C_1 \rightarrow O_1$) by employing a background mutation that disrupts ATP hydrolysis in site 2, thereby reducing gating to reversible $C_1 \leftrightarrow O_1$ transitions. REFER analysis in such a nonhydrolytic background (NBD2 Walker B aspartate mutant D1370N) revealed a clear spatial Φ -value gradient along the protein's longitudinal axis from cytoplasm to cell exterior (219, 220); Φ was close to ~ 1 for both faces of composite ATP site 2 (positions 555 and 1246; FIGURE 3A, left, red spacefill; FIGURE 3A, right, red numbers) and ~ 0.5 – 0.6 for positions in each of the four coupling helices (positions 172, 275, 961, and 1068, respectively; FIGURE 3A, purple spacefill and numbers), but ~ 0.2 for the centrally located pore residue M348 in TM6 and ~ 0 for position 117 in the first extracellular loop (FIGURE 3A, blue spacefill and numbers). This clear Φ -value gradient suggests that a spreading conformational wave is initiated at the site 2 NBD interface and propagates toward the pore (FIGURE 3B, vertical colored arrow). In particular, it suggests that in the transition state the site 2 interface is already tightly dimerized, but the pore is still closed (FIGURE 3B, center). Thus, the high enthalpy of the opening transition state ($\Delta H_{T-C}^\ddagger = \sim 100$ – 150 kJ/mol) might reflect strain at the NBD/TMD interface [(219); cf., (57)], which includes the disease hotspot position 508. Indeed, a Φ value of ~ 0.5 for position 508 suggests that this NBD position moves synchronously with nearby TMD-coupling helix 4 (220). Interestingly, a low-intermediate Φ value of ~ 0.4 was found for both faces of degenerate site 1 (positions 460 and 1348; FIGURE 3A, orange spacefill and numbers), reporting delayed movement here with respect to site 2 and suggesting that site 1 residues are still on the move in the transition state for channel opening. However, because such pronounced asymmetry cannot be detected at the level of the four coupling helices, it seems likely that the movements completed in site 1 between the transition state and the open state are localized movements confined to the site 1 NBD interface (220).

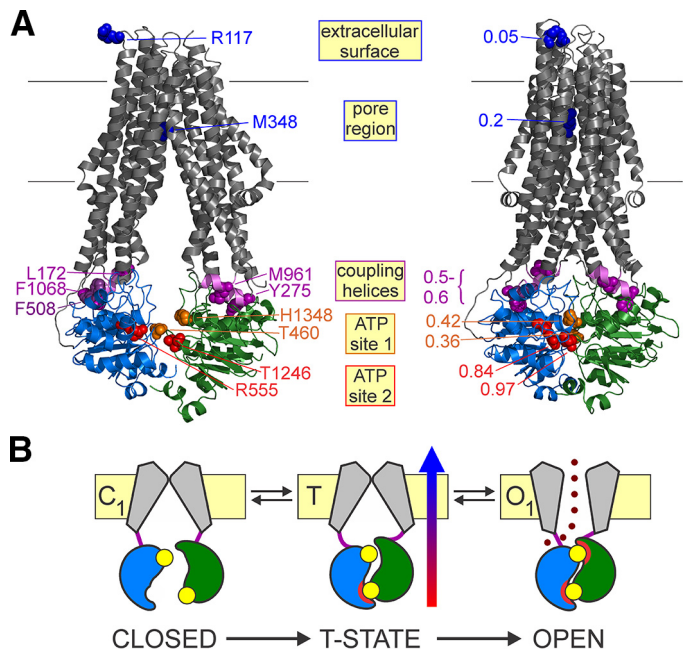


FIGURE 3. Cytosolic to extracellular Φ -value gradient and asymmetry between sites 1 and 2. **A:** Cartoon representation of homology models (52) of phosphorylated closed- (left) and open-state (right) CFTR, with color coding as in FIGURE 1A; the regulatory (R) domain is omitted. Target positions for rate-equilibrium free energy relationship (REFER) analysis are highlighted in colored spacefill (left), corresponding colored numbers illustrate estimated Φ values (right). **B:** Cartoon representation of approximate structural rearrangements during the pore opening transition as the channel transits from an ATP-bound closed state (C_1) through the transition state (T) to the ATP-bound open state (O_1). Site 1 (degenerate site), upper site; site 2 (canonical site), lower site; color coding as in FIGURE 2E. Vertical colored arrow illustrates the direction of the spreading conformational wave. Red arcs in states T and O_1 represent tight bonding across the NBD interface. [Adapted with permission from Sorum et al. (219) and Sorum et al. (220)].

D. Strictness of Coupling Between Pore-Opening Events and NBD Dimerization

Strict coupling between NBD dimerization and pore opening in CFTR has been called into question because a construct lacking NBD2 (Δ NBD2, truncated after residue 1197) displays low-probability, ATP-independent openings following phosphorylation by PKA (65, 248). Based on that observation, spontaneous openings in the absence of ATP, also seen occasionally in WT CFTR (25, 224) but robustly promoted by mutations at TMD positions 978 [ICL3 (253)] or 355 [TM6 (257)], were interpreted as reflecting pore openings in the absence of NBD dimerization. Furthermore, a resemblance was noted between CFTR and classical ligand-gated channels, such as the nicotinic acetylcholine receptor, in that phosphorylation (248), TMD mutations (253, 257), various drugs (112, 248), and ATP analogs (172) all had strongly correlated effects on spontaneous (ATP-independent) and ATP-dependent channel activity, and the effects of such allosteric modulators were energetically additive (172, 257). These analogies led to CFTR

gating being modeled as an equilibrium loop mechanism in which the ligand (ATP) can bind and unbind in both the closed-pore and the open-pore conformation, and closed/open (isomerization) transitions can occur whether or not ligand is bound. In that model, because of the thermodynamic principle of detailed balance, which constrains the product of the equilibrium constants around a kinetic cycle to be unity, higher affinity binding of the ligand in the open-channel conformation would shift the closed/open equilibrium of liganded channels toward the open state [(120); cf., (92)]. An essential feature of such an allosteric loop model [also key to the proposed reentry mechanism (113) discussed in Section IVE, below] is the postulate that in the ATP-free, spontaneous open state, the NBDs are disengaged, and the dimer interface is therefore accessible for ATP binding. Studying the accessibility of site 2 in ATP-free open channels is not straightforward, but this question was recently addressed by exploiting the enhanced spontaneous activity of the K978C/P355A double mutant, which allows quantitation of spontaneous gating parameters in micro-

scopic patches (160). In K978C/P355A channels gating in the absence of ATP, just as in WT channels gating in the presence of ATP (242) (Section IVB), energetic coupling between site 2 residues R555 (NBD1 face) and T1246 (NBD2 face) was found to change in a state-dependent manner; spontaneous open probability of the background construct is reduced by both the R555K and the T1246N single mutation, but restored in the double mutant (FIGURE 4A–B), reporting energetic coupling between these residues in the open state (FIGURE 4C). Thus, the two side chains on opposing faces of composite site 2 form a hydrogen bond in the open-pore conformation, but not in the closed-pore conformation, indicating the presence of a tightly dimerized site 2 NBD interface in the spontaneous open-channel state (FIGURE 4D), just as during normal, ATP-dependent openings (FIGURE 2E). Because a tightly dimerized NBD interface does not allow ATP binding/unbinding in the open-pore conformation, CFTR gating must be driven by principles fundamentally different from the allosteric mechanisms that underlie gating of ligand-gated channels. Thus, strict

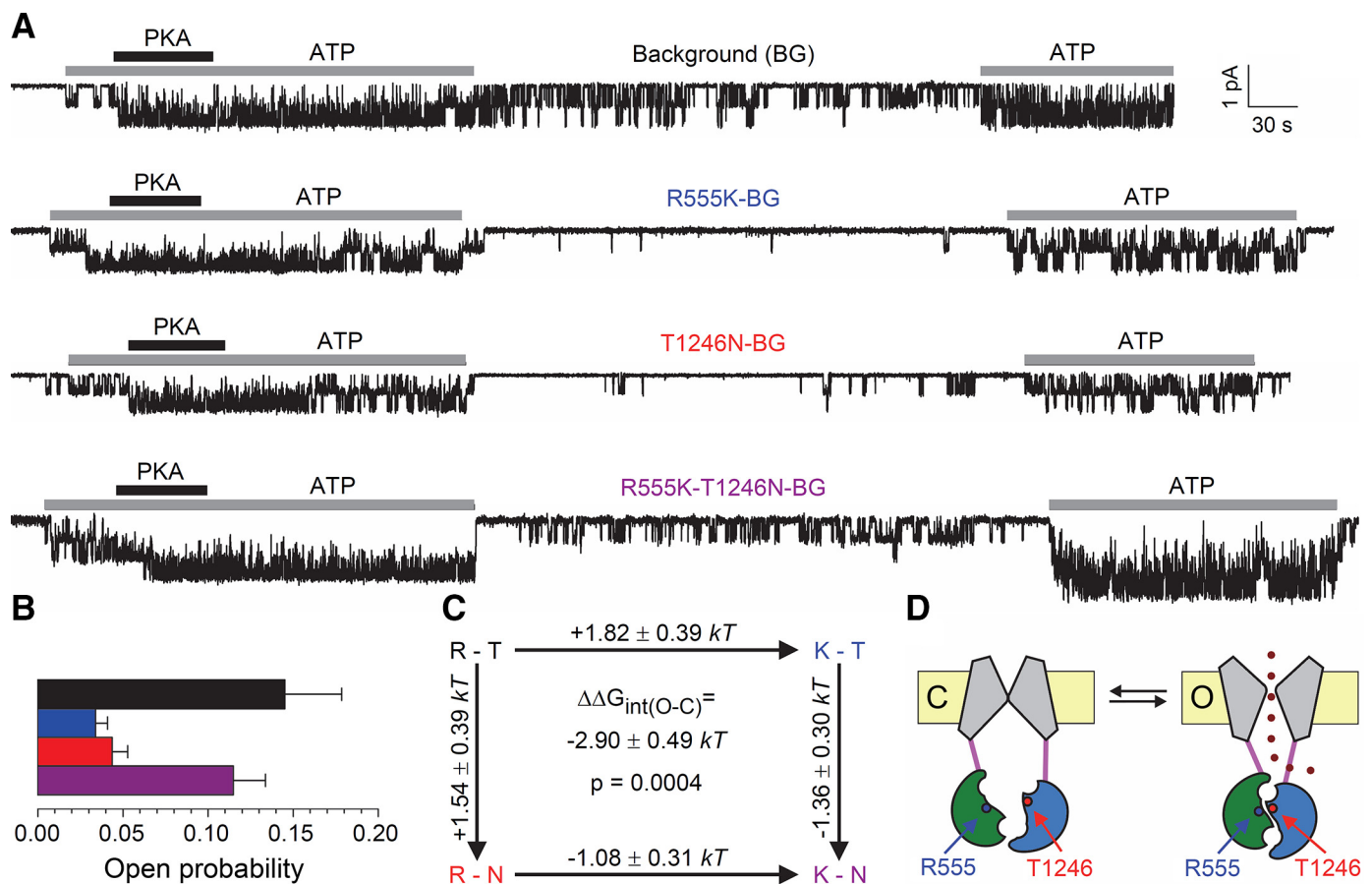


FIGURE 4. Spontaneous pore openings are also coupled to NBD dimerization. *A*: Microscopic inside-out patch recordings of CFTR background construct P355A/K978C and of channels bearing mutations R555K, T1246N, and R555K/T1246N in that background; $V_m = -80$ mV. *B*: Open probabilities of the constructs in *A* (see color coding) during the last 4 min of each 5-min ATP-free segment of recording. *C*: Thermodynamic mutant cycle illustrating mutation-induced changes in ΔG_{O-C} (numbers next to arrows); $\Delta\Delta G_{int(O-C)}$ is the difference between $\Delta\Delta G_{O-C}$ values along two parallel sides of the cycle. The four corners of the cycle are represented by the pairs of residues present at positions 555 and 1246, respectively. *D*: Cartoon depicting mechanism of spontaneous openings. Color coding as in FIGURE 1A; the R domain is not depicted. [Adapted with permission from Mihályi et al. (160)].

coupling between slow gating and NBD dimerization/dissociation seems to be an intrinsic property of the CFTR protein; ATP binding alters the energetics, but not the basic structural organization, of the open- and closed-pore conformations. The similar structural architecture of ATP-free and ATP-bound open states also readily explains correlated and additive effects on spontaneous and ATP-driven channel activity of the various allosteric modulators mentioned above [R domain phosphorylation, TMD mutations, or drug binding to TMDs (253)] through energetic stabilization or destabilization of the inherent open-state structure. A similarity between ATP-free and ATP-bound open channel structures is also consistent with inhibition of opening of disease mutant G551D CFTR by ATP binding at site 2, interpreted to reflect electrostatic repulsion between the negative charge of the aspartate in the site 2 signature sequence and that of the γ -phosphate of ATP bound to the site 2 Walker motifs (133). Because electrostatic interactions are very short range in water, such an interaction would not be expected to occur if the site 2 interfacial NBD surfaces did not approach each other and become dehydrated (i.e., if the dimer interface did not close) in the G551D mutant upon pore opening, but it is plausible if pore openings remain strictly coupled to NBD dimerization. Indeed, the aspartate side chain in position 551 does not sterically interfere with closure of the dimer interface, because introduction of large uncharged (serine) or positive (lysine) side chains are tolerated here (133). Although infrequent ATP-independent pore openings of Δ NBD2 CFTR (248) can clearly not be linked to NBD dimerization, it seems likely that upon pore opening, its remaining NBD/TMD coupling machinery undergoes movements similar to those that accompany NBD dimerization in full-length CFTR.

E. Strictness of Coupling Between Open Burst Termination and ATP Hydrolysis

How strictly CFTR gating is coupled to ATP hydrolysis has been a matter of longstanding debate. The first hint implying a nonequilibrium gating cycle came from the observation of time-asymmetric changes in permeation properties in patch-clamp records of individual gating CFTR channels (96). The kinetics of pore block of WT CFTR by the anionic buffer MOPS changes within each burst, a phenomenon that can be made evident by the presence, at small recording bandwidth, of two distinct conductance states (one low, one high) (109). The sequence of occurrence of these conductance states shows clear time asymmetry; the ratio between resolvable low-to-high (L→H) and high-to-low (H→L) transitions is ~16:1 (96), with the majority of time during each burst spent in the initial low-conductance state. Such time asymmetry is a clear violation of microscopic reversibility and indicated strong coupling between pore gating and a free-energy releasing process, here, most likely ATP hydrolysis. Indeed, the L→H transition itself was suggested to coincide with ATP hydrolysis, because it was ab-

sent under nonhydrolytic conditions (96). In apparent conflict with that conclusion of strong coupling, mutation of the NBD1 Walker A lysine (K464A) reduced ATPase activity of purified CFTR protein by ~10-fold but little affected channel gating, interpreted to suggest loose coupling between gating and catalytic activity in CFTR (192).

In single-channel recordings, transitions among closed-channel states, or among open-channel states, remain undetected. However, such invisible transitions contribute to determining the shapes of the open- and closed-dwell time distributions (which consist of mixtures of exponential components), making it possible to estimate their rates through maximum likelihood fitting (50). For equilibrium processes, the fractional amplitude of each exponential component is necessarily positive, and the distributions are therefore monotonically decaying (117). In contrast, for WT CFTR, the distribution of open burst durations is clearly peaked (FIGURE 5A). This experimental observation thus reveals an underlying nonequilibrium gating mechanism, with most open events involving two sequential steps: a slow step with a rate of $\sim 4 \text{ s}^{-1}$, followed by a fast step with a rate of $\sim 50 \text{ s}^{-1}$ (at room temperature) (61). These two sequential steps were interpreted to reflect slow ATP hydrolysis (FIGURE 2E, step $O_1 \rightarrow O_2$, rate k_1) followed by fast disruption of the posthydrolytic NBD dimer (FIGURE 2E, step $O_2 \rightarrow C_2$, rate k_2). Indeed, the rate-limiting step for WT CFTR channel closure is strongly temperature dependent, with an estimated activation enthalpy $\Delta H^\ddagger \sim 70\text{--}90 \text{ kJ/mol}$ [(57, 155) but, cf., (6)], and the similar values for ΔG^\ddagger and ΔH^\ddagger report no decrease in entropy (57). Such an isolated positive enthalpy change, unaccompanied by a change in entropy, is consistent with strain in a single chemical bond without accompanying changes in interface accessibility to solvent molecules. These observations suggest that the ATP hydrolysis step ($O_1 \rightarrow O_2$) is rate limiting for channel closure; the transition state for this step would include a still tightly dimerized composite site 2 but a strained bond between the β and γ phosphates of the occluded ATP.

Because in WT CFTR the rate of nonhydrolytic closure (FIGURE 2E, step $O_1 \rightarrow C_1$, rate k_{-1}) is likely very slow, estimated between ~ 0.03 and 0.2 s^{-1} based on the slow closing rates of various nonhydrolytic mutants, >95% of pore opening events must terminate through ATP hydrolysis, consistent with the conclusions of Gunderson and Kopito (1995) (94%). In contrast, the burst distribution of the nonhydrolytic D1370N mutant lacks a negative exponential component and is monotonically decaying (FIGURE 5B), reflecting a gating cycle truncated to reversible $C_1 \leftrightarrow O_1$ transitions (61), with rate k_{-1} ($\sim 0.5 \text{ s}^{-1}$) accelerated by this mutation, which removes a side chain involved in Mg^{2+} coordination (269). On the other hand, fitting the burst distribution of the site 1 mutant K464A (FIGURE 5C) suggested an approximately fourfold reduction in rate k_1 (i.e., allosteric slowing of ATP hydrolysis in site 2) and a >10-

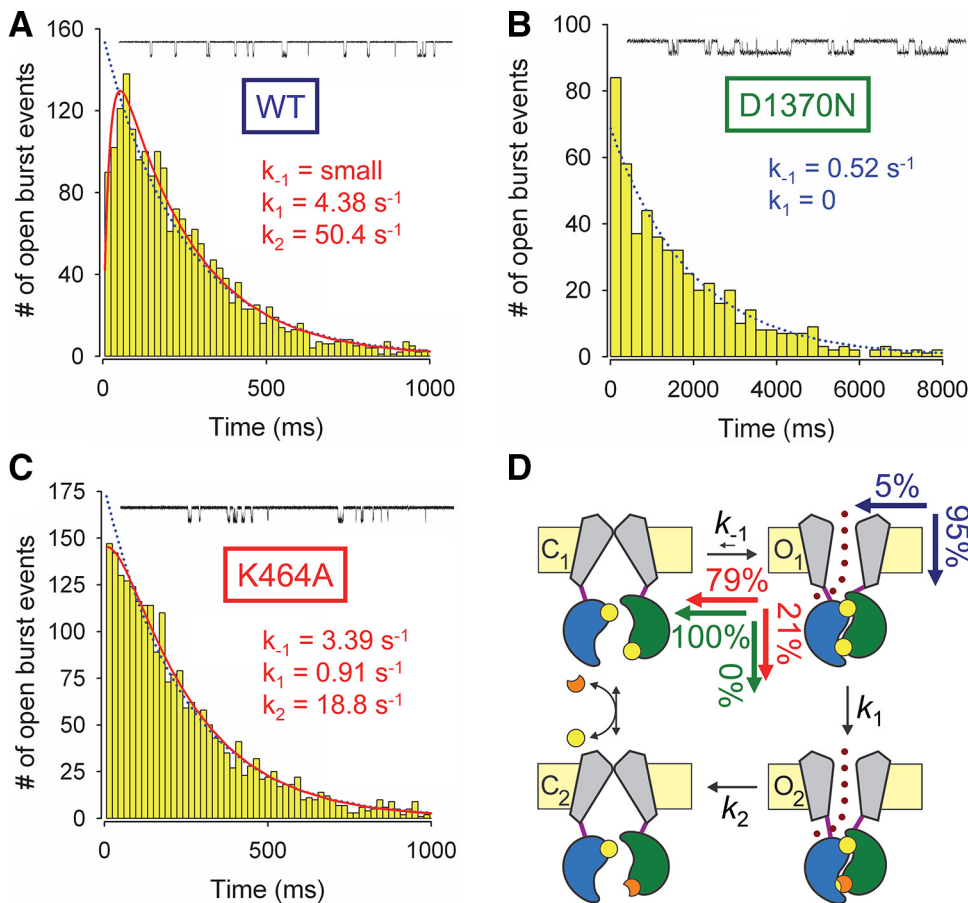


FIGURE 5. Distributions of CFTR burst durations support nonequilibrium gating. *A–C:* Distributions of burst durations for prephosphorylated wild-type (WT) (*A*), D1370N (*B*), and K464A (*C*) CFTR channels gating in 2 mM ATP at 25°C. *Solid red lines* in *A* and *C* are maximum likelihood fits to the scheme in panel *D*; in *A*, rate k_{-1} was fixed to zero. *Dotted blue lines* in *A–C* are maximum likelihood fits to a nonhydrolytic equilibrium $C_1 \leftrightarrow O_1$ scheme. Fitted rates are printed in the panels. *Insets* show 30-s segments of single-channel inward currents; $V_m = -80$ mV. *D:* Cartoon gating cycle illustrating coupling ratios. *Colored vertical and horizontal arrows and numbers* depict fractions of bursts terminated through ATP hydrolysis and nonhydrolytic NBD dimer dissociation, respectively, for WT (*blue*), K464A (*red*), and D1370N (*green*) CFTR. [Adapted with permission from Csanády et al. (61)].

fold acceleration of rate k_{-1} (61), consistent with the effect of this mutation on macroscopic closing rates in various nonhydrolytic mutant backgrounds (56, 61, 185, 243). Thus, the coupling ratio that quantifies the proportion of pore opening (burst) events that result in ATP hydrolysis [given by $k_1/(k_1 + k_{-1})$ for the scheme in **FIGURE 2E** (i.e., the ratio of the rate of hydrolysis over the sum of all rates out of the prehydrolytic open state)] may be lowered by mutations that slow ATP hydrolysis and/or accelerate nonhydrolytic dissociation of the NBD dimer; it is >0.95 for WT CFTR (strong coupling), but only ~ 0.2 for K464A (loose coupling) and 0 for nonhydrolytic mutants (no coupling) (**FIGURE 5D**, colored arrows). Such an interpretation is consistent with the ATPase measurements of Ramjeesingh and colleagues (1999) on both WT CFTR and the two Walker A lysine mutants.

More recently, time-asymmetric subconductance patterns (L→H) for single CFTR channels have been observed in the presence of the blocker 3-nitrobenzoate (60) as well as in mutants in which the native charge distribution of the intracellular pore vestibule is perturbed (113, 272). Intriguingly, for the latter mutants, multiple L→H subconductance transitions could be observed in ~ 10 – 20% of the bursts. On the assumption that L→H transitions reflect ATP hydrolysis events, L→H→L→H type bursts were interpreted to reflect two ATP hydrolysis events occurring

within a single burst [i.e., a coupling ratio > 1 (“super-coupling”)]. The phenomenon was explained by a model that postulates that the hydrolysis products ADP + P_i may be released, and a novel ATP molecule may bind at site 2, returning the channel to the prehydrolytic open state without an intervening pore closure (113). The existence of such a reentry pathway, which implies separation of the NBD dimer interface around site 2 uncoupled from pore closure, seemed consistent with the earlier finding that a brief, 1-s exposure of open CFTR channels to PP_i or AMPPNP in the presence of ATP, or immediately after ATP removal, can lock CFTR channels into a long-lasting burst without an intervening long closure. It also seemed consistent with the modest [ATP] dependence of steady-state single-channel burst durations observed for W401F (but not for WT) CFTR (114). Moreover, the CFTR potentiator drug VX-770 (ivacaftor) was shown to increase the frequency of L→H→L→H-type bursts and to prolong CFTR burst durations in a weakly [ATP]-dependent manner, prompting the interpretation that the drug acts by stabilizing the post-hydrolytic O_2 state and thus promoting the reentry pathway (112).

A major shortcoming of the reentry model is that it predicts a dissociation between the steady-state mean burst duration (τ_b) and the time constant of macroscopic current relaxation following sudden nucleotide removal (τ_{relax}). This is

because the latter reflects average survival time in the open burst state at zero nucleotide concentration (i.e., in the certain absence of reentry events). Thus, for a channel that gates at steady state, the average number of site 2 nucleotide occlusion events within a single burst is given by the ratio $\tau_b/\tau_{\text{relax}}$; that number was found to be ~ 1 under most, if not all, conditions tested, including WT CFTR and various mutants gated by either ATP or N^6 -(2-phenylethyl)-ATP (P-ATP) (56, 233) and even for WT CFTR stimulated by VX-770 (112). On the other hand, both [ATP] dependence of τ_b and the existence of $L \rightarrow H \rightarrow L \rightarrow H$ -type bursts might be accounted for by alternative explanations. First, τ_b dependence on [ATP] might arise from a differential contribution to channel activity of spontaneous openings. CFTR channels are known to open with ATP bound at only one composite site (25, 26, 185) and occasionally even in the complete absence of nucleotide (25, 160, 224, 253). Such monoliganded and unliganded (spontaneous) openings are briefer than normal diliganded openings (160, 257), and their fractional contribution, which shortens mean burst duration, is expected to be stronger at low [ATP]. Although for WT CFTR this effect is too subtle to be measurable in most studies [(24, 112, 243); but cf., (270)], it might be accentuated by mutations that perturb ATP binding at either site (114) or by drugs that increase the frequency of spontaneous openings, such as VX-770 (112). Second, how might $L \rightarrow H \rightarrow L \rightarrow H$ -type bursts arise? $L \rightarrow H$ subconductance transitions are believed to coincide with ATP hydrolysis because only the L state is readily observed under nonhydrolytic conditions (e.g., in the absence of Mg^{2+} , in the site 2 mutants D1370N, K1250A, and E1371S, or for WT channels locked open by ATP + PP_i or ATP + AMPPNP), (96, 113). However, in ABC proteins, splitting of the ATP β - γ bond is a multi-step process, as evidenced by multiple intermediate states distinguishable by blocking the hydrolysis reaction using ATP γ S, V_i , fluoroaluminate, beryllium fluoride, or different catalytic site mutations (213, 222, 236). Which of these partial steps coincides with the $L \rightarrow H$ transition is as yet unclear; some of these might be reversible, and so repeated $L \rightarrow H$ transitions might reflect multiple attempts to complete the bond-splitting reaction. Alternatively, the entire ATP hydrolysis process (step $O_1 \rightarrow O_2$; **FIGURE 2E**) might be reversible; although the ATP hydrolysis reaction with reagents and products in aqueous solution is highly exergonic, in a multi-step enzymatic process, that starts with binding of $ATP_{(aq)}$ from the bulk solution and ends with the release of products [$ADP_{(aq)} + P_{i(aq)}$] into solution, the step associated with the largest negative ΔG° need not be the bond-splitting step itself. Thus, ΔG° for the reaction ($CFTR \cdot ATP$) + $H_2O \rightarrow CFTR \cdot ADP \cdot P$, in which reagents and products are bound within the catalytic site, might not be highly negative [cf., ATP- and $ADP \cdot P$ -bound states of the F1-ATPase β subunit are in equilibrium (264)]. Of note, reversibility of step $O_1 \rightarrow O_2$ (**FIGURE 2E**) would not alter the shape of the burst dwell time distributions (61). As a third possibility, coupling between conductance state and

hydrolytic state might be only probabilistic, such that the prehydrolytic state (O_1 , **FIGURE 2E**) only favors (but is not strictly linked to) the lower conductance (L), whereas the posthydrolytic state (O_2 , **FIGURE 2E**) favors (but is not strictly linked to) the higher-conductance (H) pore conformation. None of these possible alternatives has been excluded to date.

Where this has been studied, both ATP-dependent (242) and ATP-independent (160) open channels have been found to have tightly dimerized NBDs, with ATP at site 2 occluded (see Section IVD). Given this evidence and the considerations above on our uncertainty on how to precisely link the conductance changes to events at the catalytic site, the conformational changes underlying the $L \rightarrow H$ transition are more easily interpreted as changes in the TMDs that do not alter tight NBD dimerization. As described above (Section IIC), structures for a number of ABC transporters have been obtained in outward-facing conformations (46, 67, 256) in which the extracellular portions of the TMDs, corresponding to the regions involved in forming CFTR's permeation pathway, assume diverse arrangements, whereas the NBDs remain tightly dimerized. Thus, CFTR's low conductance state might represent a conformation in which, as in the phosphorylated ATP-bound zebrafish CFTR structure (274) or the McjD transporter (46), the extracellular ends of the TM helices are arranged in a largely parallel orientation, whereas the high-conductance conformation reached at the end of the burst might be somewhat more similar to the Sav1866 structure (67) in which the extracellular ends of the TM helices further diverge. Of note, the position corresponding to R352 in human CFTR, mutations at which appear to differentially affect conductance in the O_1 and O_2 state (113), is positioned at a constriction of the permeation pathway in Sav1866-based homology models (52, 163), but in the wider intracellular vestibule in the outward-facing zebrafish CFTR structure (274) and in models based on McjD (52).

F. Role of the Degenerate ATP-Binding Site in Channel Gating

Photocrosslinking experiments using [$\alpha^{32}P$]8-azido-ATP to label the two ATP sites, and various unlabeled nucleotides to compete that labeling, identified site 1 as a high-affinity binding site with a K_d for Mg-ATP in the low micromolar range (7, 14). Furthermore, labeling of site 1 by [$\gamma^{32}P$]8-azido-ATP, without cross-linking, was shown to survive several minutes of extensive washing with nucleotide-free solution at 30°C, demonstrating poor or absent catalytic activity at the degenerate site (14). Given that the cycle time for channel gating is on the order of ~ 1 s, these biochemical findings suggested that site 1 must keep ATP bound but unhydrolyzed throughout many gating cycles, in contrast to site 2, which hydrolyzes ATP within each channel burst event. Indeed, such an asymmetry between the kinetics of

nucleotide exchange in the two sites was supported by ligand exchange experiments in which ATP and the high-affinity analog P-ATP were intermittently applied to inside-out patches. Gating of CFTR channels in P-ATP is characterized by approximately twofold prolonged bursts (slower closing) and approximately twofold shortened interbursts (faster opening), as compared with gating in ATP. However, whereas the effect on opening rate (attributed to the nucleotide bound in site 2) is observed instantaneously upon exchange of the bath nucleotide, the effect on closing rate (attributed to the nucleotide bound in site 1) appears with a delay of ~50 s (233).

What is the extent of gating-related movements in site 1? In closed channels, the NBD dimer interface must disengage occasionally even around site 1, because, albeit slowly, the nucleotide in site 1 can be clearly exchanged (233) and that is most unlikely to happen while the interface is tight. But to what extent, and how frequently, does site 1 open up? The slow nucleotide exchange rate at site 1 is affected by NBD2 signature sequence (S1347) mutations (233), suggesting that the NBD2 tail continues to contribute to ATP binding even while the pore is closed. In apparent contradiction to these findings, cysteines engineered into the signature sequence at either site 1 (S549C) or site 2 (S1347C) were accessible to small hydrophilic methanethiosulfonate (MTS) reagents in the closed, but not in the open state, and were modified equally rapidly at a rate approximating the rate of pore closure. Thus, upon pore closure, the NBD interface must open up around both ATP sites promptly and sufficiently to accommodate reagents with a diameter up to ~8 Å (37). A heterodimeric bacterial ABC transporter, Tm287–288, crystallized in the presence of AMPPNP, shows an inward-facing conformation (101) with nucleotide bound only at site 1, but with both binding sites partially open (i.e., Walker A and signature sequences are separated and accessible to the solvent and to relatively large reagents). Some contact across the site 1 interface is maintained through interactions between the Walker A loop of NBD1 and the D-loop of NBD2. In particular, the residues corresponding to CFTR's T460 in NBD1 and H1375 in NBD2 are seen to form hydrogen bonds. Maintained contact between these two residues, throughout CFTR's gating cycle, is supported by lack of gating-associated changes in their energetic coupling (223). One possible interpretation, consistent with both MTS accessibility (37) and mutant cycle (223) studies, is that closing of the pore corresponds to a partial opening of site 1, as seen in the Tm287–288 AMPPNP-bound crystal. However, functional studies on Tm287–288 (230), as well as on SUR1/K_{ATP} (176) and CFTR (243) channels, suggest that binding of AMPPNP to heterodimeric ABC proteins has a poor efficacy in altering equilibria toward the NBD-dimerized conformations. Thus, bound Mg-ATP might be more effective in maintaining the site 1 interface tightly dimerized, even immediately after pore closure, as the nucleotide exchange studies would suggest (233). One possible unifying interpretation could be that there is a

rapid equilibrium between a tightly dimerized and a partially open conformation of site 1 in closed channels: whereas the impact of NBD2 signature sequence mutations on site 1 nucleotide exchange rate (233) depends on the fraction of time a closed channel spends with site 1 dimerized, the rate of MTS modification of site-1 cysteines upon pore closure (37) reflects the rate of first passage to the dedimerized state. Thus, possibly in a closed channel, site 1 might remain in a dimerized state for most of the time but nevertheless visit the dedimerized state frequently enough to allow high-probability modification of site 1 cysteines within a single closed-channel (interburst) event. Understanding the precise range of gating-related movements in CFTR's site 1 will require a high-resolution structure of phosphorylated CFTR in a closed state with ATP bound at site 1.

What role does site 1 play in CFTR channel gating? Regardless of what the precise spatial arrangement of the most frequently populated closed-channel conformation is, significant rearrangements must occur in site 1 between that conformation and the open-channel conformation, because site 1 structural perturbations clearly alter the free energy difference between the ATP-saturated closed-pore (FIGURE 2E, C₁) and the prehydrolytic open-pore (FIGURE 2E, O₁) states (56, 185, 281). But whereas in canonical site 2 the conformational changes upon pore opening are completed already in the transition state, as reported by its large Φ value of ~1 (FIGURE 3A, right, red numbers), for degenerate site 1, the low Φ value of ~0.4 (FIGURE 3A, right, orange numbers) reports some further motion between the transition state and the open state. ATP stabilizes the open-pore conformation by acting as a molecular glue that bonds the NBD dimer interface together. Comparison of gating kinetics of ATP hydrolysis-deficient mutants in saturating ATP and of WT CFTR channels in the absence of ATP (spontaneous gating) indicates that the presence of bound ATP both speeds channel opening (FIGURE 2E, step C₁→O₁) and slows nonhydrolytic closure (FIGURE 2E, step O₁→C₁) (160). The effect on opening rate is readily explained by the bonding of the ATP glue in site 2, which is already completed in the transition state (FIGURE 3B, bottom site, red cups around ATP in states T and O₁); that glue stabilizes state T (and O₁) relative to state C, thereby lowering the energetic barrier for opening. However, slowing of nonhydrolytic closure indicates that ATP binding also stabilizes the open state (O₁) relative to the transition state (T) (i.e., ATP-bound channels, compared with spontaneously opened channels, face a higher energetic barrier to closing by simple reversal of the opening step). Indeed, the movements in site 1 that occur between the transition state and the open state might reflect the bonding of the ATP glue in the degenerate site (FIGURE 3B, top site, red cups around ATP in state O₁), which underlies this differential stabilization of O₁ compared with T. In the context of ATP-dependent gating of WT CFTR (FIGURE 2E), that bonding

effect of ATP in site 1 would explain the small value of rate $O_1 \rightarrow C_1$, which ensures strictly unidirectional, nonequilibrium cycling (FIGURE 2E, purple circular arrow; cf., FIGURE 5D). Consistent with such an interpretation, channel closure under nonhydrolytic conditions is affected by a number of structural perturbations in site 1; it is accelerated by the K464A mutation (56, 185, 243) or by deletion of the RI (54) but slowed by the H1348A mutation (56) or by P-ATP bound in site 1 (56, 233).

G. The Channel-Transporter Interface: CFTR Viewed as a Degraded Active Transporter

From an evolutionary perspective, CFTR is most closely related to the exporter class of ABC proteins that extrude a variety of substrates, against their electrochemical gradients, out of cells. To avoid instantaneous dissipation of the electrochemical gradient built up at the expense of ATP hydrolysis, exporters must have two gates, and these must never be open at the same time (83). In the inward-facing conformation of ABC exporters, a closed outer gate is formed by the converging external ends of the TM helices (8, 101, 212, 256), whereas in the outward-facing conformation, tight bundling of the cytosolic ends of the TM helices forms a closed inner gate (46, 67, 256). The inward-facing conformation thus allows high-affinity substrate binding from the cytosolic side, whereas in the outward-facing conformation, the substrate is released into the extracellular medium. The inward- to outward-facing conformational transition is driven by NBD dimerization following ATP binding (146). However, unidirectional uphill transport requires a source of external energy input. That energy source, the binding and hydrolysis of ATP, is harnessed to drive conformational changes unidirectionally, thus switching the substrate binding site from inward-facing high affinity to outward-facing low affinity in the loaded transporter and allowing release of substrate even in the face of a high extracellular concentration (13).

Based on the common evolutionary origin of CFTR and ABC exporters, and on the finding that, in CFTR, dimerized NBDs are coupled to an open, but dedimerized NBDs to a closed, pore (242); CFTR's TMDs were believed to adopt an inward-facing conformation in the closed (interburst) but an outward-facing conformation in the open (burst) state. Because the latter conformation forms a transmembrane aqueous pore permeable to anions, in CFTR, the ABC protein internal gate was proposed to have become "leaky" to anions over the course of evolution. Supported by a line of functional evidence (12, 64, 107, 252), that proposal was finally proven to be correct by the recent structures of inward- and outward-facing CFTR [(145, 273, 274); FIGURE 1E-F]. These structures also identify the structural changes that implemented CFTR's evolution from a transporter to a channel; the appearance of a lateral opening between the cytosolic ends of TM helices 4 and 6 (FIGURE 1F, right, red

arrow) provides an aqueous pathway between the cytosol and the internal vestibule, thus short-circuiting the ABC protein internal gate formed by the cytosolic TM helix bundle crossing [cf., (76, 77)]. But why has the ATP hydrolysis-driven, nonequilibrium gating cycle of CFTR been spared by evolution? The passive, electrochemically downhill chloride ion flow through CFTR could, in principle, be controlled by simple ATP binding (i.e., reversible $C_1 \leftrightarrow O_1$ transitions, see FIGURE 2E) without any need for "wasteful" ATP hydrolysis. A likely explanation is a lack of evolutionary pressure given that ATP wasting by CFTR is negligible, because P-type ATPases like the ubiquitous Na^+K^+ -ATPase transport only ~5 cations at the expense of hydrolysis of a single ATP molecule, whereas CFTR transports millions of chloride ions at the same cost. Alternatively, in addition to serving as an anion channel, CFTR might also serve as an active transporter of some, as yet unidentified, substrate. Interestingly, CFTR was found to mediate efflux of large organic anions, such as gluconate or lactobionate (142), or of reduced and oxidized glutathione (143) from the cytosolic solution but not influx of the same anions from the extracellular solution; this asymmetry was disrupted when ATP hydrolysis was prevented, using PP_i or AMP-PNP. However, the molecular mechanism of such ATP hydrolysis-dependent unidirectional export is still elusive; it is not a classical transporter-like process, as the estimated throughput rate for gluconate export [~ 40 fA, corresponding to $\sim 2.5 \times 10^5$ ions/s (142)] exceeds measured rates of ATP hydrolysis [~ 1 ATP/s (131, 145)] by five orders of magnitude.

H. Adenylate Kinase Catalytic Activity and Gating Regulation

Isolated, purified NBD1 and NBD2 of CFTR show measurable adenylate kinase (AK) activity, catalyzing reversible interconversion between ATP + AMP and two ADP molecules by direct phosphotransfer between the two nucleotides (93, 193, 194). Based on this finding, CFTR was suggested to catalyze preferentially AK, rather than ATPase reactions, in the presence of AMP levels found in living cells (195). Along these lines, partial inhibition of CFTR channel currents by ADP or the AK inhibitor P1,P5-di(adenosine-5')pentaphosphate (AP_5A), as well as subtle effects of AMP on currents evoked by low micromolar ATP, were all interpreted to reflect alterations in CFTR gating caused by modulation of its intrinsic AK activity (195, 197). However, unlike the purified isolated NBDs, full-length CFTR protein purified to homogeneity was shown to exhibit exclusively ATPase, but no significant AK, activity (193). As the ATPase turnover rate of the same preparation was comparable with that of channel bursting rates (~ 0.2 s⁻¹), intrinsic AK activity of full-length CFTR, if any, would be expected to be orders of magnitude slower than channel gating rates; indeed, even for isolated NBDs, reported AK turnover rates were in the range of 0.003–0.02 s⁻¹ [(193, 195); but, cf.,

(93)]. Interestingly, recent studies demonstrated phosphoryl transfer between γ - ^{32}P -GTP and 2-azido-AMP (2- N_3 -AMP) in membrane preparations of CFTR-overexpressing HeLa cells, and the resulting β - ^{32}P -2- N_3 -ADP product could be photocrosslinked to CFTR; moreover, that signal was weakened by CFTR site 2 mutations S1248F (196) and Q1291F (70). These results could indeed reflect some intrinsic AK activity for CFTR, but they could also be explained by the activity of an endogenous AK associated with HeLa cell membranes; reduced labeling of the CFTR mutants could then reflect impaired binding to CFTR's site 2 of the labeled β - ^{32}P -2- N_3 -ADP produced by the associated AK. Indeed, AK1 β contains a myristoylation domain and has been shown to strongly associate with membranes (49). AK also interacts with multiple enzymes involved in energy homeostasis, and at least two AK anchoring proteins have been identified [reviewed in (73)]. Specifically, AK1 directly interacts with sarcolemmal K_{ATP} channels, as demonstrated by mutual coimmunoprecipitation and AK-mediated regulation of K_{ATP} channel activity, implying strong structural and functional coupling between the two proteins (31). Thus, a definitive proof of intrinsic AK activity for CFTR will require demonstration of such activity for full-length CFTR protein under conditions that exclude the presence of associated cellular proteins.

Modulation of CFTR currents by various nucleotides and nucleotide analogs has been addressed by multiple studies and is mostly consistent with competition with ATP for sites 1 and 2 [e.g., (24, 25, 195, 203, 258)]. At least the strong inhibitory effect of ADP, caused by a slowing of channel opening and an acceleration of channel closing (24, 203, 258), is readily explained by competition with ATP for sites 2 and 1, respectively (24, 25), and cannot be linked to AK activity of CFTR, as both effects are observed also for CFTR channels bearing site 2 mutations K1250A or D1370N (25) shown to abolish AK activity even for isolated NBD2 of CFTR (93, 195). Likewise, inhibition by AP_5A of ATP-induced CFTR currents cannot be attributable to inhibition of AK activity because it is observed in the absence of AMP (i.e., in inside-out patches continuously superfused with solutions that contain ATP, but no AMP) (195).

V. REGULATION OF CFTR GATING BY R DOMAIN PHOSPHORYLATION

A. Kinases and Phosphatases Involved in CFTR Regulation

Cytosolic ATP is essential for CFTR channel gating, but ATP concentration cannot serve as a physiological regulator of channel activity; because the $K_{1/2}$ for stimulation of open probability by ATP is $\sim 50 \mu\text{M}$, CFTR channels are saturated by the millimolar ATP concentrations present in

the cytosol of living cells. ATP-dependent gating is therefore regulated through phosphorylation/dephosphorylation of the CFTR protein. PKA, the key regulator of CFTR activity, phosphorylates multiple R domain serines found in consensus motifs, a process essential for channel gating (9, 20). In addition, several other kinases have been identified that affect CFTR function. CFTR phosphorylation by protein kinase C (PKC) was shown to cause partial current activation (21, 225), and basal PKC phosphorylation of some CFTR residue(s) was claimed essential for subsequent full channel activation by PKA (35, 111). In vitro studies using an R domain peptide identified R domain serines 686 and 790 as the target sites for PKC phosphorylation (183). AMP-activated protein kinase (AMPK) binds to the COOH-terminus of CFTR and phosphorylates the CFTR protein in vitro (98), and coexpression of AMPK with CFTR in *Xenopus laevis* oocytes (98) or pharmacological activation of endogenous AMPK in a lung epithelial cell line (97) lower whole-cell CFTR currents. Tyrosine kinases, including p60c-Src and the proline-rich tyrosine kinase 2 (Pyk2), are both capable of activating CFTR currents (22, 81), and such activation is prevented by simultaneous mutation of two tyrosines at positions 625 and 627, implicating the latter residues as likely tyrosine kinase substrates (23). CaM kinase I was also found to phosphorylate a CFTR R domain peptide in vitro (183), but no effects on channel activity have so far been demonstrated (21). cGMP-dependent protein kinase isoforms have also been found to phosphorylate CFTR, an activity that is likely to play a role in the action of heat-stable enterotoxins during secretory diarrheas (82) and possibly in CFTR current activation by S-Nitrosoglutathione in an airway cell line (41). In particular, isoform II (cGKII) isolated from pig intestines was shown to phosphorylate the R domain with patterns of two-dimensional peptide mapping similar to PKA, and to result in activation of CFTR channels in heterologous expression systems and in an intestinal cell line (82).

Several phosphatases have been tested for their effectiveness in dephosphorylating CFTR. Whereas phosphatases 1 (PP1) and 2B (PP2B, calcineurin) little affect currents of prephosphorylated CFTR [(21, 149); but, cf., (80)], phosphatases 2A (PP2A) (21, 149) and 2C (PP2C) (149, 232) have both been shown to efficiently deactivate CFTR channels in inside-out patches. The relative contribution of these two phosphatases to CFTR regulation in vivo is likely cell type specific. Among exogenous phosphatases frequently used for in vitro studies, alkaline phosphatase does not affect CFTR activity (21), whereas lambda phosphatase deactivates CFTR (81) and abolishes detectable phosphorylation of CFTR protein purified from resting cells (145).

B. Target Sites of PKA

PKA phosphorylates serines and threonines of target proteins found in consensus motifs of the form R-R/K-X-S/T

(dibasic sites) or R-X(-X)-S/T (monobasic sites), with a preference for dibasic motifs (116). The R domain sequence in CFTR (a.a. ~640 to ~840) contains nine dibasic and several monobasic PKA consensus motifs; a further serine in a dibasic motif, S422, localizes to the RI segment of NBD1. Out of this pool of potentially phosphorylatable residues a large number of studies have identified at least nine positions that are phosphorylated by PKA either in vivo or in vitro (**TABLE 1**). Although found in a dibasic motif, serine 686 was not seen to be phosphorylated by PKA, but instead was found to be a substrate for PKC (183). To our knowledge, phosphorylation by PKA of threonine 788, located in a dibasic motif, has not yet been demonstrated.

Under in vitro conditions gradual phosphorylation of an R domain peptide by PKA causes incremental electrophoretic mobility shifts, allowing visual discrimination of up to six distinct phosphoforms that appear with different kinetics (**FIGURE 6A**). Two-dimensional peptide mapping and mass spectrometric analysis of the phosphoforms revealed that phosphorylation of serine 737 causes the largest mobility shift, and identified serine 768 as being among the first to become phosphorylated (58, 183).

C. Stimulatory and Inhibitory Phosphorylation Sites

In inside-out patches, in the presence of saturating ATP but various concentrations of the active catalytic subunit of PKA (**FIGURE 6B**), the steady-state open probability of single CFTR channels shows a roughly hyperbolic dependence on PKA concentration [(58); **FIGURE 6C**, red symbols]. Because membrane-associated endogenous phosphatase activity is independent of the amount of applied kinase, at steady state the R domain is expected to become phosphorylated to a higher stoichiometry when the applied PKA concentration is higher. The implication is that channel open probability is not regulated in an all-or-none fashion by PKA, but is rather roughly proportional to the degree (stoichiometry) of R domain phosphorylation. Thus, most PKA target serines might be classified as “stimulatory PKA sites.” Accordingly, mutation to alanine of four, eight (199), or ten (34) con-

sus serines substantially reduced channel open probability in the presence of ATP and PKA. Surprisingly, however, even channels lacking all 10 serines located in dibasic PKA sites retain substantial phosphorylation-dependent channel activity with a maximal open probability almost 50% of that of WT CFTR (154), implying large functional redundancy among PKA target serines. Just as different PKA target sites are phosphorylated with different kinetics, the rates of dephosphorylation of individual phosphoserines by membrane-associated endogenous phosphatases are likely diverse; in inside-out patches excised from various cell types (9, 55, 250), macroscopic CFTR currents decline with a biexponential time course following sudden removal (or inhibition) of PKA (**FIGURE 6D**). An initial rapid partial current decline (within seconds) is followed by a much slower decay (over minutes), suggesting the existence of a relatively stable, partially phosphorylated state of CFTR distinguishable from the fully phosphorylated state by approximately two- to threefold shorter mean burst durations and approximately twofold longer interburst durations (55).

Whereas alanine replacement of most PKA target serines negatively affects channel activation, mutation of serines 737 and 768 were found to increase the sensitivity of whole-cell CFTR currents toward activation by 3-isobutyl-1-methylxanthine (IBMX), which activates endogenous PKA by elevating cellular cAMP levels (260). Classification of serines 737 and 768 as inhibitory PKA sites was further supported by slightly and robustly elevated open probabilities, respectively, of S737A and S768A CFTR channels in inside-out patches [(237); but, cf. (100)]. The S768A mutation increases the sensitivity for channel activation by PKA, resulting in substantial CFTR currents already at the low endogenous PKA activity of resting, unstimulated cells but also increases maximal open probability (**FIGURE 6C**, blue symbols), mainly by lengthening mean burst durations. These effects appear to be direct effects on channel gating, as the kinetics and degree of phosphorylation of other PKA target serines remain largely unaffected in the mutant (58, 100). The in vivo relevance of inhibitory CFTR regulation might be twofold. First, by shifting the PKA dose response

Table 1. CFTR positions phosphorylated by PKA in vivo or in vitro

Positions					In Vitro/In Vivo			Reference	
660	700	712	737	768	795	813	CFTR in vitro	43	
660			737		795	813	CFTR in vivo	43	
660	700		737	768	795	813	CFTR in vitro	183	
			753*				CFTR in vitro	206	
422	660	700	712	737	768	795	NBD1-R in vitro	231	
660	700	712	737	753*	768	795	813	CFTR in vitro	168
660	700	712	737		768	795	CFTR in vivo†	58	

*Monobasic site. †Resting *Xenopus laevis* oocytes.

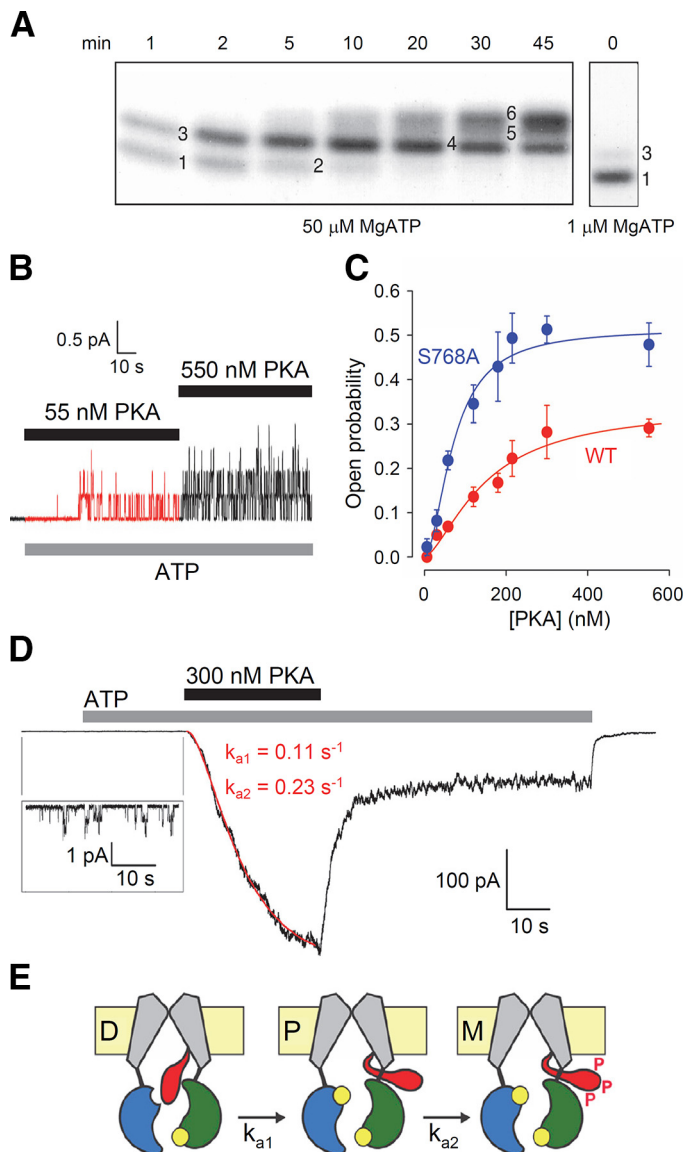


FIGURE 6. Regulation of CFTR channel activity through phosphorylation by PKA. **A:** Time course of phosphorylation of an R domain peptide [amino acid position (a.a.) 645–835] by PKA resolved by SDS/PAGE. Autoradiogram shows samples incubated for the indicated time intervals in 1 or 50 μM [as indicated] $[\gamma^{32}\text{P}]\text{-ATP}$ and 0.2 $\mu\text{g}/\text{ml}$ PKA catalytic subunit. Six distinct resolvable bands are numbered. **B:** Inside-out patch recording showing activity of four WT CFTR channels exposed to 55 and then 550 nM PKA catalytic subunit in the presence of 2 mM Mg-ATP; $V_m = +40$ mV. **C:** Steady-state open probability of WT (red symbols) and S768A (blue symbols) CFTR channels gating in 2 mM ATP and various concentrations of PKA catalytic subunit, plotted as a function of [PKA]. Solid lines are fits to the Hill equation; $P_{o,\text{max}} = 0.34 \pm 0.06$, $K_{0.5} = 149 \pm 46$ nM, and $n_H = 1.5 \pm 0.5$ for WT and $P_{o,\text{max}} = 0.51 \pm 0.05$, $K_{0.5} = 71 \pm 12$ nM, and $n_H = 1.8 \pm 0.5$ for S768A. **D:** Macroscopic CFTR current elicited in an inside-out patch by exposure to 2 mM Mg-ATP (gray bar) and 300 nM PKA catalytic subunit (black bar); $V_m = -80$ mV. Activation time course is fitted (red line) to a sequential two-step mechanism of the form closed \rightarrow closed \rightarrow active. **E:** Cartoon model of two-step channel activation; color coding as in **FIGURE 2E**; R domain, red tongue; D, dephosphorylated; P, phosphorylatable; M, maximally phosphorylated. Occasional spontaneous release of the unphosphorylated regulatory (R) domain (step D \rightarrow P) allows its phosphorylation by PKA (step P \rightarrow M). [Adapted with permission from Csanády et al. (58) (A–C) and Liu et al. (145) (D–E)].

curve to the right, phosphorylation of serine 768 by PKA, already detectable at basal PKA activity levels, might dampen the WT CFTR current response to low levels of PKA stimulation (**FIGURE 6C**). Second, serine 768 was also identified as the target site for phosphorylation by inhibitory AMPK (119, 123), so its phosphorylation might represent a mechanism to adjust CFTR activity to the metabolic state of the cell.

D. Molecular Mechanism of Gating Regulation by Phosphorylation

PKA-dependent regulation of CFTR activity can be largely ascribed to an inhibitory influence of the unphosphorylated R domain on channel gating, which is relieved upon phosphorylation. Whereas unphosphorylated WT CFTR channels show negligible open probability, a construct in which a large part (a.a. 708–835) of the R domain is deleted (ΔR CFTR) is substantially active without phosphorylation (200). Similarly, deletion of the entire R domain (a.a. 634–836) by coexpression of CFTR segments 1–633 and 837–1480 (cut- ΔR CFTR) yields channels that are active before phosphorylation, whereas channels merely split in two, but still containing the R domain, obtained by coexpression of CFTR segments 1–633 and 634–1480, remain strictly regulated by PKA (55).

In addition to loss of an inhibitory effect, a direct stimulation of channel gating by the phosphorylated R domain also seems to contribute to the full gating response of CFTR to PKA, as unphosphorylated ΔR CFTR is slightly stimulated by superfusion with a phosphorylated R domain peptide (150, 262). Accordingly, open probability of unphosphorylated cut- ΔR CFTR is somewhat lower than that of fully phosphorylated split channels containing the R domain (55). Quantitative analysis suggests that disinhibition accounts for ~ 50 -fold, whereas direct stimulation by the phosphorylated R domain accounts for an additional approximate twofold increase in open probability, amounting to an ~ 100 -fold total enhancement of WT CFTR channel currents by PKA (54).

In search for the biophysical mechanism that underlies the regulatory effect of the R domain, a number of observations have been made. Pull-down assays documented phosphorylation-dependent interactions of the R domain with other parts of the channel (29, 36), including the lasso motif (**FIGURE 1E**, red), which is located at CFTR's cytoplasmic NH₂ terminus (166) and has been shown to also act as an interaction hub for other proteins (167). Introduction of stable negative charges by replacement of up to eight R domain PKA target serines with aspartates (199) or glutamates (4, 18) resulted in a small, but substantial, activity before exposure to exogenous PKA, although some part of that small activity might have reflected basal phosphorylation of remaining serines by endogenous kinases. In any case, given

the existence of both inhibitory and stimulatory sites, mere accumulation of negative charge in the R domain is unlikely to explain channel activation by phosphorylation; rather, conformational changes must also play a role.

Several mechanisms of phosphorylation-dependent regulation of CFTR gating had been proposed in the past. The unphosphorylated R domain was suggested to act as a plug that physically occludes the pore (199, 200). Phosphorylation was suggested to increase the affinity of ATP for binding to the NBDs (131, 154, 262). Prompted by their spatial positioning and high mobilities in the NBD1 structure, as well as their inclusion of phosphorylatable serines, the RI and RE segments were suggested to impede NBD dimerization while unphosphorylated (130). However, split Δ RI CFTR channels lacking residues 415–432, as well as split Δ RE channels lacking residues 634–667, and Δ RE channels with the only phosphorylatable serine in the RI mutated (Δ RE/S422A) all retained unaltered, strict PKA-dependence of channel activity (54). Moreover, even the low-level ATP-independent activity of CFTR channels with the entire NBD2 domain (a.a. 1198–1480) deleted (Δ NBD2) remains fully dependent on phosphorylation by PKA, suggesting that the R domain exerts its modulatory effect by acting directly on the TMD extensions (248). Finally, because phosphorylation little affected [α - 32 P]8-azido-ATP labeling of NBD1, or of NBD2, in the presence of V_i , phosphorylation was suggested to modulate coupling between ATP hydrolysis cycles and gating movements, similar to an automobile clutch (14).

A recent breakthrough toward a clear mechanistic picture has come with the first high-resolution structures of unphosphorylated CFTR (145, 273). Although in those structures the R domain is not well resolved, consistent with the suggested lack of a well-defined structure, its clearly visible density is wedged in between the two NBDs and among the cytosolic extensions of the TM helices. Such an arrangement is sterically incompatible both with a transition to an outward-facing TMD conformation and with NBD dimerization, explaining the inhibitory effect of the unphosphorylated R domain on channel gating. A single resolvable α -helix wedged in between the TM helices, believed to correspond to residues 825–843 of the R domain (FIGURE 1E, yellow surface plot), is likely important for inhibition, as severing that helix by coexpression of CFTR segments 1–835 and 837–1480 results in channels that display substantial phosphorylation-independent channel activity (55). In light of the occluded localization of the unphosphorylated R domain (cartooned as a red tongue in FIGURE 6E), how does PKA gain access to its target serines? Possibly, occasional spontaneous release of the unphosphorylated R domain peptide from its occluded position (FIGURE 6E, left; D = dephosphorylated) renders it accessible to the kinase (FIGURE 6E, center; P = phosphorylatable) which, by phosphorylating its serines, traps the R domain in its released

conformational ensemble (FIGURE 6E, right; M = maximally phosphorylated), no longer incompatible with an outward-facing (open-pore) TMD conformation. Consistent with occasional release of the unphosphorylated R domain, dephosphorylated CFTR protein displays a small, but measurable, ATPase activity (131, 145), and, also in the presence of ATP, unphosphorylated CFTR channels are seen to gate with a small, but discernible, open probability [FIGURE 6D, inset (145)]; neither process is compatible with the wedged-in position of the R domain seen in the unphosphorylated structures. Moreover, the time course of macroscopic CFTR current activation upon exposure to PKA is clearly sigmoidal (FIGURE 6D) and can be reasonably well fitted assuming two sequential slow steps in the activation process (FIGURE 6D, red curve): the slowest step might reflect the spontaneous R domain release (FIGURE 6E, step D \rightarrow P, rate k_{a1}) and the subsequent step, R domain phosphorylation (FIGURE 6E, step P \rightarrow M, rate k_{a2}).

Open questions remain. It is still unclear whether, in unphosphorylated CFTR, ATP hydrolysis might happen without concomitant pore opening, as implied by the automobile clutch model. On the one hand, based on the available structures, it is unclear how NBD dimerization (required for ATP hydrolysis) might occur without concomitant pore opening. But, on the other hand, although phosphorylation clearly robustly stimulates ATPase activity, the 8- (145) to 15-fold (131) difference in ATPase rates measured for PKA-versus phosphatase-treated-purified CFTR protein seems to fall short of explaining the \sim 100-fold stimulation of channel currents upon PKA exposure [FIGURE 6D (54)], unless specific gating changes are invoked. Possibly, some of the basal ATPase activity measured for dephosphorylated CFTR might reflect a minute contamination by some highly active ATPase; given the turnover rate of \sim 1 s $^{-1}$ for CFTR, but up to \sim 1000 s $^{-1}$ for many other ATPases, a 0.01% contamination of a CFTR protein preparation by such an ATPase might account for a basal activity \sim 10% of that of phosphorylated CFTR, possibly contributing to the much lower apparent stimulation of ATPase than of channel activity by phosphorylation. A further uncertainty is the mechanism of the approximately twofold stimulation of channel open probability by the phosphorylated R domain, an action apparently distinct from the \sim 50-fold stimulation that results from the disinhibitory effect of phosphorylating, or deleting, the R domain. Kinetic analysis suggests the approximately twofold stimulation reflects in part slowing of channel closure (55), but the absence of any density for the R domain in the cryo-EM structure of phosphorylated CFTR precludes speculation as to how that might occur.

VI. TARGETING CFTR FUNCTION TO TREAT DISEASE

Although for decades the treatment of CF has largely focused on treating the symptoms of the disease, in recent

years, new drugs have emerged that directly bind to CFTR and so target the primary molecular defect. Potentiators are small molecules that enhance CFTR open probability, thus offering hope to restore channel activity decreased by Class III (and IV) CF mutations. In contrast, pharmacological agents aimed at amending the protein folding/processing defect caused by Class II CF mutations are called “correctors.” Because the most common CF mutation, $\Delta F508$, belongs to both classes, effective treatment of the majority of CF patients will likely require a viable combination of corrector and potentiator drugs. The following paragraphs provide a brief overview of what is known about how presently available potentiators work.

The feasibility of designing practically useful potentiators was signaled by early identification of a number of compounds that stimulate CFTR channel gating when applied *in vitro*. Replacement of ATP with various analogs such as P-ATP (280), 2'- and 3'-deoxy-ATP (3) and 2'-deoxy-P-ATP (161) increases open probability for WT CFTR and even more so for mutants with low open probabilities. The structurally unrelated natural plant compounds genistein (105, 247), capsaicin (2), and curcumin (19, 248) were shown to increase CFTR activity with apparent affinities in the tens-of-micromolar range. All three compounds act by simultaneously speeding channel opening and delaying channel closure and likely share overlapping binding sites, as the effects of genistein and capsaicin (2), or of genistein and curcumin (19), are competitive. The negatively charged voltage-dependent pore blocker NPPB (276) was later found to strongly potentiate channel open probability, and this potentiator effect was retained, without pore block, in the uncharged amide analog NPPB-AM (250). NPPB similarly increases the rates of opening and of nonhydrolytic closure of WT CFTR (59), suggesting that it decreases the energetic barrier for the $C_1 \leftrightarrow O_1$ step (FIGURE 2E); interestingly, thanks to CFTR's nonequilibrium gating cycle, such a catalyst effect might enhance opening rate without speeding normal (hydrolytic) closure. In fact, NPPB also slows hydrolytic channel closing rate by slowing the ATP hydrolysis step [FIGURE 2E, step $O_1 \rightarrow O_2$ (59)]. These two distinct kinetic effects can be ascribed, respectively, to the 3-nitrobenzoate and 3-phenylpropylamine moieties of the parent compound (60). In addition, NPPB also increases open probability of the G551D mutant (134), which opens preferentially with site 2 vacant (133), suggesting that it might either stabilize the monoliganded open state more than the transition state for the $C_1 \leftrightarrow O_1$ step or stabilize only the monoliganded open state in the mutant.

The first potentiator evaluated in clinical trials was VX-770 (ivacaftor), identified by Vertex Pharmaceuticals using high-throughput screening. VX-770 very effectively stimulates CFTR channels carrying the common Class III mutation G551D (~2% of CF alleles), but was also found to enhance $\Delta F508$ CFTR activity *in vitro* (238). Later work

demonstrated the drug's efficacy on a number of other less frequent Class III (and Class IV) mutants (267). At present, the drug is approved in most Western countries for the treatment of CF patients carrying G551D and some other rare mutant alleles, all of which strongly impact gating. *In vitro* mechanistic studies of VX-770 action revealed current stimulation for both WT CFTR and for nonhydrolytic mutants. Kinetically, VX-770 acts by increasing channel opening rate and by slowing both hydrolytic and nonhydrolytic closing rate (112, 125, 134). Although more complex mechanisms have been suggested [see Section IVE (112)], the simplest explanation of these kinetic effects is a stabilization of state O_1 (relative to both C_1 and O_2 ; FIGURE 2E) by the drug; just as for the binding of ATP itself (see Section IVF), VX-770 stabilizes the transition state (T, FIGURE 3B) for opening (modestly increasing rate k_{CO}), but stabilizes state O_1 even more (decreasing rate k_{-1}). Insofar as the rarely visited unliganded open state of CFTR is structurally similar to state O_1 [see Section IVD (160)], such a mechanism would also explain the observed stimulation by VX-770 of spontaneous channel activity in the absence of ATP (74, 112). Similar fold potentiation of nonhydrolytic mutants, K464A CFTR, and WT CFTR channels, which visit the posthydrolytic state O_2 in none, in a small proportion, or in all of the open-burst events, respectively, suggests that any effect on stability of the posthydrolytic state O_2 (112) is likely to be minor (126). Consistent with its extremely hydrophobic nature ($\log P$, ~6.3) the binding site for VX-770 is believed to be located in the membrane-spanning region of CFTR (112).

The clinical success of administering VX-770 in combination with corrector compounds to treat patients carrying $\Delta F508$ alleles has, so far, been limited (244). This disappointing result might be due to a demonstrated negative impact of VX-770 on $\Delta F508$ CFTR biogenesis, and particularly on its stability at the plasma membrane. Thus, the potentiator appears to effectively counteract the action of coadministered corrector drugs, VX-809 (lumacaftor), and VX-661 (45, 240). Surprisingly, a number of structurally diverse potentiators were found to cause a similar reduction in $\Delta F508$ CFTR plasma membrane density (240). As mentioned above, F508 is positioned at the transmission interface that connects the TMDs and NBD1 on the outer side of the “socket” in which CH4 (the “ball” element of the joint, see Section IIC) fits. A conserved, short α -helix completes the socket in most ABC protein NBDs (see FIGURE 1B, *green helix* in NBD2) but is absent from CFTR's NBD1. It is possible that the reduced metabolic stability of potentiator-bound $\Delta F508$ CFTR at the plasma membrane might result from the increased frequency of opening, and hence increased exposure of the fragile mutant, lacking the socket-completing phenylalanine, to the high molecular strain of the opening transition state [(6, 57, 155), see Section IVC]. Consistent with this interpretation, mutations, such as E1371S, that decrease the frequency of pore-opening events

by greatly prolonging burst duration, were seen to protect $\Delta F508$ CFTR from VX-770–induced peripheral instability (240). These considerations suggest that potentiators that increase burst duration, and/or strongly reduce the strain in the opening transition state (59, 60), might be better suited for treatment of patients carrying the $\Delta F508$ mutation. Given the very large number of CFTR mutations known to cause CF, this observation highlights how precision potentiator development might need to be tailored according to the CFTR genotype, as potentiators developed for potency/efficacy on $\Delta F508$ CFTR might not provide maximal therapeutic benefit to all CF patients.

Recently, the potentiator GLPG1837, developed by Abbvie–Galapagos, has also entered clinical trials. Although GLPG1837 was found to be more effective on G551D and G1349D CFTR than VX-770, the mechanisms of action of the two drugs seem similar; indeed, GLPG1837 also potentiates both WT CFTR and nonhydrolytic mutants and acts by speeding channel opening and by slowing both hydrolytic and nonhydrolytic pore closure (265). Thus, just as for VX-770, a plausible mechanism for GLPG1837 might be stabilization of state O_1 relative to C_1 , O_2 (FIGURE 2A), and T (FIGURE 3B). In line with such an explanation, GLPG1837 also stimulates spontaneous CFTR opening (265). In contrast to NPPB, which acts synergistically with VX-770, suggesting distinct binding sites, GLPG1837 and VX-770 act competitively, suggesting that binding of these two drugs is mutually exclusive (i.e., that their binding sites might overlap) (265).

Several additional laboratories are actively involved in CFTR potentiator development. Employing high-throughput screening, the Verkman group was the first to identify potentiators with low micromolar (84) or submicromolar (152, 180) affinities based on a variety of structurally unrelated chemical scaffolds. Furthermore, some of their recently identified potentiators have been shown not to reduce plasma membrane density of $\Delta F508$ CFTR or to interfere with the corrector effect of VX-809 and are, therefore, promising candidates for CF therapy of patients carrying $\Delta F508$, or similar phenotype alleles (182). Other groups have identified potential lead compounds capable of increasing CFTR open probability [(79, 127, 179), <https://www.cff.org/Trials/Pipeline/details/91/QBW251>]. However, so far, the mechanisms of action of all these compounds have not been studied in detail.

The recognition that CFTR plays a vital physiological role in regulating transepithelial fluid movement has prompted researchers to start considering it as a pharmacological target for treatment of disorders other than CF. Potentiators might be useful for the treatment of other airway diseases sharing characteristics with CF, such as mucus stasis and CFTR dysfunction/inhibition. One such area of clinical interest is the treatment of chronic obstructive pulmonary

disease (191, 214). Focusing, instead, on CFTR expressed in intestinal epithelia, initial results suggest CFTR potentiators can outperform currently approved treatments for constipation (47, 217).

In contrast, CFTR inhibitors might provide benefit in diseases characterized by excessive transepithelial fluid movement. Such compounds could help prevent cyst formation in autosomal dominant polycystic kidney disease (132, 263) and could be crucial in preventing death by dehydration caused by secretory diarrheas (e.g., following cholera infection), especially in situations in which obtaining safe water for oral rehydration therapy is problematic (229). The voltage-dependent pore blocker GlyH-101 that acts from outside the cell has been described (Section IIID). CFTR_{inh}-172 (3-[(3-trifluoromethyl)phenyl]-5-[(4-carboxyphenyl)methylene]-2-thioxo-4-thiazolidinone) was identified by high-throughput screening as a membrane-permeant compound that inhibits CFTR currents in a voltage-independent manner with a K_I of ~ 300 nM (151). Studies addressing the mechanism of this inhibition concluded that CFTR_{inh}-172 does not act as a pore blocker, but rather as a gating modifier that delays pore opening and accelerates pore closure (124, 228). More recently, higher-potency benzopyrimido-pyrrolo-oxazinedione compounds have been identified that bind at site 2 in competition with ATP, thus impeding channel opening (118). The nanomolar potency attained with these compounds might make such drugs specific enough to avoid short-term toxicity at non-target ATP binding sites.

VII. CONCLUDING REMARKS

Almost three decades after the cloning of the CFTR gene, our understanding of CFTR structure and function has seen tremendous progress; meanwhile, high-throughput screening has led to the development of potentiator and corrector drugs that are finding their way to clinical application. There are undoubtedly still major gaps in our knowledge that need to be filled. These include unraveling what an open channel looks like and what state the outward-facing zebrafish CFTR structure represents, clarifying the existence and functional significance of reentry events, determining the extent of interface separation in the degenerate site of closed channels during gating, dissecting possible conformations of the R domain and their dependence on phosphorylation, and mapping protein/protein interactions of CFTR with scaffolding proteins and with other channels and transporters. That notwithstanding, with the recent breakthrough provided by the first high-resolution structures, CFTR research has transitioned into a new era, one that holds the promise of exploiting atomic-level structural information and advances in mechanistic understanding of CFTR molecular motions to guide drug development. There is now well-grounded hope that decades of basic research could soon strongly impact human health, result-

ing in novel treatments for a variety of disorders and an effective causative treatment for both common and rare forms of CF.

GRANTS

Supported by Cystic Fibrosis Trust Project no. SRC 005 and Sparks Grant reference no. 15UCL04 (to P. Vergani), and Hungarian Academy of Sciences Lendület Grant LP2017–14/2017 and Cystic Fibrosis Foundation Research Grant CSANAD17G0 (to L. Csanády).

DISCLOSURES

No conflicts of interest, financial or otherwise, are declared by the author(s).

REFERENCES

- Ai T, Bompadre SG, Sohma Y, Wang X, Li M, Hwang TC. Direct effects of 9-anthracene compounds on cystic fibrosis transmembrane conductance regulator gating. *Pflügers Arch* 449: 88–95, 2004. doi:10.1007/s00424-004-1317-y.
- Ai T, Bompadre SG, Wang X, Hu S, Li M, Hwang TC. Capsaicin potentiates wild-type and mutant cystic fibrosis transmembrane conductance regulator chloride-channel currents. *Mol Pharmacol* 65: 1415–1426, 2004. doi:10.1124/mol.65.6.1415.
- Aleksandrov AA, Aleksandrov L, Riordan JR. Nucleoside triphosphate pentose ring impact on CFTR gating and hydrolysis. *FEBS Lett* 518: 183–188, 2002. doi:10.1016/S0014-5793(02)02698-4.
- Aleksandrov AA, Chang X, Aleksandrov L, Riordan JR. The non-hydrolytic pathway of cystic fibrosis transmembrane conductance regulator ion channel gating. *J Physiol* 528: 259–265, 2000. doi:10.1111/j.1469-7793.2000.00259.x.
- Aleksandrov AA, Cui L, Riordan JR. Relationship between nucleotide binding and ion channel gating in cystic fibrosis transmembrane conductance regulator. *J Physiol* 587: 2875–2886, 2009. doi:10.1113/jphysiol.2009.170258.
- Aleksandrov AA, Riordan JR. Regulation of CFTR ion channel gating by MgATP. *FEBS Lett* 431: 97–101, 1998. doi:10.1016/S0014-5793(98)00713-3.
- Aleksandrov L, Aleksandrov AA, Chang XB, Riordan JR. The First Nucleotide Binding Domain of Cystic Fibrosis Transmembrane Conductance Regulator Is a Site of Stable Nucleotide Interaction, whereas the Second Is a Site of Rapid Turnover. *J Biol Chem* 277: 15419–15425, 2002. doi:10.1074/jbc.M111713200.
- Aller SG, Yu J, Ward A, Weng Y, Chittaboina S, Zhuo R, Harrell PM, Trinh YT, Zhang Q, Urbatsch IL, Chang G. Structure of P-glycoprotein reveals a molecular basis for poly-specific drug binding. *Science* 323: 1718–1722, 2009. doi:10.1126/science.1168750.
- Anderson MP, Berger HA, Rich DP, Gregory RJ, Smith AE, Welsh MJ. Nucleoside triphosphates are required to open the CFTR chloride channel. *Cell* 67: 775–784, 1991. doi:10.1016/0092-8674(91)90072-7.
- Auerbach A. How to turn the reaction coordinate into time. *J Gen Physiol* 130: 543–546, 2007. doi:10.1085/jgp.200709898.
- Bai Y, Li M, Hwang TC. Dual roles of the sixth transmembrane segment of the CFTR chloride channel in gating and permeation. *J Gen Physiol* 136: 293–309, 2010. doi:10.1085/jgp.201010480.
- Bai Y, Li M, Hwang TC. Structural basis for the channel function of a degraded ABC transporter, CFTR (ABCC7). *J Gen Physiol* 138: 495–507, 2011. doi:10.1085/jgp.201110705.
- Bársony O, Szalóki G, Türk D, Tarapcsák S, Gutay-Tóth Z, Bacsó Z, Holb JJ, Székölgyi L, Szabó G, Csanády L, Szakács G, Goda K. A single active catalytic site is sufficient to promote transport in P-glycoprotein. *Sci Rep* 6: 24810, 2016. doi:10.1038/srep24810.
- Basso C, Vergani P, Nairn AC, Gadsby DC. Prolonged nonhydrolytic interaction of nucleotide with CFTR's NH₂-terminal nucleotide binding domain and its role in channel gating. *J Gen Physiol* 122: 333–348, 2003. doi:10.1085/jgp.200308798.
- Baukowitz T, Hwang TC, Nairn AC, Gadsby DC. Coupling of CFTR Cl⁻ channel gating to an ATP hydrolysis cycle. *Neuron* 12: 473–482, 1994. doi:10.1016/0896-6273(94)90206-2.
- Bear CE, Li CH, Kartner N, Bridges RJ, Jensen TJ, Ramjeesingh M, Riordan JR. Purification and functional reconstitution of the cystic fibrosis transmembrane conductance regulator (CFTR). *Cell* 68: 809–818, 1992. doi:10.1016/0092-8674(92)90155-6.
- Beck EJ, Yang Y, Yaemsiri S, Raghuram V. Conformational changes in a pore-lining helix coupled to cystic fibrosis transmembrane conductance regulator channel gating. *J Biol Chem* 283: 4957–4966, 2008. doi:10.1074/jbc.M702235200.
- Becq F, Verrier B, Chang XB, Riordan JR, Hanrahan JW. cAMP- and Ca²⁺-independent activation of cystic fibrosis transmembrane conductance regulator channels by phenylimidazothiazole drugs. *J Biol Chem* 271: 16171–16179, 1996. doi:10.1074/jbc.271.27.16171.
- Berger AL, Randak CO, Ostedgaard LS, Karp PH, Vermeer DW, Welsh MJ. Curcumin stimulates cystic fibrosis transmembrane conductance regulator Cl⁻ channel activity. *J Biol Chem* 280: 5221–5226, 2005. doi:10.1074/jbc.M412972200.
- Berger HA, Anderson MP, Gregory RJ, Thompson S, Howard PW, Maurer RA, Muligan R, Smith AE, Welsh MJ. Identification and regulation of the cystic fibrosis transmembrane conductance regulator-generated chloride channel. *J Clin Invest* 88: 1422–1431, 1991. doi:10.1172/JCI115450.
- Berger HA, Travis SM, Welsh MJ. Regulation of the cystic fibrosis transmembrane conductance regulator Cl⁻ channel by specific protein kinases and protein phosphatases. *J Biol Chem* 268: 2037–2047, 1993.
- Billet A, Jia Y, Jensen T, Riordan JR, Hanrahan JW. Regulation of the cystic fibrosis transmembrane conductance regulator anion channel by tyrosine phosphorylation. *FASEB J* 29: 3945–3953, 2015. doi:10.1096/fj.15-273151. An addendum to this article is available at <http://dx.doi.org/10.1080/19336950.2015.1126010>.
- Billet A, Jia Y, Jensen TJ, Hou YX, Chang XB, Riordan JR, Hanrahan JW. Potential sites of CFTR activation by tyrosine kinases. *Channels (Austin)* 10: 247–251, 2016. doi:10.1080/19336950.2015.1126010. An addendum to this article is available at <http://dx.doi.org/10.1096/fj.15-273151>.
- Bompadre SG, Ai T, Cho JH, Wang X, Sohma Y, Li M, Hwang TC. CFTR gating I: Characterization of the ATP-dependent gating of a phosphorylation-independent CFTR channel (DeltaR-CFTR). *J Gen Physiol* 125: 361–375, 2005. doi:10.1085/jgp.200409227.
- Bompadre SG, Cho JH, Wang X, Zou X, Sohma Y, Li M, Hwang TC. CFTR gating II: Effects of nucleotide binding on the stability of open states. *J Gen Physiol* 125: 377–394, 2005. doi:10.1085/jgp.200409228.
- Bompadre SG, Sohma Y, Li M, Hwang TC. G551D and G1349D, two CF-associated mutations in the signature sequences of CFTR, exhibit distinct gating defects. *J Gen Physiol* 129: 285–298, 2007. doi:10.1085/jgp.200609667.
- Boucher RC. Regulation of airway surface liquid volume by human airway epithelia. *Pflügers Arch* 445: 495–498, 2003. doi:10.1007/s00424-002-0955-1.
- Boucher RC, Stutts MJ, Knowles MR, Cantley L, Gatzky JT. Na⁺ transport in cystic fibrosis respiratory epithelia. Abnormal basal rate and response to adenylate cyclase activation. *J Clin Invest* 78: 1245–1252, 1986. doi:10.1172/JCI112708.
- Bozoky Z, Krzeminski M, Muhandiram R, Birtley JR, Al-Zahrani A, Thomas PJ, Frizzell RA, Ford RC, Forman-Kay JD. Regulatory R region of the CFTR chloride channel is a dynamic integrator of phospho-dependent intra- and intermolecular interactions. *Proc Natl Acad Sci USA* 110: E4427–E4436, 2013. doi:10.1073/pnas.1315104110.
- Cai Z, Scott-Ward TS, Sheppard DN. Voltage-dependent gating of the cystic fibrosis transmembrane conductance regulator Cl⁻ channel. *J Gen Physiol* 122: 605–620, 2003. doi:10.1085/jgp.200308921.
- Carrasco AJ, Dzeja PP, Alekseev AE, Pucar D, Zingman LV, Abraham MR, Hodgson D, Bienengraeber M, Puceat M, Janssen E, Wieringa B, Terzic A. Adenylate kinase phosphotransfer communicates cellular energetic signals to ATP-sensitive potassium channels. *Proc Natl Acad Sci USA* 98: 7623–7628, 2001. doi:10.1073/pnas.121038198.

32. Carson MR, Travis SM, Welsh MJ. The two nucleotide-binding domains of cystic fibrosis transmembrane conductance regulator (CFTR) have distinct functions in controlling channel activity. *J Biol Chem* 270: 1711–1717, 1995. doi:[10.1074/jbc.270.4.1711](https://doi.org/10.1074/jbc.270.4.1711).
33. Chan KW, Csanády L, Seto-Young D, Nairn AC, Gadsby DC. Severed molecules functionally define the boundaries of the cystic fibrosis transmembrane conductance regulator's NH₂-terminal nucleotide binding domain. *J Gen Physiol* 116: 163–180, 2000. doi:[10.1085/jgp.116.2.163](https://doi.org/10.1085/jgp.116.2.163).
34. Chang XB, Tabcharani JA, Hou YX, Jensen TJ, Kartner N, Alon N, Hanrahan JW, Riordan JR. Protein kinase A (PKA) still activates CFTR chloride channel after mutagenesis of all 10 PKA consensus phosphorylation sites. *J Biol Chem* 268: 11304–11311, 1993.
35. Chappe V, Hinkson DA, Zhu T, Chang XB, Riordan JR, Hanrahan JW. Phosphorylation of protein kinase C sites in NBD1 and the R domain control CFTR channel activation by PKA. *J Physiol* 548: 39–52, 2003. doi:[10.1113/jphysiol.2002.035790](https://doi.org/10.1113/jphysiol.2002.035790).
36. Chappe V, Irvine T, Liao J, Evagelidis A, Hanrahan JW. Phosphorylation of CFTR by PKA promotes binding of the regulatory domain. *EMBO J* 24: 2730–2740, 2005. doi:[10.1038/sj.emboj.7600747](https://doi.org/10.1038/sj.emboj.7600747).
37. Chaves LAP, Gadsby DC. Cysteine accessibility probes timing and extent of NBD separation along the dimer interface in gating CFTR channels. *J Gen Physiol* 145: 261–283, 2015. doi:[10.1085/jgp.201411347](https://doi.org/10.1085/jgp.201411347).
38. Chen J, Lu G, Lin J, Davidson AL, Quioco FA. A tweezers-like motion of the ATP-binding cassette dimer in an ABC transport cycle. *Mol Cell* 12: 651–661, 2003. doi:[10.1016/j.molcel.2003.08.004](https://doi.org/10.1016/j.molcel.2003.08.004).
39. Chen JH, Stoltz DA, Karp PH, Ernst SE, Pezzulo AA, Moninger TO, Rector MV, Reznikov LR, Launspach JL, Chaloner K, Zabner J, Welsh MJ. Loss of anion transport without increased sodium absorption characterizes newborn porcine cystic fibrosis airway epithelia. *Cell* 143: 911–923, 2010. doi:[10.1016/j.cell.2010.11.029](https://doi.org/10.1016/j.cell.2010.11.029).
40. Chen JH, Xu W, Sheppard DN. Altering intracellular pH reveals the kinetic basis of intraburst gating in the CFTR Cl⁻ channel. *J Physiol* 595: 1059–1076, 2017. doi:[10.1113/JP273205](https://doi.org/10.1113/JP273205).
41. Chen L, Patel RP, Teng X, Bosworth CA, Lancaster JR Jr, Matalon S. Mechanisms of cystic fibrosis transmembrane conductance regulator activation by S-nitrosoglutathione. *J Biol Chem* 281: 9190–9199, 2006. doi:[10.1074/jbc.M513231200](https://doi.org/10.1074/jbc.M513231200).
42. Cheng SH, Gregory RJ, Marshall J, Paul S, Souza DW, White GA, O'Riordan CR, Smith AE. Defective intracellular transport and processing of CFTR is the molecular basis of most cystic fibrosis. *Cell* 63: 827–834, 1990. doi:[10.1016/0092-8674\(90\)90148-8](https://doi.org/10.1016/0092-8674(90)90148-8).
43. Cheng SH, Rich DP, Marshall J, Gregory RJ, Welsh MJ, Smith AE. Phosphorylation of the R domain by cAMP-dependent protein kinase regulates the CFTR chloride channel. *Cell* 66: 1027–1036, 1991. doi:[10.1016/0092-8674\(91\)90446-6](https://doi.org/10.1016/0092-8674(91)90446-6).
44. Chinet TC, Fullton JM, Yankaskas JR, Boucher RC, Stutts MJ. Mechanism of sodium hyperabsorption in cultured cystic fibrosis nasal epithelium: a patch-clamp study. *Am J Physiol* 266: C1061–C1068, 1994. doi:[10.1152/ajpcell.1994.266.4.C1061](https://doi.org/10.1152/ajpcell.1994.266.4.C1061).
45. Cholon DM, Quinney NL, Fulcher ML, Esther CR Jr, Das J, Dokholyan NV, Randell SH, Boucher RC, Gentsch M. Potentiator ivacaftor abrogates pharmacological correction of ΔF508 CFTR in cystic fibrosis. *Sci Transl Med* 6: 246ra96, 2014. doi:[10.1126/scitranslmed.3008680](https://doi.org/10.1126/scitranslmed.3008680).
46. Choudhury HG, Tong Z, Mathavan I, Li Y, Iwata S, Zirah S, Rebuffat S, van Veen HW, Beis K. Structure of an antibacterial peptide ATP-binding cassette transporter in a novel outward occluded state. *Proc Natl Acad Sci USA* 111: 9145–9150, 2014. doi:[10.1073/pnas.1320506111](https://doi.org/10.1073/pnas.1320506111).
47. Cil O, Phuan PW, Son JH, Zhu JS, Ku CK, Tabib NA, Teuthorn AP, Ferrera L, Zachos NC, Lin R, Galiotta LJ, Donowitz M, Kurth MJ, Verkman AS. Phenylquinoxalinone CFTR activator as potential prosecretory therapy for constipation. *Transl Res* 182: 14–26.e4, 2017. doi:[10.1016/j.trsl.2016.10.003](https://doi.org/10.1016/j.trsl.2016.10.003).
48. Cohn JA, Nairn AC, Marino CR, Melhus O, Kole J. Characterization of the cystic fibrosis transmembrane conductance regulator in a colonocyte cell line. *Proc Natl Acad Sci USA* 89: 2340–2344, 1992. doi:[10.1073/pnas.89.6.2340](https://doi.org/10.1073/pnas.89.6.2340).
49. Collavin L, Lazarevic D, Utrera R, Marzinotto S, Monte M, Schneider C. wt p53 dependent expression of a membrane-associated isoform of adenylate kinase. *Oncogene* 18: 5879–5888, 1999. doi:[10.1038/sj.onc.1202970](https://doi.org/10.1038/sj.onc.1202970).
50. Colquhoun D, Sigworth FJ. *Single channel recording* (Sakmann B, Neher E, editors). New York: Plenum Press, 1995.
51. Corradi V, Gu RX, Vergani P, Tieleman DP. Structure of Transmembrane Helix 8 and Possible Membrane Defects in CFTR. *Biophys J* 114: 1751–1754, 2018. doi:[10.1016/j.bpj.2018.03.003](https://doi.org/10.1016/j.bpj.2018.03.003).
52. Corradi V, Vergani P, Tieleman DP. Cystic fibrosis transmembrane conductance regulator (CFTR): closed and open state channel models. *J Biol Chem* 290: 22891–22906, 2015. doi:[10.1074/jbc.M115.665125](https://doi.org/10.1074/jbc.M115.665125).
53. Csanády L. Application of rate-equilibrium free energy relationship analysis to non-equilibrium ion channel gating mechanisms. *J Gen Physiol* 134: 129–136, 2009. doi:[10.1085/jgp.200910268](https://doi.org/10.1085/jgp.200910268).
54. Csanády L, Chan KW, Nairn AC, Gadsby DC. Functional roles of nonconserved structural segments in CFTR's NH₂-terminal nucleotide binding domain. *J Gen Physiol* 125: 43–55, 2005. doi:[10.1085/jgp.200409174](https://doi.org/10.1085/jgp.200409174).
55. Csanády L, Chan KW, Seto-Young D, Kopsco DC, Nairn AC, Gadsby DC. Severed channels probe regulation of gating of cystic fibrosis transmembrane conductance regulator by its cytoplasmic domains. *J Gen Physiol* 116: 477–500, 2000. doi:[10.1085/jgp.116.3.477](https://doi.org/10.1085/jgp.116.3.477).
56. Csanády L, Mihályi C, Szollosi A, Töröcsik B, Vergani P. Conformational changes in the catalytically inactive nucleotide-binding site of CFTR. *J Gen Physiol* 142: 61–73, 2013. doi:[10.1085/jgp.201210954](https://doi.org/10.1085/jgp.201210954).
57. Csanády L, Nairn AC, Gadsby DC. Thermodynamics of CFTR channel gating: a spreading conformational change initiates an irreversible gating cycle. *J Gen Physiol* 128: 523–533, 2006. doi:[10.1085/jgp.200609558](https://doi.org/10.1085/jgp.200609558).
58. Csanády L, Seto-Young D, Chan KW, Cenciarelli C, Angel BB, Qin J, McLachlin DT, Krutchinsky AN, Chait BT, Nairn AC, Gadsby DC. Preferential phosphorylation of R-domain Serine 768 dampens activation of CFTR channels by PKA. *J Gen Physiol* 125: 171–186, 2005. doi:[10.1085/jgp.200409076](https://doi.org/10.1085/jgp.200409076).
59. Csanády L, Töröcsik B. Catalyst-like modulation of transition states for CFTR channel opening and closing: new stimulation strategy exploits nonequilibrium gating. *J Gen Physiol* 143: 269–287, 2014. doi:[10.1085/jgp.201311089](https://doi.org/10.1085/jgp.201311089).
60. Csanády L, Töröcsik B. Structure-activity analysis of a CFTR channel potentiator: Distinct molecular parts underlie dual gating effects. *J Gen Physiol* 144: 321–336, 2014. doi:[10.1085/jgp.201411246](https://doi.org/10.1085/jgp.201411246).
61. Csanády L, Vergani P, Gadsby DC. Strict coupling between CFTR's catalytic cycle and gating of its Cl⁻ ion pore revealed by distributions of open channel burst durations. *Proc Natl Acad Sci USA* 107: 1241–1246, 2010. doi:[10.1073/pnas.0911061107](https://doi.org/10.1073/pnas.0911061107).
62. Cui G, McCarty NA. Murine and human CFTR exhibit different sensitivities to CFTR potentiators. *Am J Physiol Lung Cell Mol Physiol* 309: L687–L699, 2015. doi:[10.1152/ajplung.00181.2015](https://doi.org/10.1152/ajplung.00181.2015).
63. Cui G, Song B, Turki HW, McCarty NA. Differential contribution of TM6 and TM12 to the pore of CFTR identified by three sulfonylurea-based blockers. *Pflügers Arch* 463: 405–418, 2012. doi:[10.1007/s00424-011-1035-1](https://doi.org/10.1007/s00424-011-1035-1).
64. Cui G, Rahman KS, Infield DT, Kuang C, Prince CZ, McCarty NA. Three charged amino acids in extracellular loop 1 are involved in maintaining the outer pore architecture of CFTR. *J Gen Physiol* 144: 159–179, 2014. doi:[10.1085/jgp.201311122](https://doi.org/10.1085/jgp.201311122).
65. Cui L, Aleksandrov L, Chang XB, Hou YX, He L, Hegedus T, Gentsch M, Aleksandrov A, Balch WE, Riordan JR. Domain interdependence in the biosynthetic assembly of CFTR. *J Mol Biol* 365: 981–994, 2007. doi:[10.1016/j.jmb.2006.10.086](https://doi.org/10.1016/j.jmb.2006.10.086).
66. Dalemans W, Barby P, Champigny G, Jallat S, Dott K, Dreyer D, Crystal RG, Pavirani A, Lecocq JP, Lazdunski M. Altered chloride ion channel kinetics associated with the delta F508 cystic fibrosis mutation. *Nature* 354: 526–528, 1991. doi:[10.1038/354526a0](https://doi.org/10.1038/354526a0).
67. Dawson RJP, Locher KP. Structure of a bacterial multidrug ABC transporter. *Nature* 443: 180–185, 2006. doi:[10.1038/nature05155](https://doi.org/10.1038/nature05155).
68. De Boeck K, Amaral MD. Progress in therapies for cystic fibrosis. *Lancet Respir Med* 4: 662–674, 2016. doi:[10.1016/S2213-2600\(16\)00023-0](https://doi.org/10.1016/S2213-2600(16)00023-0).
69. Dean M, Annilo T. Evolution of the ATP-binding cassette (ABC) transporter superfamily in vertebrates. *Annu Rev Genomics Hum Genet* 6: 123–142, 2005. doi:[10.1146/annurev.genom.6.080604.162122](https://doi.org/10.1146/annurev.genom.6.080604.162122).

70. Dong Q, Ernst SE, Ostedgaard LS, Shah VS, Ver Heul AR, Welsh MJ, Randak CO. Mutating the Conserved Q-loop Glutamine 1291 Selectively Disrupts Adenylate Kinase-dependent Channel Gating of the ATP-binding Cassette (ABC) Adenylate Kinase Cystic Fibrosis Transmembrane Conductance Regulator (CFTR) and Reduces Channel Function in Primary Human Airway Epithelia. *J Biol Chem* 290: 14140–14153, 2015. doi:10.1074/jbc.M114.611616.
71. Dousmanis AG, Nairn AC, Gadsby DC. Distinct Mg(2+)-dependent steps rate limit opening and closing of a single CFTR Cl(-) channel. *J Gen Physiol* 119: 545–559, 2002. doi:10.1085/jgp.20028594.
72. Dulhanty AM, Riordan JR. Phosphorylation by cAMP-dependent protein kinase causes a conformational change in the R domain of the cystic fibrosis transmembrane conductance regulator. *Biochemistry* 33: 4072–4079, 1994. doi:10.1021/bi00179a036.
73. Dzeja P, Terzic A. Adenylate kinase and AMP signaling networks: metabolic monitoring, signal communication and body energy sensing. *Int J Mol Sci* 10: 1729–1772, 2009. doi:10.3390/ijms10041729.
74. Eckford PD, Li C, Ramjeesingh M, Bear CE. Cystic fibrosis transmembrane conductance regulator (CFTR) potentiator VX-770 (ivacaftor) opens the defective channel gate of mutant CFTR in a phosphorylation-dependent but ATP-independent manner. *J Biol Chem* 287: 36639–36649, 2012. doi:10.1074/jbc.M112.393637.
75. El Hiani Y, Linsdell P. Changes in accessibility of cytoplasmic substances to the pore associated with activation of the cystic fibrosis transmembrane conductance regulator chloride channel. *J Biol Chem* 285: 32126–32140, 2010. doi:10.1074/jbc.M110.113332.
76. El Hiani Y, Linsdell P. Functional Architecture of the Cytoplasmic Entrance to the Cystic Fibrosis Transmembrane Conductance Regulator Chloride Channel Pore. *J Biol Chem* 290: 15855–15865, 2015. doi:10.1074/jbc.M115.656181.
77. El Hiani Y, Negoda A, Linsdell P. Cytoplasmic pathway followed by chloride ions to enter the CFTR channel pore. *Cell Mol Life Sci* 73: 1917–1925, 2016. doi:10.1007/s00018-015-2113-x.
78. Fatehi M, Linsdell P. Novel residues lining the CFTR chloride channel pore identified by functional modification of introduced cysteines. *J Membr Biol* 228: 151–164, 2009. doi:10.1007/s00232-009-9167-3.
79. Favia M, Mancini MT, Bezzerri V, Guerra L, Lasela O, Abbattiscianni AC, Debellis L, Reshkin SJ, Gambari R, Cabrini G, Casavola V. Trimethylangelicin promotes the functional rescue of mutant F508del CFTR protein in cystic fibrosis airway cells. *Am J Physiol Lung Cell Mol Physiol* 307: L48–L61, 2014. doi:10.1152/ajplung.00305.2013.
80. Fischer H, Illek B, Machen TE. Regulation of CFTR by protein phosphatase 2B and protein kinase C. *Pflugers Arch* 436: 175–181, 1998. doi:10.1007/s004240050620.
81. Fischer H, Machen TE. The tyrosine kinase p60c-src regulates the fast gate of the cystic fibrosis transmembrane conductance regulator chloride channel. *Biophys J* 71: 3073–3082, 1996. doi:10.1016/S0006-3495(96)79501-2.
82. French PJ, Bijman J, Edixhoven M, Vaandrager AB, Scholte BJ, Lohmann SM, Nairn AC, de Jonge HR. Isotype-specific activation of cystic fibrosis transmembrane conductance regulator-chloride channels by cGMP-dependent protein kinase II. *J Biol Chem* 270: 26626–26631, 1995. doi:10.1074/jbc.270.44.26626.
83. Gadsby DC. Ion channels versus ion pumps: the principal difference, in principle. *Nat Rev Mol Cell Biol* 10: 344–352, 2009. doi:10.1038/nrm2668.
84. Galiotta LJ, Springsteel MF, Eda M, Niedzinski EJ, By K, Haddadin MJ, Kurth MJ, Nantz MH, Verkman AS. Novel CFTR chloride channel activators identified by screening of combinatorial libraries based on flavone and benzoquinolizinium lead compounds. *J Biol Chem* 276: 19723–19728, 2001. doi:10.1074/jbc.M101892200.
85. Gao X, Bai Y, Hwang TC. Cysteine scanning of CFTR's first transmembrane segment reveals its plausible roles in gating and permeation. *Biophys J* 104: 786–797, 2013. doi:10.1016/j.bpj.2012.12.048.
86. Gao X, Hwang TC. Spatial positioning of CFTR's pore-lining residues affirms an asymmetrical contribution of transmembrane segments to the anion permeation pathway. *J Gen Physiol* 147: 407–422, 2016. doi:10.1085/jgp.201511557.
87. Gao X, Hwang TC. Localizing a gate in CFTR. *Proc Natl Acad Sci USA* 112: 2461–2466, 2015. doi:10.1073/pnas.1420676112.
88. Ge N, Muise CN, Gong X, Linsdell P. Direct comparison of the functional roles played by different transmembrane regions in the cystic fibrosis transmembrane conductance regulator chloride channel pore. *J Biol Chem* 279: 55283–55289, 2004. doi:10.1074/jbc.M411935200.
89. Gentzsch M, Dang H, Dang Y, Garcia-Caballero A, Suchindran H, Boucher RC, Stutts MJ. The cystic fibrosis transmembrane conductance regulator impedes proteolytic stimulation of the epithelial Na+ channel. *J Biol Chem* 285: 32227–32232, 2010. doi:10.1074/jbc.M110.155259.
90. Gong X, Burbridge SM, Cowley EA, Linsdell P. Molecular determinants of Au(CN)(2)(-) binding and permeability within the cystic fibrosis transmembrane conductance regulator Cl(-) channel pore. *J Physiol* 540: 39–47, 2002. doi:10.1113/jphysiol.2001.013235.
91. Gray MA, Pollard CE, Harris A, Coleman L, Greenwell JR, Argent BE. Anion selectivity and block of the small-conductance chloride channel on pancreatic duct cells. *Am J Physiol* 259: C752–C761, 1990. doi:10.1152/ajpcell.1990.259.5.C752.
92. Grosman C, Auerbach A. The dissociation of acetylcholine from open nicotinic receptor channels. *Proc Natl Acad Sci USA* 98: 14102–14107, 2001. doi:10.1073/pnas.251402498.
93. Gross CH, Abdul-Manan N, Fulghum J, Lippe J, Liu X, Prabhakar P, Brennan D, Willis MS, Faerman C, Connelly P, Raybuck S, Moore J. Nucleotide-binding domains of cystic fibrosis transmembrane conductance regulator, an ABC transporter, catalyze adenylate kinase activity but not ATP hydrolysis. *J Biol Chem* 281: 4058–4068, 2006. doi:10.1074/jbc.M511113200.
94. Grunwald E. Structure-energy relations, reaction mechanism, and disparity of progress of concerted reaction events. *J Am Chem Soc* 107: 125–133, 1985. doi:10.1021/ja00287a023.
95. Gunderson KL, Kopito RR. Effects of pyrophosphate and nucleotide analogs suggest a role for ATP hydrolysis in cystic fibrosis transmembrane regulator channel gating. *J Biol Chem* 269: 19349–19353, 1994.
96. Gunderson KL, Kopito RR. Conformational states of CFTR associated with channel gating: the role ATP binding and hydrolysis. *Cell* 82: 231–239, 1995. doi:10.1016/0092-8674(95)90310-0.
97. Hallows KR, McCane JE, Kemp BE, Witters LA, Foskett JK. Regulation of channel gating by AMP-activated protein kinase modulates cystic fibrosis transmembrane conductance regulator activity in lung submucosal cells. *J Biol Chem* 278: 998–1004, 2003. doi:10.1074/jbc.M210621200.
98. Hallows KR, Raghuram V, Kemp BE, Witters LA, Foskett JK. Inhibition of cystic fibrosis transmembrane conductance regulator by novel interaction with the metabolic sensor AMP-activated protein kinase. *J Clin Invest* 105: 1711–1721, 2000. doi:10.1172/JCI9622.
99. He L, Aleksandrov AA, Serohijos AWR, Hegedus T, Aleksandrov LA, Cui L, Dokholyan NV, Riordan JR. Multiple membrane-cytoplasmic domain contacts in the cystic fibrosis transmembrane conductance regulator (CFTR) mediate regulation of channel gating. *J Biol Chem* 283: 26383–26390, 2008. doi:10.1074/jbc.M803894200.
100. Hegedus T, Aleksandrov A, Mengos A, Cui L, Jensen TJ, Riordan JR. Role of individual R domain phosphorylation sites in CFTR regulation by protein kinase A. *Biochim Biophys Acta* 1788: 1341–1349, 2009. doi:10.1016/j.bbame.2009.03.015.
101. Hohl M, Briand C, Grütter MG, Seeger MA. Crystal structure of a heterodimeric ABC transporter in its inward-facing conformation. *Nat Struct Mol Biol* 19: 395–402, 2012. doi:10.1038/nsmb.2267.
102. Hou Y, Cui L, Riordan JR, Chang X. Allosteric interactions between the two non-equivalent nucleotide binding domains of multidrug resistance protein MRP1. *J Biol Chem* 275: 20280–20287, 2000. doi:10.1074/jbc.M001109200.
103. Hwang TC, Nagel G, Nairn AC, Gadsby DC. Regulation of the gating of cystic fibrosis transmembrane conductance regulator Cl channels by phosphorylation and ATP hydrolysis. *Proc Natl Acad Sci USA* 91: 4698–4702, 1994. doi:10.1073/pnas.91.11.4698.
104. Hwang TC, Yeh JT, Zhang J, Yu YC, Yeh HI, Destefano S. Structural mechanisms of CFTR function and dysfunction. *J Gen Physiol* 150: 539–570, 2018.
105. Illek B, Fischer H, Santos GF, Widdicombe JH, Machen TE, Reenstra WW. cAMP-independent activation of CFTR Cl channels by the tyrosine kinase inhibitor genistein. *Am J Physiol* 268: C886–C893, 1995. doi:10.1152/ajpcell.1995.268.4.C886.

106. Illek B, Tam AW, Fischer H, Machen TE. Anion selectivity of apical membrane conductance of Calu 3 human airway epithelium. *Pflugers Arch* 437: 812–822, 1999. doi:10.1007/s004240050850.
107. Infield DT, Cui G, Kuang C, McCarty NA. Positioning of extracellular loop 1 affects pore gating of the cystic fibrosis transmembrane conductance regulator. *Am J Physiol Lung Cell Mol Physiol* 310: L403–L414, 2016. doi:10.1152/ajplung.00259.2015.
108. Ishiguro H, Steward MC, Naruse S, Ko SB, Goto H, Case RM, Kondo T, Yamamoto A. CFTR functions as a bicarbonate channel in pancreatic duct cells. *J Gen Physiol* 133: 315–326, 2009. doi:10.1085/jgp.200810122.
109. Ishihara H, Welsh MJ. Block by MOPS reveals a conformation change in the CFTR pore produced by ATP hydrolysis. *Am J Physiol* 273: C1278–C1289, 1997. doi:10.1152/ajpcell.1997.273.4.C1278.
110. Itani OA, Chen JH, Karp PH, Ernst S, Keshavjee S, Parekh K, Klesney-Tait J, Zabner J, Welsh MJ. Human cystic fibrosis airway epithelia have reduced Cl⁻ conductance but not increased Na⁺ conductance. *Proc Natl Acad Sci USA* 108: 10260–10265, 2011. doi:10.1073/pnas.1106695108.
111. Jia Y, Mathews CJ, Hanrahan JW. Phosphorylation by protein kinase C is required for acute activation of cystic fibrosis transmembrane conductance regulator by protein kinase A. *J Biol Chem* 272: 4978–4984, 1997. doi:10.1074/jbc.272.8.4978.
112. Jih KY, Hwang TC. VX-770 potentiates CFTR function by promoting decoupling between the gating cycle and ATP hydrolysis cycle. *Proc Natl Acad Sci USA* 110: 4404–4409, 2013. doi:10.1073/pnas.1215982110.
113. Jih KY, Sohma Y, Hwang TC. Nonintegral stoichiometry in CFTR gating revealed by a pore-lining mutation. *J Gen Physiol* 140: 347–359, 2012. doi:10.1085/jgp.201210834.
114. Jih KY, Sohma Y, Li M, Hwang TC. Identification of a novel post-hydrolytic state in CFTR gating. *J Gen Physiol* 139: 359–370, 2012. doi:10.1085/jgp.201210789.
115. Karpowich N, Martsinkevich O, Millen L, Yuan YR, Dai PL, MacVey K, Thomas PJ, Hunt JF. Crystal structures of the MJ1267 ATP binding cassette reveal an induced-fit effect at the ATPase active site of an ABC transporter. *Structure* 9: 571–586, 2001. doi:10.1016/S0969-2126(01)00617-7.
116. Kennelly PJ, Krebs EG. Consensus sequences as substrate specificity determinants for protein kinases and protein phosphatases. *J Biol Chem* 266: 15555–15558, 1991.
117. Kijima S, Kijima H. Statistical analysis of channel current from a membrane patch. I. Some stochastic properties of ion channels or molecular systems in equilibrium. *J Theor Biol* 128: 423–434, 1987. doi:10.1016/S0022-5193(87)80188-1.
118. Kim Y, Anderson MO, Park J, Lee MG, Namkung W, Verkman AS. Benzopyrimido-pyrrolo-oxazine-dione (R)-BPO-27 Inhibits CFTR Chloride Channel Gating by Competition with ATP. *Mol Pharmacol* 88: 689–696, 2015. doi:10.1124/mol.115.098368.
119. King JD Jr, Fitch AC, Lee JK, McCane JE, Mak DO, Foskett JK, Hallows KR. AMP-activated protein kinase phosphorylation of the R domain inhibits PKA stimulation of CFTR. *Am J Physiol Cell Physiol* 297: C94–C101, 2009. doi:10.1152/ajpcell.00677.2008.
120. Kirk KL, Wang W. A unified view of cystic fibrosis transmembrane conductance regulator (CFTR) gating: combining the allostereism of a ligand-gated channel with the enzymatic activity of an ATP-binding cassette (ABC) transporter. *J Biol Chem* 286: 12813–12819, 2011. doi:10.1074/jbc.R111.219634.
121. Knowles M, Gatzky J, Boucher R. Relative ion permeability of normal and cystic fibrosis nasal epithelium. *J Clin Invest* 71: 1410–1417, 1983. doi:10.1172/JCI110894.
122. Knowles MR, Stutts MJ, Spock A, Fischer N, Gatzky JT, Boucher RC. Abnormal ion permeation through cystic fibrosis respiratory epithelium. *Science* 221: 1067–1070, 1983. doi:10.1126/science.6308769.
123. Kongsuphol P, Cassidy D, Hieke B, Trehan KJ, Schreiber R, Mehta A, Kunzelmann K. Mechanistic insight into control of CFTR by AMPK. *J Biol Chem* 284: 5645–5653, 2009. doi:10.1074/jbc.M806780200.
124. Kopeikin Z, Sohma Y, Li M, Hwang TC. On the mechanism of CFTR inhibition by a thiazolidinone derivative. *J Gen Physiol* 136: 659–671, 2010. doi:10.1085/jgp.201010518.
125. Kopeikin Z, Yuksek Z, Yang HY, Bompadre SG. Combined effects of VX-770 and VX-809 on several functional abnormalities of F508del-CFTR channels. *J Cyst Fibros* 13: 508–514, 2014. doi:10.1016/j.jcf.2014.04.003.
126. Langron E, Prins S, Vergani P. Potentiation of the cystic fibrosis transmembrane conductance regulator by VX-770 involves stabilization of the pre-hydrolytic O1 state. *Br J Pharmacol* 175: 3990–4002, 2018. doi:10.1111/bph.14475.
127. Laselva O, Molinski S, Casavola V, Bear CE. The investigational Cystic Fibrosis drug Trimethylangelicin directly modulates CFTR by stabilizing the first membrane-spanning domain. *Biochem Pharmacol* 119: 85–92, 2016. doi:10.1016/j.bcp.2016.09.005.
128. Lazrak A, Jurkuvenaite A, Chen L, Keeling KM, Collawn JF, Bedwell DM, Matalon S. Enhancement of alveolar epithelial sodium channel activity with decreased cystic fibrosis transmembrane conductance regulator expression in mouse lung. *Am J Physiol Lung Cell Mol Physiol* 301: L557–L567, 2011. doi:10.1152/ajplung.00094.2011.
129. Lee MG, Ohana E, Park HW, Yang D, Muallem S. Molecular mechanism of pancreatic and salivary gland fluid and HCO₃ secretion. *Physiol Rev* 92: 39–74, 2012. doi:10.1152/physrev.00011.2011.
130. Lewis HA, Buchanan SG, Burley SK, Connors K, Dickey M, Dorwart M, Fowler R, Gao X, Guggino WB, Hendrickson WA, Hunt JF, Kearins MC, Lorimer D, Maloney PC, Post KW, Rajashankar KR, Rutter ME, Sauder JM, Shriver S, Thibodeau PH, Thomas PJ, Zhang M, Zhao X, Emtage S. Structure of nucleotide-binding domain 1 of the cystic fibrosis transmembrane conductance regulator. *EMBO J* 23: 282–293, 2004. doi:10.1038/sj.emboj.7600040.
131. Li C, Ramjeesingh M, Wang W, Garami E, Hewryk M, Lee D, Rommens JM, Galley K, Bear CE. ATPase activity of the cystic fibrosis transmembrane conductance regulator. *J Biol Chem* 271: 28463–28468, 1996. doi:10.1074/jbc.271.45.28463.
132. Li H, Yang W, Mendes F, Amaral MD, Sheppard DN. Impact of the cystic fibrosis mutation F508del-CFTR on renal cyst formation and growth. *Am J Physiol Renal Physiol* 303: F1176–F1186, 2012. doi:10.1152/ajprenal.00130.2012.
133. Lin WY, Jih KY, Hwang TC. A single amino acid substitution in CFTR converts ATP to an inhibitory ligand. *J Gen Physiol* 144: 311–320, 2014. doi:10.1085/jgp.201411247.
134. Lin WY, Sohma Y, Hwang TC. Synergistic Potentiation of Cystic Fibrosis Transmembrane Conductance Regulator Gating by Two Chemically Distinct Potentiators, Ivacaftor (VX-770) and 5-Nitro-2-(3-Phenylpropylamino) Benzoate. *Mol Pharmacol* 90: 275–285, 2016. doi:10.1124/mol.116.104570.
135. Linsdell P. Relationship between anion binding and anion permeability revealed by mutagenesis within the cystic fibrosis transmembrane conductance regulator chloride channel pore. *J Physiol* 531: 51–66, 2001. doi:10.1111/j.1469-7793.2001.0051j.x.
136. Linsdell P. Thiocyanate as a probe of the cystic fibrosis transmembrane conductance regulator chloride channel pore. *Can J Physiol Pharmacol* 79: 573–579, 2001. doi:10.1139/y01-041.
137. Linsdell P. Location of a common inhibitor binding site in the cytoplasmic vestibule of the cystic fibrosis transmembrane conductance regulator chloride channel pore. *J Biol Chem* 280: 8945–8950, 2005. doi:10.1074/jbc.M414354200.
138. Linsdell P. Interactions between permeant and blocking anions inside the CFTR chloride channel pore. *Biochim Biophys Acta* 1848: 1573–1590, 2015. doi:10.1016/j.bbamem.2015.04.004.
139. Linsdell P. Anion conductance selectivity mechanism of the CFTR chloride channel. *Biochim Biophys Acta* 1858: 740–747, 2016. doi:10.1016/j.bbamem.2016.01.009.
140. Linsdell P, Evagelidis A, Hanrahan JW. Molecular determinants of anion selectivity in the cystic fibrosis transmembrane conductance regulator chloride channel pore. *Biophys J* 78: 2973–2982, 2000. doi:10.1016/S0006-3495(00)76836-6.
141. Linsdell P, Hanrahan JW. Disulphonic stilbene block of cystic fibrosis transmembrane conductance regulator Cl⁻ channels expressed in a mammalian cell line and its regulation by a critical pore residue. *J Physiol* 496: 687–693, 1996. doi:10.1113/jphysiol.1996.sp021719.
142. Linsdell P, Hanrahan JW. Adenosine triphosphate-dependent asymmetry of anion permeation in the cystic fibrosis transmembrane conductance regulator chloride channel. *J Gen Physiol* 111: 601–614, 1998. doi:10.1085/jgp.111.4.601.
143. Linsdell P, Hanrahan JW. Glutathione permeability of CFTR. *Am J Physiol* 275: C323–C326, 1998. doi:10.1152/ajpcell.1998.275.1.C323.
144. Linsdell P, Tabcharani JA, Rommens JM, Hou YX, Chang XB, Tsui LC, Riordan JR, Hanrahan JW. Permeability of wild-type and mutant cystic fibrosis transmembrane conductance regulator chloride channels to polyatomic anions. *J Gen Physiol* 110: 355–364, 1997. doi:10.1085/jgp.110.4.355.

145. Liu F, Zhang Z, Csanády L, Gadsby DC, Chen J. Molecular Structure of the Human CFTR Ion Channel. *Cell* 169: 85–95.e8, 2017. doi:10.1016/j.cell.2017.02.024.
146. Locher KP. Structure and mechanism of ATP-binding cassette transporters. *Philos Trans R Soc Lond B Biol Sci* 364: 239–245, 2009. doi:10.1098/rstb.2008.0125.
147. Locher KP. Mechanistic diversity in ATP-binding cassette (ABC) transporters. *Nat Struct Mol Biol* 23: 487–493, 2016. doi:10.1038/nsmb.3216.
148. Lukacs GL, Verkman AS. CFTR: folding, misfolding and correcting the Δ F508 conformational defect. *Trends Mol Med* 18: 81–91, 2012. doi:10.1016/j.molmed.2011.10.003.
149. Luo J, Pato MD, Riordan JR, Hanrahan JW. Differential regulation of single CFTR channels by PP2C, PP2A, and other phosphatases. *Am J Physiol* 274: C1397–C1410, 1998. doi:10.1152/ajpcell.1998.274.5.C1397.
150. Ma J, Zhao J, Drumm ML, Xie J, Davis PB. Function of the R domain in the cystic fibrosis transmembrane conductance regulator chloride channel. *J Biol Chem* 272: 28133–28141, 1997. doi:10.1074/jbc.272.44.28133.
151. Ma T, Thiagarajah JR, Yang H, Sonawane ND, Folli C, Galiotta LJ, Verkman AS. Thiazolidinone CFTR inhibitor identified by high-throughput screening blocks cholera toxin-induced intestinal fluid secretion. *J Clin Invest* 110: 1651–1658, 2002. doi:10.1172/JCI0216112.
152. Ma T, Vetrivel L, Yang H, Pedemonte N, Zegarra-Moran O, Galiotta LJ, Verkman AS. High-affinity activators of cystic fibrosis transmembrane conductance regulator (CFTR) chloride conductance identified by high-throughput screening. *J Biol Chem* 277: 37235–37241, 2002. doi:10.1074/jbc.M205932200.
153. Marcus RA. Theoretical relations among rate constants, barriers, and bronsted slopes of chemical reactions. *J Phys Chem* 72: 891–899, 1968. doi:10.1021/j100849a019.
154. Mathews CJ, Tabcharani JA, Chang XB, Jensen TJ, Riordan JR, Hanrahan JW. Dibasic protein kinase A sites regulate bursting rate and nucleotide sensitivity of the cystic fibrosis transmembrane conductance regulator chloride channel. *J Physiol* 508: 365–377, 1998. doi:10.1111/j.1469-7793.1998.365bq.x.
155. Mathews CJ, Tabcharani JA, Hanrahan JW. The CFTR chloride channel: nucleotide interactions and temperature-dependent gating. *J Membr Biol* 163: 55–66, 1998. doi:10.1007/s002329900370.
156. McCarty NA, McDonough S, Cohen BN, Riordan JR, Davidson N, Lester HA. Voltage-dependent block of the cystic fibrosis transmembrane conductance regulator Cl⁻ channel by two closely related arylaminobenzoates. *J Gen Physiol* 102: 1–23, 1993. doi:10.1085/jgp.102.1.1.
157. McCarty NA, Zhang ZR. Identification of a region of strong discrimination in the pore of CFTR. *Am J Physiol Lung Cell Mol Physiol* 281: L852–L867, 2001. doi:10.1152/ajplung.2001.281.4.L852.
158. McDonough S, Davidson N, Lester HA, McCarty NA. Novel pore-lining residues in CFTR that govern permeation and open-channel block. *Neuron* 13: 623–634, 1994. doi:10.1016/0896-6273(94)90030-2.
159. Mense M, Vergani P, White DM, Altberg G, Nairn AC, Gadsby DC. In vivo phosphorylation of CFTR promotes formation of a nucleotide-binding domain heterodimer. *EMBO J* 25: 4728–4739, 2006. doi:10.1038/sj.emboj.7601373.
160. Mihályi C, Töröcsik B, Csanády L. Obligate coupling of CFTR pore opening to tight nucleotide-binding domain dimerization. *eLife* 5: e18164, 2016. doi:10.7554/eLife.18164.
161. Miki H, Zhou Z, Li M, Hwang TC, Bompadre SG. Potentiation of disease-associated cystic fibrosis transmembrane conductance regulator mutants by hydrolyzable ATP analogs. *J Biol Chem* 285: 19967–19975, 2010. doi:10.1074/jbc.M109.092684.
162. Moody JE, Millen L, Binns D, Hunt JF, Thomas PJ. Cooperative, ATP-dependent association of the nucleotide binding cassettes during the catalytic cycle of ATP-binding cassette transporters. *J Biol Chem* 277: 21111–21114, 2002. doi:10.1074/jbc.C200228200.
163. Mornon JP, Hoffmann B, Jonic S, Lehn P, Callebaut I. Full-open and closed CFTR channels, with lateral tunnels from the cytoplasm and an alternative position of the F508 region, as revealed by molecular dynamics. *Cell Mol Life Sci* 72: 1377–1403, 2015. doi:10.1007/s00018-014-1749-2.
164. Muanprasat C, Sonawane ND, Salinas D, Taddei A, Galiotta LJ, Verkman AS. Discovery of glycine hydrazide pore-occluding CFTR inhibitors: mechanism, structure-activity analysis, and in vivo efficacy. *J Gen Physiol* 124: 125–137, 2004. doi:10.1085/jgp.200409059.
165. Nagel G, Barbry P, Chabot H, Brochiero E, Hartung K, Grygorczyk R. CFTR fails to inhibit the epithelial sodium channel ENaC expressed in *Xenopus laevis* oocytes. *J Physiol* 564: 671–682, 2005. doi:10.1113/jphysiol.2004.079046.
166. Naren AP, Cornet-Boyaka E, Fu J, Villain M, Blalock JE, Quick MW, Kirk KL. CFTR chloride channel regulation by an interdomain interaction. *Science* 286: 544–548, 1999. doi:10.1126/science.286.5439.544.
167. Naren AP, Quick MW, Collawn JF, Nelson DJ, Kirk KL. Syntaxin 1A inhibits CFTR chloride channels by means of domain-specific protein-protein interactions. *Proc Natl Acad Sci USA* 95: 10972–10977, 1998. doi:10.1073/pnas.95.18.10972.
168. Neville DC, Rozanas CR, Price EM, Gruis DB, Verkman AS, Townsend RR. Evidence for phosphorylation of serine 753 in CFTR using a novel metal-ion affinity resin and matrix-assisted laser desorption mass spectrometry. *Protein Sci* 6: 2436–2445, 1997. doi:10.1002/pro.5560061117.
169. Norimatsu Y, Ivetaç A, Alexander C, O'Donnell N, Frye L, Sansom MSP, Dawson DC. Locating a plausible binding site for an open-channel blocker, GlyH-101, in the pore of the cystic fibrosis transmembrane conductance regulator. *Mol Pharmacol* 82: 1042–1055, 2012. doi:10.1124/mol.112.080267.
170. O'Donoghue DL, Dua V, Moss GW, Vergani P. Increased apical Na⁺ permeability in cystic fibrosis is supported by a quantitative model of epithelial ion transport. *J Physiol* 591: 3681–3692, 2013. doi:10.1113/jphysiol.2013.253955.
171. O'Sullivan BP, Freedman SD. Cystic fibrosis. *Lancet* 373: 1891–1904, 2009. doi:10.1016/S0140-6736(09)60327-5.
172. Okeyo G, Wang W, Wei S, Kirk KL. Converting nonhydrolyzable nucleotides to strong cystic fibrosis transmembrane conductance regulator (CFTR) agonists by gain of function (GOF) mutations. *J Biol Chem* 288: 17122–17133, 2013. doi:10.1074/jbc.M112.442582.
173. Okiyoneda T, Barrière H, Bagdány M, Rabeh WM, Du K, Höfheld J, Young JC, Lukacs GL. Peripheral protein quality control removes unfolded CFTR from the plasma membrane. *Science* 329: 805–810, 2010. doi:10.1126/science.1191542.
174. Oldham ML, Chen J. Snapshots of the maltose transporter during ATP hydrolysis. *Proc Natl Acad Sci USA* 108: 15152–15156, 2011. doi:10.1073/pnas.1108858108.
175. Orelle C, Dalmas O, Gros P, Di Pietro A, Jault JM. The conserved glutamate residue adjacent to the Walker-B motif is the catalytic base for ATP hydrolysis in the ATP-binding cassette transporter BmrA. *J Biol Chem* 278: 47002–47008, 2003. doi:10.1074/jbc.M308268200.
176. Ortiz D, Gossack L, Quast U, Bryan J. Reinterpreting the action of ATP analogs on K(ATP) channels. *J Biol Chem* 288: 18894–18902, 2013. doi:10.1074/jbc.M113.476887.
177. Ostedgaard LS, Baldursson O, Vermeer DW, Welsh MJ, Robertson AD. A functional R domain from cystic fibrosis transmembrane conductance regulator is predominantly unstructured in solution. *Proc Natl Acad Sci USA* 97: 5657–5662, 2000. doi:10.1073/pnas.100588797.
178. Park HW, Nam JH, Kim JY, Namkung W, Yoon JS, Lee JS, Kim KS, Venglovecz V, Gray MA, Kim KH, Lee MG. Dynamic regulation of CFTR bicarbonate permeability by [Cl⁻]_{ji} and its role in pancreatic bicarbonate secretion. *Gastroenterology* 139: 620–631, 2010. doi:10.1053/j.gastro.2010.04.004.
179. Park J, Khloya P, Seo Y, Kumar S, Lee HK, Jeon DK, Jo S, Sharma PK, Namkung W. Potentiation of Δ F508- and G551D-CFTR-mediated Cl⁻ current by novel hydroxypyrazolines. *PLoS One* 11: e0149131, 2016. doi:10.1371/journal.pone.0149131.
180. Pedemonte N, Sonawane ND, Taddei A, Hu J, Zegarra-Moran O, Suen YF, Robins LI, Dicus CW, Willenbring D, Nantz MH, Kurth MJ, Galiotta LJ, Verkman AS. Phenylglycine and sulfonamide correctors of defective Δ F508 and G551D cystic fibrosis transmembrane conductance regulator chloride-channel gating. *Mol Pharmacol* 67: 1797–1807, 2005. doi:10.1124/mol.105.010959.
181. Pezzullo AA, Tang XX, Hoegger MJ, Abou Alaiwa MH, Ramachandran S, Moninger TO, Karp PH, Wohlford-Lenane CL, Haagsman HP, van Eijk M, Bánfi B, Horswill AR, Stoltz DA, McCray PB Jr, Welsh MJ, Zabner J. Reduced airway surface pH impairs bacterial killing in the porcine cystic fibrosis lung. *Nature* 487: 109–113, 2012. doi:10.1038/nature11130.

182. Phuan PW, Veit G, Tan JA, Finkbeiner WE, Lukacs GL, Verkman AS. Potentiators of Defective $\Delta F508$ -CFTR Gating that Do Not Interfere with Corrector Action. *Mol Pharmacol* 88: 791–799, 2015. doi:10.1124/mol.115.099689.
183. Picciotto MR, Cohn JA, Bertuzzi G, Greengard P, Nairn AC. Phosphorylation of the cystic fibrosis transmembrane conductance regulator. *J Biol Chem* 267: 12742–12752, 1992.
184. Poulsen JH, Fischer H, Illek B, Machen TE. Bicarbonate conductance and pH regulatory capability of cystic fibrosis transmembrane conductance regulator. *Proc Natl Acad Sci USA* 91: 5340–5344, 1994. doi:10.1073/pnas.91.12.5340.
185. Powe AC Jr, Al-Nakkash L, Li M, Hwang TC. Mutation of Walker-A lysine 464 in cystic fibrosis transmembrane conductance regulator reveals functional interaction between its nucleotide-binding domains. *J Physiol* 539: 333–346, 2002. doi:10.1113/jphysiol.2001.013162.
186. Procko E, Ferrin-O'Connell I, Ng SL, Gaudet R. Distinct structural and functional properties of the ATPase sites in an asymmetric ABC transporter. *Mol Cell* 24: 51–62, 2006. doi:10.1016/j.molcel.2006.07.034.
187. Procko E, O'Mara ML, Bennett WFD, Tieleman DP, Gaudet R. The mechanism of ABC transporters: general lessons from structural and functional studies of an antigenic peptide transporter. *FASEB J* 23: 1287–1302, 2009. doi:10.1096/fj.08-121855.
188. Qian F, El Hiani Y, Linsdell P. Functional arrangement of the 12th transmembrane region in the CFTR chloride channel pore based on functional investigation of a cysteine-less CFTR variant. *Pflügers Arch* 462: 559–571, 2011. doi:10.1007/s00424-011-0998-2.
189. Quinton PM. The neglected ion: HCO₃⁻. *Nat Med* 7: 292–293, 2001. doi:10.1038/85429.
190. Quinton PM, Bijman J. Higher bioelectric potentials due to decreased chloride absorption in the sweat glands of patients with cystic fibrosis. *N Engl J Med* 308: 1185–1189, 1983. doi:10.1056/NEJM198305193082002.
191. Raju SV, Lin VY, Liu L, McNicholas CM, Karki S, Sloane PA, Tang L, Jackson PL, Wang W, Wilson L, Macon KJ, Mazur M, Kappes JC, DeLucas LJ, Barnes S, Kirk K, Tearney GJ, Rowe SM. The Cystic Fibrosis Transmembrane Conductance Regulator Potentiator Ivacaftor Augments Mucociliary Clearance Abrogating Cystic Fibrosis Transmembrane Conductance Regulator Inhibition by Cigarette Smoke. *Am J Respir Cell Mol Biol* 56: 99–108, 2017. doi:10.1165/rmb.2016-0226OC.
192. Ramjeesingh M, Li C, Garami E, Huan LJ, Galley K, Wang Y, Bear CE. Walker mutations reveal loose relationship between catalytic and channel-gating activities of purified CFTR (cystic fibrosis transmembrane conductance regulator). *Biochemistry* 38: 1463–1468, 1999. doi:10.1021/bi982243y.
193. Ramjeesingh M, Ugwu F, Stratford FL, Huan LJ, Li C, Bear CE. The intact CFTR protein mediates ATPase rather than adenylate kinase activity. *Biochem J* 412: 315–321, 2008. doi:10.1042/BJ20071719.
194. Randak C, Neth P, Auerswald EA, Eckerskorn C, Assfalg-Machleidt I, Machleidt W. A recombinant polypeptide model of the second nucleotide-binding fold of the cystic fibrosis transmembrane conductance regulator functions as an active ATPase, GT-Pase and adenylate kinase. *FEBS Lett* 410: 180–186, 1997. doi:10.1016/S0014-5793(97)00574-7.
195. Randak C, Welsh MJ. An intrinsic adenylate kinase activity regulates gating of the ABC transporter CFTR. *Cell* 115: 837–850, 2003. doi:10.1016/S0092-8674(03)00983-8.
196. Randak CO, Ver Heul AR, Welsh MJ. Demonstration of phosphoryl group transfer indicates that the ATP-binding cassette (ABC) transporter cystic fibrosis transmembrane conductance regulator (CFTR) exhibits adenylate kinase activity. *J Biol Chem* 287: 36105–36110, 2012. doi:10.1074/jbc.M112.408450.
197. Randak CO, Welsh MJ. ADP inhibits function of the ABC transporter cystic fibrosis transmembrane conductance regulator via its adenylate kinase activity. *Proc Natl Acad Sci USA* 102: 2216–2220, 2005. doi:10.1073/pnas.0409787102.
198. Reddy MM, Quinton PM. Control of dynamic CFTR selectivity by glutamate and ATP in epithelial cells. *Nature* 423: 756–760, 2003. doi:10.1038/nature01694.
199. Rich DP, Berger HA, Cheng SH, Travis SM, Saxena M, Smith AE, Welsh MJ. Regulation of the cystic fibrosis transmembrane conductance regulator Cl⁻ channel by negative charge in the R domain. *J Biol Chem* 268: 20259–20267, 1993.
200. Rich DP, Gregory RJ, Anderson MP, Manavalan P, Smith AE, Welsh MJ. Effect of deleting the R domain on CFTR-generated chloride channels. *Science* 253: 205–207, 1991. doi:10.1126/science.1712985.
201. Riordan JR, Rommens JM, Kerem B, Alon N, Rozmahel R, Grzelczak Z, Zielenski J, Lok S, Plavsic N, Chou JL, et al. Identification of the cystic fibrosis gene: cloning and characterization of complementary DNA. *Science* 245: 1066–1073, 1989. doi:10.1126/science.2475911.
202. Saint-Criq V, Gray MA. Role of CFTR in epithelial physiology. *Cell Mol Life Sci* 74: 93–115, 2017. doi:10.1007/s00018-016-2391-y.
203. Schultz BD, Venglarik CJ, Bridges RJ, Frizzell RA. Regulation of CFTR Cl⁻ channel gating by ADP and ATP analogues. *J Gen Physiol* 105: 329–361, 1995. doi:10.1085/jgp.105.3.329.
204. Scott-Ward TS, Cai Z, Dawson ES, Doherty A, Da Paula AC, Davidson H, Porteous DJ, Wainwright BJ, Amaral MD, Sheppard DN, Boyd AC. Chimeric constructs endow the human CFTR Cl⁻ channel with the gating behavior of murine CFTR. *Proc Natl Acad Sci USA* 104: 16365–16370, 2007. doi:10.1073/pnas.0701562104.
205. Sebastian A, Rishishwar L, Wang J, Bernard KF, Conley AB, McCarty NA, Jordan IK. Origin and evolution of the cystic fibrosis transmembrane regulator protein R domain. *Gene* 523: 137–146, 2013. doi:10.1016/j.gene.2013.02.050.
206. Seibert FS, Tabcharani JA, Chang XB, Dulhanty AM, Mathews C, Hanrahan JW, Riordan JR. cAMP-dependent protein kinase-mediated phosphorylation of cystic fibrosis transmembrane conductance regulator residue Ser-753 and its role in channel activation. *J Biol Chem* 270: 2158–2162, 1995. doi:10.1074/jbc.270.5.2158.
207. Serohijos AWR, Hegedus T, Aleksandrov AA, He L, Cui L, Dokholyan NV, Riordan JR. Phenylalanine-508 mediates a cytoplasmic-membrane domain contact in the CFTR 3D structure crucial to assembly and channel function. *Proc Natl Acad Sci USA* 105: 3256–3261, 2008. doi:10.1073/pnas.0800254105.
208. Shah VS, Ernst S, Tang XX, Karp PH, Parker CP, Ostedgaard LS, Welsh MJ. Relationships among CFTR expression, HCO₃⁻ secretion, and host defense may inform gene- and cell-based cystic fibrosis therapies. *Proc Natl Acad Sci USA* 113: 5382–5387, 2016. doi:10.1073/pnas.1604905113.
210. Shah VS, Meyerholz DK, Tang XX, Reznikov L, Abou Alaiwa M, Ernst SE, Karp PH, Wohlford-Lenane CL, Heilmann KP, Leidinger MR, Allen PD, Zabner J, McCray PB Jr, Ostedgaard LS, Stoltz DA, Randak CO, Welsh MJ. Airway acidification initiates host defense abnormalities in cystic fibrosis mice. *Science* 351: 503–507, 2016. doi:10.1126/science.1255899.
211. Sheppard DN, Robinson KA. Mechanism of glibenclamide inhibition of cystic fibrosis transmembrane conductance regulator Cl⁻ channels expressed in a murine cell line. *J Physiol* 503: 333–346, 1997. doi:10.1111/j.1469-7793.1997.333bh.x.
212. Shintre CA, Pike AC, Li Q, Kim JJ, Barr AJ, Goubin S, Shrestha L, Yang J, Berridge G, Ross J, Stansfeld PJ, Sansom MS, Edwards AM, Bountra C, Marsden BD, von Delft F, Bullock AN, Gileadi O, Burgess-Brown NA, Carpenter EP. Structures of ABCB10, a human ATP-binding cassette transporter in apo- and nucleotide-bound states. *Proc Natl Acad Sci USA* 110: 9710–9715, 2013. doi:10.1073/pnas.1217042110.
213. Siarheyeva A, Liu R, Sharom FJ. Characterization of an asymmetric occluded state of P-glycoprotein with two bound nucleotides: implications for catalysis. *J Biol Chem* 285: 7575–7586, 2010. doi:10.1074/jbc.M109.047290.
214. Sloane PA, Shastry S, Wilhelm A, Courville C, Tang LP, Backer K, Levin E, Raju SV, Li Y, Mazur M, Byan-Parker S, Grizzle W, Sorscher EJ, Dransfield MT, Rowe SM. A pharmacologic approach to acquired cystic fibrosis transmembrane conductance regulator dysfunction in smoking related lung disease. *PLoS One* 7: e39809, 2012. doi:10.1371/journal.pone.0039809.
215. Smith PC, Karpowich N, Millen L, Moody JE, Rosen J, Thomas PJ, Hunt JF. ATP binding to the motor domain from an ABC transporter drives formation of a nucleotide sandwich dimer. *Mol Cell* 10: 139–149, 2002. doi:10.1016/S1097-2765(02)00576-2.
216. Smith SS, Steinle ED, Meyerhoff ME, Dawson DC. Cystic fibrosis transmembrane conductance regulator. Physical basis for lyotropic anion selectivity patterns. *J Gen Physiol* 114: 799–818, 1999. doi:10.1085/jgp.114.6.799.
217. Son JH, Zhu JS, Phuan PW, Cil O, Teuthorn AP, Ku CK, Lee S, Verkman AS, Kurth MJ. High-Potency Phenylquinoxalinone Cystic Fibrosis Transmembrane Conductance Regulator (CFTR) Activators. *J Med Chem* 60: 2401–2410, 2017. doi:10.1021/acs.jmedchem.6b01759.

218. Sonawane ND, Zhao D, Zegarra-Moran O, Galiotta LJ, Verkman AS. Nanomolar CFTR inhibition by pore-occluding divalent polyethylene glycol-malonic acid hydrazides. *Chem Biol* 15: 718–728, 2008. doi:10.1016/j.chembiol.2008.05.015.
219. Sorum B, Czégé D, Csanády L. Timing of CFTR pore opening and structure of its transition state. *Cell* 163: 724–733, 2015. doi:10.1016/j.cell.2015.09.052.
220. Sorum B, Töröcsik B, Csanády L. Asymmetry of movements in CFTR's two ATP sites during pore opening serves their distinct functions. *eLife* 6: e29013, 2017. doi:10.7554/eLife.29013.
221. St Aubin CN, Zhou JJ, Linsdell P. Identification of a second blocker binding site at the cytoplasmic mouth of the cystic fibrosis transmembrane conductance regulator chloride channel pore. *Mol Pharmacol* 71: 1360–1368, 2007. doi:10.1124/mol.106.031732.
222. Szakács G, Ozvegy C, Bakos E, Sarkadi B, Váradi A. Transition-state formation in ATPase-negative mutants of human MDRI protein. *Biochem Biophys Res Commun* 276: 1314–1319, 2000. doi:10.1006/bbrc.2000.3576.
223. Szollosi A, Muallem DR, Csanády L, Vergani P. Mutant cycles at CFTR's non-canonical ATP-binding site support little interface separation during gating. *J Gen Physiol* 137: 549–562, 2011. doi:10.1085/jgp.201110608.
224. Szollosi A, Vergani P, Csanády L. Involvement of F1296 and N1303 of CFTR in induced-fit conformational change in response to ATP binding at NBD2. *J Gen Physiol* 136: 407–423, 2010. doi:10.1085/jgp.201010434.
225. Tabcharani JA, Chang XB, Riordan JR, Hanrahan JW. Phosphorylation-regulated Cl-channel in CHO cells stably expressing the cystic fibrosis gene. *Nature* 352: 628–631, 1991. doi:10.1038/352628a0.
226. Tabcharani JA, Linsdell P, Hanrahan JW. Halide permeation in wild-type and mutant cystic fibrosis transmembrane conductance regulator chloride channels. *J Gen Physiol* 110: 341–354, 1997. doi:10.1085/jgp.110.4.341.
227. Tabcharani JA, Rommens JM, Hou YX, Chang XB, Tsui LC, Riordan JR, Hanrahan JW. Multi-ion pore behaviour in the CFTR chloride channel. *Nature* 366: 79–82, 1993. doi:10.1038/366079a0.
228. Taddei A, Folli C, Zegarra-Moran O, Fanen P, Verkman AS, Galiotta LJ. Altered channel gating mechanism for CFTR inhibition by a high-affinity thiazolidinone blocker. *FEBS Lett* 558: 52–56, 2004. doi:10.1016/S0014-5793(04)00011-0.
229. Thiagarajah JR, Donowitz M, Verkman AS. Secretory diarrhoea: mechanisms and emerging therapies. *Nat Rev Gastroenterol Hepatol* 12: 446–457, 2015. doi:10.1038/nrgastro.2015.111.
230. Timachi MH, Hutter CA, Hohl M, Assafa T, Böhm S, Mittal A, Seeger MA, Bordignon E. Exploring conformational equilibria of a heterodimeric ABC transporter. *eLife* 6: e20236, 2017. doi:10.7554/eLife.20236.
231. Townsend RR, Lipniunas PH, Tulk BM, Verkman AS. Identification of protein kinase A phosphorylation sites on NBD1 and R domains of CFTR using electrospray mass spectrometry with selective phosphate ion monitoring. *Protein Sci* 5: 1865–1873, 1996. doi:10.1002/pro.5560050912.
232. Travis SM, Berger HA, Welsh MJ. Protein phosphatase 2C dephosphorylates and inactivates cystic fibrosis transmembrane conductance regulator. *Proc Natl Acad Sci USA* 94: 11055–11060, 1997. doi:10.1073/pnas.94.20.11055.
233. Tsai MF, Li M, Hwang TC. Stable ATP binding mediated by a partial NBD dimer of the CFTR chloride channel. *J Gen Physiol* 135: 399–414, 2010. doi:10.1085/jgp.201010399.
234. Tsai MF, Shimizu H, Sohma Y, Li M, Hwang TC. State-dependent modulation of CFTR gating by pyrophosphate. *J Gen Physiol* 133: 405–419, 2009. doi:10.1085/jgp.200810186.
235. Ueda K, Inagaki N, Seino S. MgADP antagonism to Mg²⁺-independent ATP binding of the sulfonyleurea receptor SUR1. *J Biol Chem* 272: 22983–22986, 1997. doi:10.1074/jbc.272.37.22983.
236. Urbatsch IL, Julien M, Carrier I, Rousseau ME, Cayrol R, Gros P. Mutational analysis of conserved carboxylate residues in the nucleotide binding sites of P-glycoprotein. *Biochemistry* 39: 14138–14149, 2000. doi:10.1021/bi001128w.
237. Vais H, Zhang R, Reenstra WW. Dibasic phosphorylation sites in the R domain of CFTR have stimulatory and inhibitory effects on channel activation. *Am J Physiol Cell Physiol* 287: C737–C745, 2004. doi:10.1152/ajpcell.00504.2003.
238. Van Goor F, Hadida S, Grootenhuys PDJ, Burton B, Cao D, Neuberger T, Turnbull A, Singh A, Joubbran J, Hazlewood A, Zhou J, McCartney J, Arumugam V, Decker C, Yang J, Young C, Olson ER, Wine JJ, Frizzell RA, Ashlock M, Negulescu P. Rescue of CF airway epithelial cell function in vitro by a CFTR potentiator, VX-770. *Proc Natl Acad Sci USA* 106: 18825–18830, 2009. doi:10.1073/pnas.0904709106.
239. Van Goor F, Hadida S, Grootenhuys PDJ, Burton B, Stack JH, Straley KS, Decker CJ, Miller M, McCartney J, Olson ER, Wine JJ, Frizzell RA, Ashlock M, Negulescu PA. Correction of the F508del-CFTR protein processing defect in vitro by the investigational drug VX-809. *Proc Natl Acad Sci USA* 108: 18843–18848, 2011. doi:10.1073/pnas.1105787108.
240. Veit G, Avramescu RG, Perdomo D, Phuan PW, Bagdany M, Apaja PM, Borot F, Szollosi D, Wu YS, Finkbeiner WE, Hegedus T, Verkman AS, Lukacs GL. Some gating potentiators, including VX-770, diminish $\Delta F508$ -CFTR functional expression. *Sci Transl Med* 6: 246ra97, 2014. doi:10.1126/scitranslmed.3008889.
241. Venglarik CJ, Schultz BD, Frizzell RA, Bridges RJ. ATP alters current fluctuations of cystic fibrosis transmembrane conductance regulator: evidence for a three-state activation mechanism. *J Gen Physiol* 104: 123–146, 1994. doi:10.1085/jgp.104.1.123.
242. Vergani P, Lockless SW, Nairn AC, Gadsby DC. CFTR channel opening by ATP-driven tight dimerization of its nucleotide-binding domains. *Nature* 433: 876–880, 2005. doi:10.1038/nature03313.
243. Vergani P, Nairn AC, Gadsby DC. On the mechanism of MgATP-dependent gating of CFTR Cl⁻ channels. *J Gen Physiol* 121: 17–36, 2003. doi:10.1085/jgp.20028673.
244. Wainwright CE, Elborn JS, Ramsey BW, Marigowda G, Huang X, Cipolli M, Colombo C, Davies JC, De Boeck K, Flume PA, Konstan MW, McColley SA, McCoy K, McKone EF, Munck A, Ratjen F, Rowe SM, Waltz D, Boyle MP; TRAFFIC Study Group; TRANSPORT Study Group. Lumacaftor-ivacaftor in Patients with Cystic Fibrosis Homozygous for Phe508del CFTR. *N Engl J Med* 373: 220–231, 2015. doi:10.1056/NEJMoa1409547.
245. Walker JE, Saraste M, Runswick MJ, Gay NJ. Distantly related sequences in the alpha and beta-subunits of ATP synthase, myosin, kinases and other ATP-requiring enzymes and a common nucleotide binding fold. *EMBO J* 1: 945–951, 1982. doi:10.1002/j.1460-2075.1982.tb01276.x.
246. Wang F, Zeltwanger S, Hu S, Hwang TC. Deletion of phenylalanine 508 causes attenuated phosphorylation-dependent activation of CFTR chloride channels. *J Physiol* 524: 637–648, 2000. doi:10.1111/j.1469-7793.2000.00637.x.
247. Wang F, Zeltwanger S, Yang IC, Nairn AC, Hwang TC. Actions of genistein on cystic fibrosis transmembrane conductance regulator channel gating. Evidence for two binding sites with opposite effects. *J Gen Physiol* 111: 477–490, 1998. doi:10.1085/jgp.111.3.477.
248. Wang W, Bernard K, Li G, Kirk KL. Curcumin opens cystic fibrosis transmembrane conductance regulator channels by a novel mechanism that requires neither ATP binding nor dimerization of the nucleotide-binding domains. *J Biol Chem* 282: 4533–4544, 2007. doi:10.1074/jbc.M609942200.
249. Wang W, He Z, O'Shaughnessy TJ, Rux J, Reenstra WW. Domain-domain associations in cystic fibrosis transmembrane conductance regulator. *Am J Physiol Cell Physiol* 282: C1170–C1180, 2002. doi:10.1152/ajpcell.00337.2001.
250. Wang W, Li G, Clancy JP, Kirk KL. Activating cystic fibrosis transmembrane conductance regulator channels with pore blocker analogs. *J Biol Chem* 280: 23622–23630, 2005. doi:10.1074/jbc.M503118200.
251. Wang W, Okeyo GO, Tao B, Hong JS, Kirk KL. Thermally unstable gating of the most common cystic fibrosis mutant channel ($\Delta F508$): "rescue" by suppressor mutations in nucleotide binding domain I and by constitutive mutations in the cytosolic loops. *J Biol Chem* 286: 41937–41948, 2011. doi:10.1074/jbc.M111.296061.
252. Wang W, Roessler BC, Kirk KL. An electrostatic interaction at the tetrahelix bundle promotes phosphorylation-dependent cystic fibrosis transmembrane conductance regulator (CFTR) channel opening. *J Biol Chem* 289: 30364–30378, 2014. doi:10.1074/jbc.M114.595710.
253. Wang W, Wu J, Bernard K, Li G, Wang G, Bevensee MO, Kirk KL. ATP-independent CFTR channel gating and allosteric modulation by phosphorylation. *Proc Natl Acad Sci USA* 107: 3888–3893, 2010. doi:10.1073/pnas.0913001107.
254. Wang W, El Hiani Y, Linsdell P. Alignment of transmembrane regions in the cystic fibrosis transmembrane conductance regulator chloride channel pore. *J Gen Physiol* 138: 165–178, 2011. doi:10.1085/jgp.201110605.

255. Wang W, El Hiani Y, Rubaiy HN, Linsdell P. Relative contribution of different transmembrane segments to the CFTR chloride channel pore. *Pflügers Arch* 466: 477–490, 2014. doi:10.1007/s00424-013-1317-x.
256. Ward A, Reyes CL, Yu J, Roth CB, Chang G. Flexibility in the ABC transporter MsbA: Alternating access with a twist. *Proc Natl Acad Sci USA* 104: 19005–19010, 2007. doi:10.1073/pnas.0709388104.
257. Wei S, Roesler BC, Chauvet S, Guo J, Hartman JL IV, Kirk KL. Conserved allosteric hot spots in the transmembrane domains of cystic fibrosis transmembrane conductance regulator (CFTR) channels and multidrug resistance protein (MRP) pumps. *J Biol Chem* 289: 19942–19957, 2014. doi:10.1074/jbc.M114.562116.
258. Weinreich F, Riordan JR, Nagel G. Dual effects of ADP and adenylylimidodiphosphate on CFTR channel kinetics show binding to two different nucleotide binding sites. *J Gen Physiol* 114: 55–70, 1999. doi:10.1085/jgp.114.1.55.
259. Widdicombe JH, Welsh MJ, Finkbeiner WE. Cystic fibrosis decreases the apical membrane chloride permeability of monolayers cultured from cells of tracheal epithelium. *Proc Natl Acad Sci USA* 82: 6167–6171, 1985. doi:10.1073/pnas.82.18.6167.
260. Wilkinson DJ, Strong TV, Mansoura MK, Wood DL, Smith SS, Collins FS, Dawson DC. CFTR activation: additive effects of stimulatory and inhibitory phosphorylation sites in the R domain. *Am J Physiol* 273: L127–L133, 1997.
261. Winter MC, Sheppard DN, Carson MR, Welsh MJ. Effect of ATP concentration on CFTR Cl⁻ channels: a kinetic analysis of channel regulation. *Biophys J* 66: 1398–1403, 1994. doi:10.1016/S0006-3495(94)80930-0.
262. Winter MC, Welsh MJ. Stimulation of CFTR activity by its phosphorylated R domain. *Nature* 389: 294–296, 1997. doi:10.1038/38514.
263. Yang B, Sonawane ND, Zhao D, Somlo S, Verkman AS. Small-molecule CFTR inhibitors slow cyst growth in polycystic kidney disease. *J Am Soc Nephrol* 19: 1300–1310, 2008. doi:10.1681/ASN.2007070828.
264. Yasuda R, Noji H, Yoshida M, Kinoshita K Jr, Itoh H. Resolution of distinct rotational substeps by submillisecond kinetic analysis of F1-ATPase. *Nature* 410: 898–904, 2001. doi:10.1038/35073513.
265. Yeh HI, Sohma Y, Conrath K, Hwang TC. A common mechanism for CFTR potentiators. *J Gen Physiol* 149: 1105–1118, 2017. doi:10.1085/jgp.201711886.
266. Yeh HI, Yeh JT, Hwang TC. Modulation of CFTR gating by permeant ions. *J Gen Physiol* 145: 47–60, 2015. doi:10.1085/jgp.201411272.
267. Yu H, Burton B, Huang CJ, Worley J, Cao D, Johnson JP Jr, Urrutia A, Joubbran J, Seepersaud S, Sussky K, Hoffman BJ, Van Goor F. Ivacaftor potentiation of multiple CFTR channels with gating mutations. *J Cyst Fibros* 11: 237–245, 2012. doi:10.1016/j.jcf.2011.12.005.
268. Yuan YR, Blecker S, Martsinkevich O, Millen L, Thomas PJ, Hunt JF. The crystal structure of the MJ0796 ATP-binding cassette. Implications for the structural consequences of ATP hydrolysis in the active site of an ABC transporter. *J Biol Chem* 276: 32313–32321, 2001. doi:10.1074/jbc.M100758200.
269. Zaitseva J, Jenewein S, Jumpertz T, Holland IB, Schmitt L. H662 is the linchpin of ATP hydrolysis in the nucleotide-binding domain of the ABC transporter HlyB. *EMBO J* 24: 1901–1910, 2005. doi:10.1038/sj.emboj.7600657.
270. Zeltwanger S, Wang F, Wang GT, Gillis KD, Hwang TC. Gating of cystic fibrosis transmembrane conductance regulator chloride channels by adenosine triphosphate hydrolysis. Quantitative analysis of a cyclic gating scheme. *J Gen Physiol* 113: 541–554, 1999. doi:10.1085/jgp.113.4.541.
271. Zhang J, Hwang TC. The Fifth Transmembrane Segment of Cystic Fibrosis Transmembrane Conductance Regulator Contributes to Its Anion Permeation Pathway. *Biochemistry* 54: 3839–3850, 2015. doi:10.1021/acs.biochem.5b00427.
272. Zhang J, Hwang TC. Electrostatic tuning of the pre- and post-hydrolytic open states in CFTR. *J Gen Physiol* 149: 355–372, 2017. doi:10.1085/jgp.201611664.
273. Zhang Z, Chen J. Atomic Structure of the Cystic Fibrosis Transmembrane Conductance Regulator. *Cell* 167: 1586–1597.e9, 2016. doi:10.1016/j.cell.2016.11.014.
274. Zhang Z, Liu F, Chen J. Conformational Changes of CFTR upon Phosphorylation and ATP Binding. *Cell* 170: 483–491.e8, 2017. doi:10.1016/j.cell.2017.06.041.
275. Zhang ZR, McDonough SI, McCarty NA. Interaction between permeation and gating in a putative pore domain mutant in the cystic fibrosis transmembrane conductance regulator. *Biophys J* 79: 298–313, 2000. doi:10.1016/S0006-3495(00)76292-8.
276. Zhang ZR, Zeltwanger S, McCarty NA. Direct comparison of NPPB and DPC as probes of CFTR expressed in *Xenopus* oocytes. *J Membr Biol* 175: 35–52, 2000. doi:10.1007/s002320001053.
277. Zhou Y, Pearson JE, Auerbach A. Phi-value analysis of a linear, sequential reaction mechanism: theory and application to ion channel gating. *Biophys J* 89: 3680–3685, 2005. doi:10.1529/biophysj.105.067215.
278. Zhou Z, Hu S, Hwang TC. Voltage-dependent flickery block of an open cystic fibrosis transmembrane conductance regulator (CFTR) channel pore. *J Physiol* 532: 435–448, 2001. doi:10.1111/j.1469-7793.2001.0435f.x.
279. Zhou Z, Hu S, Hwang TC. Probing an open CFTR pore with organic anion blockers. *J Gen Physiol* 120: 647–662, 2002. doi:10.1085/jgp.20028685.
280. Zhou Z, Wang X, Li M, Sohma Y, Zou X, Hwang TC. High affinity ATP/ADP analogues as new tools for studying CFTR gating. *J Physiol* 569: 447–457, 2005. doi:10.1113/jphysiol.2005.095083.
281. Zhou Z, Wang X, Liu HY, Zou X, Li M, Hwang TC. The two ATP binding sites of cystic fibrosis transmembrane conductance regulator (CFTR) play distinct roles in gating kinetics and energetics. *J Gen Physiol* 128: 413–422, 2006. doi:10.1085/jgp.200609622.
282. Zielenski J, Tsui LC. Cystic fibrosis: genotypic and phenotypic variations. *Annu Rev Genet* 29: 777–807, 1995. doi:10.1146/annurev.ge.29.120195.004021.